東北大学機関リポジトリ
TOUR
Tohoku University Repository

Circuits for appetitive responses of Drosophila

著者	THOMA VLADIMIROS
学位授与機関	Tohoku University
学位授与番号	11301甲第16685号
URL	http://hdl.handle.net/10097/63057

博士論文

Circuits for appetitive responses of Drosophila
（ショウジョウバエの味覚行動を司る神経回路についての研究）

平成 27 年度

東北大学大学院生命科学研究科
生命機能科学専攻
Vladimiros Thoma

Dissertation

Circuits for appetitive responses of *Drosophila*

Vladimiros Thoma

Contents

Table of Figures 4
List of Abbreviations 5
Summary 8
1. Introduction 9
1.1. Taste qualities in mammals and invertebrates 9
1.2. Structure of the *Drosophila* taste system 10
1.2.1. Taste organs of Drosophila 10
1.2.2. Structure of taste sensilla 12
1.2.3. Projections of gustatory receptor neurons to the central nervous system 12
1.3. Functions of the *Drosophila* taste system 14
1.3.1. Taste receptors in mammals and Drosophila 16
1.3.2. Drosophila gustatory receptors in taste perception 16
1.3.3. Drosophila ionotropic receptors in taste perception 20
1.3.4. Drosophila pickpocket channels in taste perception 20
1.3.5. Drosophila transient receptor potential channels in taste perception 21
1.3.6. Taste information processing in sensory neurons 22
1.3.7. Coordination of feeding behavior 23
1.3.8. Functions of 'atypical' taste organs 24
1.3.9. Role of taste in courtship behavior 24
1.4. Taste processing in the *Drosophila* central nervous system 25
1.4.1. Modulation of sweet taste neurons by starvation 26
1.4.2. Motor neurons controlling feeding behaviors 26
1.4.3. Taste circuits for associative learning 27
1.5. *Drosophila* as a model organism 28
1.5.1. General advantages of Drosophila 28
1.5.2. Genetic tools in Drosophila: GAL4/UAS system 29
1.5.3. Intersectional approaches and other binary expression systems 31
2. Materials and Methods 33
2.1. Fly strains 33

2.2. Immunohistochemistry and anatomical analysis 34
2.3. Generation of single-cell flp-outs 35
2.4. Behavioral experiments 35
2.4.1. Sugar preference assay 36
2.4.2. Proboscis extension reflex 37
2.4.3. Olfactory learning 37
2.5. Quantification of fly locomotion 38
2.6. Mathematical model of sugar preference 39
2.7. Statistics 41
3. Results 43
3.1. Sugar preference assay 43
3.2. Sweet taste receptor neurons are diferentially required for sugar choice 45
3.3. *Gr64f* and *Gr5a* lines label overlapping but distinct populations of cells 47
3.4. An intersectional approach selectively labels ascending tarsal GRNs 50
3.5. Ascending sweet taste receptor neurons in the tarsi are required for early appetitive responses 51
3.6. Sugar detection triggers rapid suppression of locomotion 57
3.7. Segmental tarsal sweet taste receptor neurons are required for sugar-induced locomotion suppression. 60
3.8. A mathematical model accurately predicts sugar preference 63
3.9. A neuronal silencing screen reveals candidate neurons for sugar preference 66
4. Discussion 69
4.1. Summary of results 69
4.2. Sensillar position relates to gustatory receptor neuron function 69
4.3. Functional dissociation in tarsal sweet taste receptor neurons 71
4.4. Roles of different taste organs in *Drosophila* 73
4.4.1. Role of labellar GRNs 74
4.4.2. Role of pharyngeal GRNs 75
4.5. Higher order neurons for sugar preference 77
References 79
Acknowledgements 101

Non-self contributions 103

Table of Figures

Figure 1: Taste sensilla and taste organs of *Drosophila*.. 11
Figure 2: Projections of gustatory receptor neurons to the central nervous system. 13
Figure 3: Feeding behavior of *Drosophila*. 15
Figure 4: Taste receptors in the mouse and fly. 17
Figure 5: Projections of gustatory receptor neurons are segregated based on taste quality. 23
Figure 6: Examples of genetic tools in *Drosophila*.. 30
Figure 7: The sugar preference assay. 43
Figure 8: Quantification and characterization of sugar preference in wild-type flies. 44
Figure 9: Sweet taste receptor neurons are differentially required for sugar preference. 45
Figure 10: Expression patterns of sweet Gr-GAL4 in the gnathal ganglia and foreleg tarsi. 46
Figure 11: Comparison of *Gr5a-GAL4* and *Gr64f-GAL4* expression in the central nervous system. 47
Figure 12: Comparison of *Gr5a-LexA* and *Gr64f-GAL4* in the same fly. 48
Figure 13: Single-cell labeling of tarsal gustatory receptor neurons in the central nervous system. 49
Figure 14: Expression pattern of Gr(64f–5a) flies. 50
Figure 15: atGRNs are required for sugar preference and feeding initiation. 52
Figure 16: Comparison of *Gr64f-LexA* and *Gr64a-GAL4* expression in the proboscis and brain. 53
Figure 17: Blocking with Gr(64f–5a) leaves labellar sweet taste receptor neurons functionally intact. 54
Figure 18: Behavioral and anatomical characterization of *Gr43a-GAL4*. 55
Figure 19: Blocking atGRNs with Gr(61a–5a) decreases 2 M sucrose preference. 56
Figure 20: Blocking atGRNs impairs short-term appetitive olfactory learning. 57
Figure 21: Hungry wild-type flies suppress their locomotion in the presence of sugar. 58
Figure 22: Quantification of sugar-induced suppression of locomotion in wild-type flies. 59
Figure 23: *Gr5a* cells are necessary for sugar-induced turning suppression. 61
Figure 24: *Gr5a* cells are necessary for sugar-induced linear velocity suppression. 62
Figure 25: Sweet taste receptor neurons in the labellum are not required for sugar-induced locomotion suppression. 63
Figure 26: A mathematical model can predict sugar preference. 64
Figure 27: A neuronal silencing screen for identification of neurons involved in sugar preference. 66
Figure 28: Candidate neurons for sugar preference. 68
Figure 29: Distinct subsets of tarsal sweet taste receptor neurons are tuned to different facets of the early appetitive response.. 71
Figure 30: Roles of taste receptor neurons in different taste organs of *Drosophila*. 74

List of Abbreviations

7TM	Seven Transmembrane Domain
atGRN	Ascending Tarsal Gustatory Receptor Neuron
CNS	Central Nervous System
CPG	Central Pattern Generator
CvC	Cervical Connective
DA	Dopamine
DCSO	Dorsal Cibarial Sense Organ
DEET	*N, N*-diethyl-*m*-toluamide
Flp	Flippase
FRT	Flippase Recognition Target
GABA	γ-aminobutiric acid
GFP	Green Fluorescent Protein
GNG	Gnathal Ganglia
GPCR	G protein-coupled receptor
GR	Gustatory Receptor
GRASP	GFP Reconstitution Across Synaptic Partners

Gr-GAL4	Gustatory receptor-GAL4
GRN	Gustatory Receptor Neuron
IR	Ionotropic Receptor
Kir	Kir2.1::eGFP (inwardly rectifying K^+ channel fused to GFP)
L-DOPA	L-3, 4-dihydroxyphenylalanine
LI	Learning Index
LSO	Labral Sense Organ
MB	Mushroom Body
MN	Mesothoracic ganglia
MtN	Metathoracic ganglia
NP-GAL4	Enhancer-trap GAL4 generated from the Nippon Project
OA	Octopamine
ORN	Olfactory Receptor Neurons
PAM	Protocerebral Anterior Medial
PBS	Phosphate-Buffered Saline
PBS-Tx	Phosphate-Buffered Saline with 0.1% Triton X-100
PER	Proboscis Extension Reflex

PI	Preference Index
PN	Protothoracic ganglia
ppk	Pickpocket
PPL1	Paired Posterior Lateral 1
SEG	Suboesophageal Ganglion
Shi^{ts1}	$Shibire^{ts1}$ (temperature-sensitive, dominant negative Dynamin allele)
SOG	Suboesophageal Ganglion
stGRN	Segmental Tarsal Gustatory Receptor Neuron
TRP	Transient Receptor Potential
UAS	Upstream Activating Sequence
VCSO	Ventral Cibarial Sense Organ
VNC	Ventral Nerve Cord
VUM	Ventral Unpaired Median

Summary

Finding appropriate food sources that are nutritious and non-toxic is crucial for survival. Like other animals, insects detect nonvolatile chemicals with specialized taste receptors. However, unlike mammals, where taste organs are exclusively located in the mouth, insects have taste receptors in multiple organs, including the proboscis and legs. The role of different taste organs in regulating feeding behavior remains poorly understood.

Here, the sweet taste receptor neurons of *Drosophila melanogaster* are used as a model to address this question. Using a neuronal silencing approach, the function of subsets of sweet taste receptor neurons in sugar preference is investigated. These experiments show that sweet taste receptor neurons in the legs, but not the proboscis, are crucial for sugar preference.

Leg neurons fall into two anatomically distinct classes. One class of leg neurons projects directly to the brain, whereas the other projects locally to thoracic ganglia. These two classes drive distinct early appetitive responses: brain-projecting cells are important for feeding initiation, whereas locally projecting cells control sugar-induced locomotion suppression. Interestingly, sugar preference can be accurately predicted from these two early appetitive responses. Information from leg cells may be conveyed to higher-order neurons that are also required for sugar preference. Taken together, these results highlight the functional specialization within the *Drosophila* taste system and help understand how early appetitive responses are coordinated to promote rapid and efficient choice behavior.

1. Introduction

1.1. Taste qualities in mammals and invertebrates

Finding nutritious food and appropriate mates are essential for all animals. Foraging for food can be guided by a combination of sensory modalities. However, it is the taste of a potential meal that ultimately determines if it will be ingested or rejected. Taste organs, being located near the entrance of the digestive system, are optimally positioned to act as the last gatekeeper before ingestion. In insects such as *Drosophila*, taste has additional functions, for example in mate selection.

Detection of tastants in mammals typically involves perception of five basic taste qualities: sweet (taste of sugars), bitter (taste of toxic substances e.g. alkaloids), sour (taste of acids), salt (taste of Na^+ and other ions) and umami (taste of amino acids)[1]. *Drosophila* is able to perceive a similar set of taste qualities[2]. Interestingly, some animals have lost the ability to sense certain taste qualities, presumably as a consequence of a specialized feeding niche[3,4]. Other taste qualities such as the taste of water, carbonation, fat and pheromones are known to exist in mammals and/or invertebrates[5].

Drosophila and mammals can detect similar taste qualities, but their taste systems also share important differences. One of the most striking differences is in structure: in mammals, the tongue is the main taste organ, while in fruit flies the taste sensors are distributed throughout the body. In the following sections, the *Drosophila* taste system will be examined in terms of its structure and functions.

1.2. Structure of the *Drosophila* taste system

The basic component of the *Drosophila* taste system is the sensillum, a hair-like structure that contains the taste receptors[6]. Taste sensilla can be categorized into two broad types: taste hairs (or taste bristles) are longer in size, while taste pegs (or papillae) are shorter and have simpler structures[7] (Figure 1a, b). Taste sensilla can be found in several parts of the *Drosophila* body, both internally and externally (Figure 1c). Below, the structure of the taste organs of the fruit fly and their sensilla are described in detail.

1.2.1. Taste organs of Drosophila

Sensilla can be found in the labellum, pharynx, leg tarsi, wing margins and female ovipositor[6] (Figure 1c). The labellum has traditionally been thought of as the 'main' taste organ in *Drosophila*[8], perhaps due to the presence of multiple sensilla, and analogous to the mammalian tongue, because it sits at the entrance of the digestive system. It houses 62 taste hairs and a comparable number of taste pegs, equally distributed between its two lobes (Figure 1d)[7]. Taste pegs are located on the internal surface of the labellum and are exposed when the two lobes open to allow ingestion (Figure 1e). The proboscis also contains other internal organs, located inside the pharynx. The labral sense organ (LSO) sits directly behind the oral opening, while the ventral cibarial sense organ (VCSO) and dorsal cibarial sense organ (DCSO) are located more proximally (Figure 1e). The LSO and VCSO contain 6 taste sensilla, while the DCSO contains 4 taste sensilla[9,10]. In the legs, taste hairs are most concentrated in the distal-most five segments, called tarsal segments, with fewer taste bristles in the tibiae[11]. Forelegs contain more taste hairs than midlegs or hindlegs[11,12]. A recent study examined taste hair anatomy, *Gr-GAL4* expression and electrophysiological responses and identified approximately 28 taste hairs

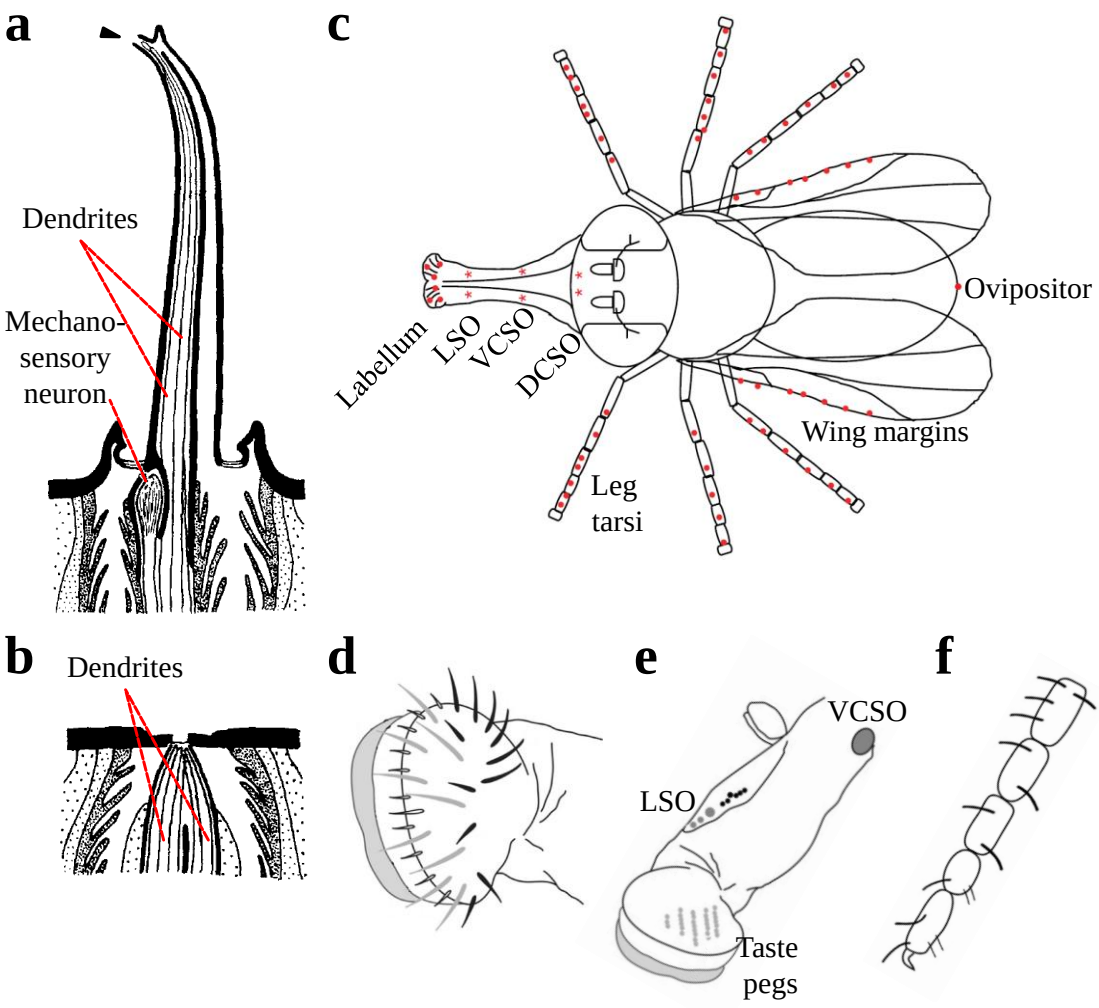

Figure 1: Taste sensilla and taste organs of *Drosophila*. (a-b) Structure of a labellar taste hair (a) and a LSO taste peg (b). Taste cells project dendrites into the hollow interiors of these structures. Taste hairs and taste pegs possess a terminal pore (arrowhead in (a)) through which chemicals can enter. (c) Schematic of the taste organs of *Drosophila*. External organs are indicated with red circles; internal organs are indicated with red asterisks. (d) Schematic of the labellum, indicating the position of the 31 taste hairs in each lobe. Taste hairs are categorized into long, intermediate and short, indicated in gray, black and white respectively. (e) Schematic of the proboscis, indicating the position of the taste pegs, LSO and VCSO, which are internal taste organs. (f) Schematic of the five tarsi of a female *Drosophila* foreleg, indicating the position of taste hairs. Most taste hairs exist in pairs. (LSO labral sense organ; VCSO ventral cibarial sense organ; DCSO dorsal cibarial sense organ. Modified from[6, 11, 67].

in the foreleg tarsi of female flies[11], a somewhat greater number than that in previous studies (Figure 1f)[12,13]. Interestingly, male forelegs contain more taste hairs than female forelegs[11,12,14], presumably because additional hairs are involved in pheromone detection, which is important for

courtship[15]. Each wing also contains approximately 40 taste hairs positioned along its margins[6]. Finally, approximately 13 putative taste hairs are found on the female ovipositor[6].

1.2.2. Structure of taste sensilla

Taste sensilla are hollow structures innervated by taste cells (Figure 1a, b). Unlike mammals, where tastants are sensed by modified epithelial cells, *Drosophila* taste cells are neurons[5,16]. *Drosophila* gustatory receptor neurons (GRNs) extend dendrites towards the hollow interior of the sensillum, have cell bodies in the periphery and project axons towards the central nervous system (CNS)[6]. Tastants can enter the sensillum through a pore at its tip and are dissolved in the hemolymph that fills it, which enables detection by GRNs. Most taste hairs in the labellum, legs and wings are innervated by four GRNs and a mechanosensory neuron that sits at the base of the taste hair[6,17]. These cells express taste receptors tuned to a specific taste quality in a mostly non-overlapping manner, an observation in line with taste hair recording studies (see section 1.3).

1.2.3. Projections of gustatory receptor neurons to the central nervous system

GRN axons bundle according to taste organ to form distinct nerves (Figure 2a). Labellar GRN projections bundle with axons from olfactory receptor neurons (ORNs) in the maxillary palps to form the labial nerves, while pharyngeal GRNs project to the brain via the pharyngeal/accessory pharyngeal nerves[51,60,62]. All GRN projections from the proboscis terminate in a specific area of the fly brain, called the gnathal ganglia (GNG)[18], but also known as the suboesophageal ganglion (SOG/SEG)[6,8,19-22] (Figure 2a-c). Because most GRN projections terminate in this area, the GNG are thought to be the taste center of the insect brain[21]. These

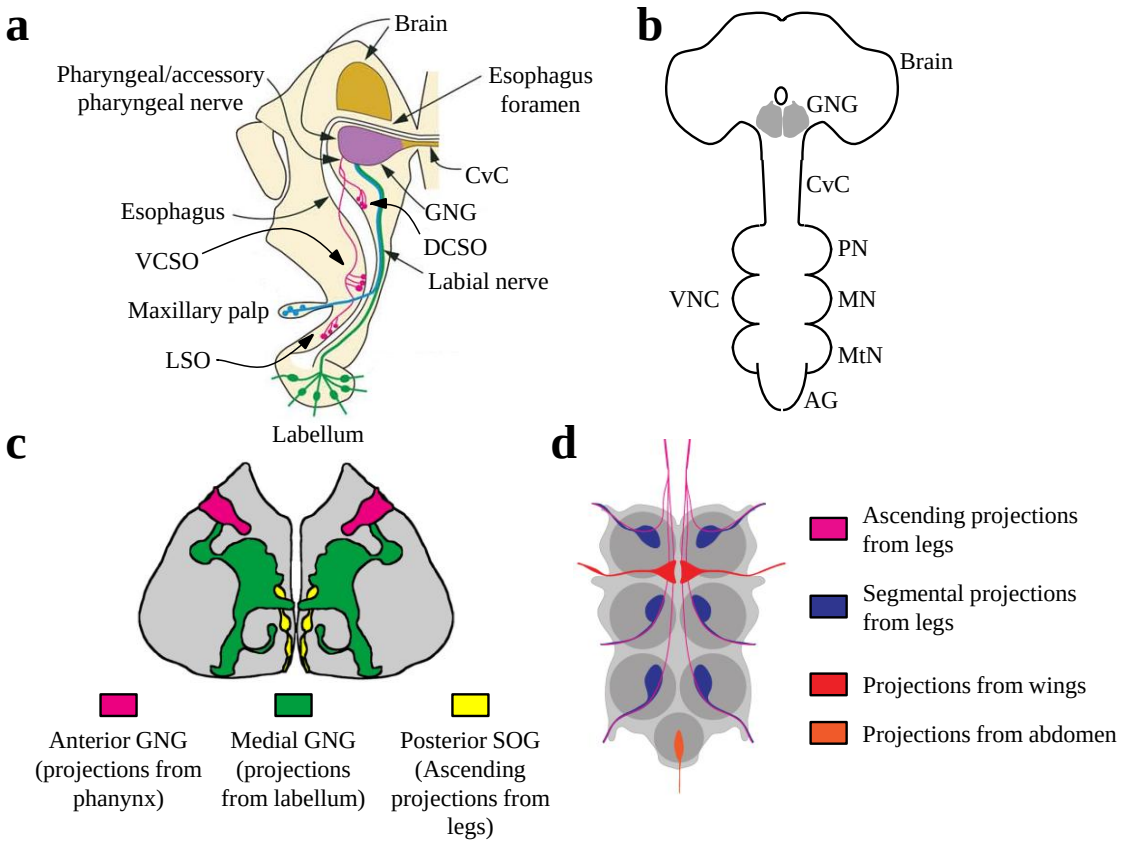

Figure 2: Projections of gustatory receptor neurons to the central nervous system. (a) Schematic of *Drosophila* head. Cephalic taste organs and their projections to the brain are indicated. Axonal projections from gustatory receptor neurons form distinct nerves, some of which project to the gnathal ganglia in the brain. (b) Schematic of the *Drosophila* central nervous system. The gnathal ganglia, thought to be the 'taste center' of the fly brain, are shown in gray. (c) Projections from different taste organs innervate distinct regions of the gnathal ganglia. Here, projections from sweet taste receptor neurons are shown. (d) Projections from different non-cephalic taste organs have distinct innervations patterns in the ventral nerve cord. LSO labral sense organ; VCSO ventral cibarial sense organ; DCSO dorsal cibarial sense organ; GNG gnathal ganglia; CvC cervical connective; VNC ventral nerve cord; PN prothoracic ganglia; MN mesothoracic ganglia; MtN metathoracic ganglia; AG abdominal ganglion. Adapted from[21, 87].

nerves terminate in discrete areas of the GNG: the pharyngeal/accessory pharyngeal nerves project to the anterodorsal GNG, while the labial nerves project more medially (Figure 2c).

GRNs from the legs project to the ventral nerve cord (VNC), according to leg position: neurons from fore-, mid- and hindlegs project to the pro-, meso- or metathoracic ganglia (PN, MN, MtN), respectively (Figure 2b, d). Interestingly, some leg GRNs terminate in the VNC,

while others continue through the cervical connective (CvC) and terminate in the GNG[6,8,19-22]. Brain-projecting GRNs in the legs terminate in the posterior GNG (Figure 2a, c).

1.3. Functions of the *Drosophila* taste system

Two opposing models can be used to explain taste coding in the brain: the labeled line model and the across-fiber model. In the labeled line model, sensory cells respond to specific taste qualities and transmit information directly to the brain. In the across-fiber model, taste cells differentially respond to multiple taste qualities, with downstream neurons ultimately separating the different qualities. Behavioral, physiological and anatomical data demonstrate that *Drosophila* makes use of a labeled line model to code for stimuli of opposing valence[5]. However, some taste qualities of same valence can be detected by overlapping sets of GRNs. For example, sweet GRNs are required for acceptance of fatty acids[23] and some respond to low concentrations of salt[24], whereas bitter taste cells also respond to high concentrations of salts[24]. Nevertheless, representations of appetitive and aversive substances are completely separated.

With regards to behavior, the *Drosophila* taste system has been most studied for its role in feeding. Hungry flies typically extend their proboscises when appetitive stimuli are applied on their tarsi or labella, a response suppressed by the inclusion of aversive substances[25]. This robust behavioral response, called the proboscis extension reflex (PER), provides an easy readout of taste-driven behavior. However, the detailed ethology of fly feeding remains less explored (Figure 3). Food elicits multiple behaviors that appear to be sequentially organized: stimulation of leg GRNs triggers proboscis extension, followed by stimulation of labellar GRNs; consequently, opening of the labellum exposes the taste pegs and ingestion is initiated (Figure

3b, c). Pharyngeal GRNs may monitor food quality during ingestion[26]. However, feeding does not strictly adhere to this hierarchical organization, since labellar stimulation also elicits PER[25] and since spontaneous PER/ingestion can occur without taste hairs in the labellum/legs, albeit with lower frequency[27].

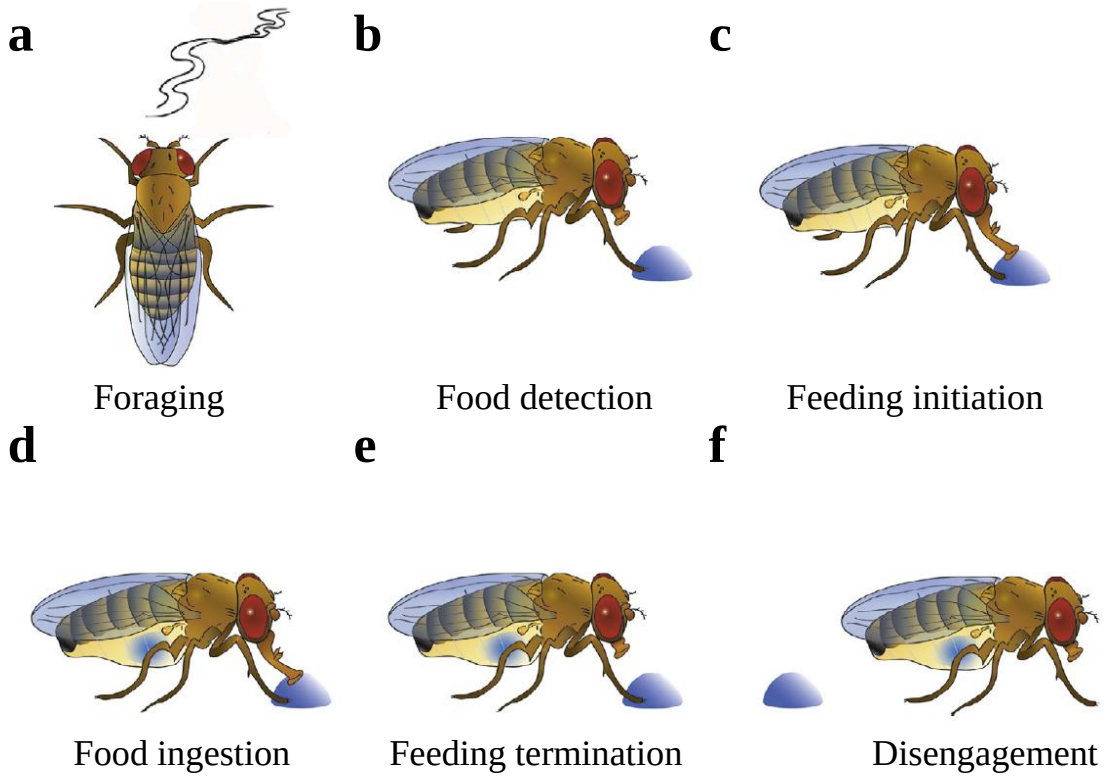

Figure 3: Feeding behavior of *Drosophila*. (a) Foraging relies on taste, but also other sensory modalities (e.g. olfaction) that may guide flies to a potential food source. (b) Initial contact with an acceptable food source, presumably with the legs, triggers early appetitive responses, such as locomotion arrest, lowering of posture and extension of the proboscis. (c) Extension of the proboscis allows feeding initiation. The labial palps open and food sucking commences. Taste receptor neurons in the labellum may play a role in feeding during this stage. (d) Food ingestion proceeds until the fly is satiated. Internal taste organs located in the pharynx are important for sustained feeding at this stage. (e) Feeding is terminated by retraction of the proboscis when the fly is satiated and eventually the fly disengages (f). Modified from[28].

Early electrophysiological studies took advantage of the accessibility of labellar taste hairs to show that they contain up to four functionally distinct taste cells: one that responds to sugars (S cell), one that responds to water (W cell), one that responds to low concentrations of

salt (L1 cell) and one that responds to bitter substances and high concentrations of salt (L2 cell) (reviewed in[29]). Later studies showed that this functional specialization is owed to a largely non-overlapping expression of receptors tuned to different taste qualities[8,22,30,31]. Taste receptors of *Drosophila* are discussed in greated detail below.

1.3.1. Taste receptors in mammals and Drosophila

Although mammals and fruit flies can perceive similar taste qualities, their taste receptors are not structurally related. In mammals, G protein-coupled receptors (GPCRs) are involved in the perception of bitter, sweet and umami taste qualities (Figure 4a-c). Bitter tastants are detected by a family of T2R receptors[32], sweet tastants are detected by the T1R2-T1R3 heterodimer[16] and umami tastants are detected by the T1R1-T1R3 heterodimer[33] and metabotropic glutamate receptors[34,35]. In insects, the most intensely studied taste receptors are the so-called gustatory receptors (GRs)[36], a family of 68 seven transmembrane domain (7TM) proteins related to olfactory receptors[37] that differ from GPCRs[38] (Figure 4a-c). Other genes have also been shown to encode taste receptors in *Drosophila*; these include ionotropic receptors (IRs; Figure 4d)[39], pickpocket (ppk) channels (Figure 4e)[15,30,40-44] and transient receptor potential (TRP) channels[45-47] (Figure 4c). These genes have diverse functions, often not limited to taste. Their roles in taste perception are discussed below, with particular emphasis to their ligands, structure and function.

1.3.2. Drosophila gustatory receptors in taste perception

The largest and best understood family of *Drosophila* taste receptors is the GRs (Figure 4f). GRs are functionally diverse: while most are involved in sensing basic taste qualities, they also include two olfactory receptors[48,49], a heat sensor[50] and a potential light sensor in larvae[51].

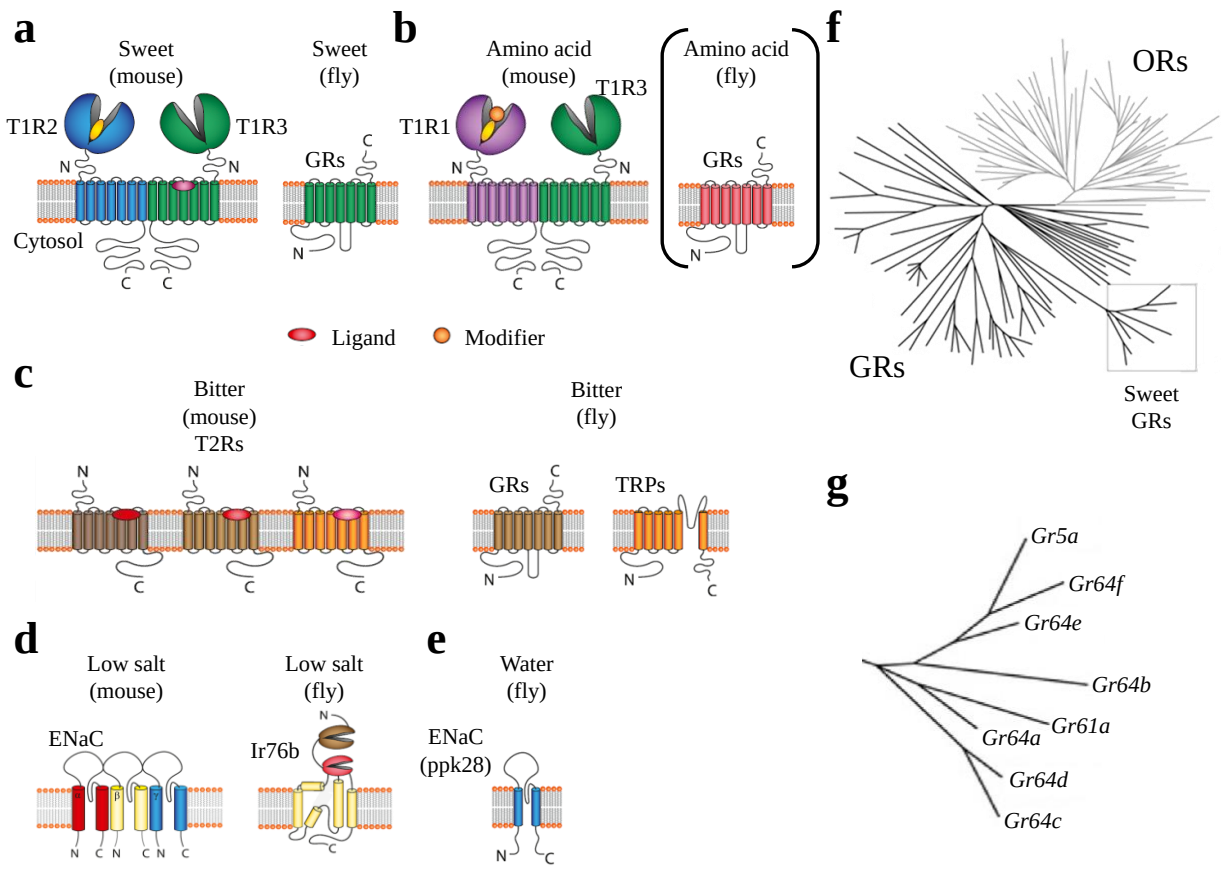

Figure 4: Taste receptors in the mouse and fly. (a) Sweet taste receptors. (b) Amino acid taste receptors. (c) Bitter taste receptors. (d) Low salt concentration taste receptors. (e) Water taste receptor. (f) Phylogenetic tree of fly chemoreceptors. A family of sweet taste receptors is indicated with a box. (e) Blow-up of box in (f). TR taste receptor; GR gustatory receptor; ENaC epithelial sodium channel; IR ionotropic receptor; ppk pickpocket channel. (a-e) modified from[5]; (f-g) modified from[19].

The first GR linked to taste was *Gr5a*, which codes for a receptor for trehalose[52-54] (a yeast sugar). Seven more GRs share sequence similarity with *Gr5a*: *Gr61a* and the six members of the *Gr64* cluster (*Gr64a-f*) (Figure 4g)[19]. Further characterization of these GRs revealed that most are tuned to subsets of sweet substances: *Gr5a* is not only required for trehalose, but also other sugars, including glucose[19]; *Gr61a* is tuned to glucose[55], *Gr64a* to sucrose, maltose and other sugars[19,56] and *Gr64e* to glycerol, which is not a sugar but nevertheless is attractive to flies[57]. *Gr64f* is required for sensing trehalose and is needed in combination with *Gr64a* for behavioral and physiological responses to sucrose, maltose and glucose[58]. The functions of

Gr64b, *Gr64c* and *Gr64d* remain unknown. *Gr43a*, a more distantly related GR, is a fructose receptor[59]. It is worth noting that findings from different laboratories are occasionally contradictory, suggesting that conclusions also depend on the specific mutants and methodologies used in the studies. For example, *Gr64f* was proposed as a sugar co-receptor because: (1) it has the broadest expression pattern[19], (2) responses to trehalose are abolished in *ΔGr64* mutants[60] and reduced upon *Gr64f* knock-down[58] and (3) the impaired responses to sucrose, maltose and glucose in *ΔGr64* flies are fully rescued only upon introduction of both *Gr64a* and *Gr64f*[58]. However, a recent study questions this conclusion by showing that ectopic expression of individual sweet GRs in olfactory neurons confers robust responses to sugars, and that expression of sweet GR combinations does not result in an increase in responses[61]. The authors of this latter study suggest that *Gr5a* and *Gr64a* are the main sweet GRs of *Drosophila*, because: (1) they are necessary and sufficient for behavioral and physiological responses to distinct, but complementary sets of sugars[19,61] and (2) eliminating both GR genes results in sugar-blind flies[19]. Nevertheless, this conclusion is controversial, because a different *Gr64a* mutant did not show any behavioral defect when the labellum was stimulated with sugars[62]. In line with this, a *Gr64a-GAL4* knock-in line lacks expression in the labellum. Fujii *et al.* speculate that such inconsistencies can be attributed to technical limitations in the *Gr64* family mutants. Taken together, these findings suggest that sweet GRs and their ligands do not share a simple one-to-one relationship; instead, responses to most sugars are influenced by multiple sweet GRs.

The majority of GRs are thought to be bitter taste receptors. The function of only a few bitter GRs has been addressed directly. The emerging picture is that, like sugar GRs, bitter substances recruit multiple bitter GRs to elicit behavioral and physiological responses. For example, responses to caffeine require *Gr33a*[63], *Gr66a*[64] and *Gr93a*[65]. Similarly, taste responses

to the insect repellant *N*, *N*-diethyl-*m*-toluamide (DEET) require *Gr32a*, *Gr33a* and *Gr66a*[66]. Other bitter GRs, such as *Gr47a* (a strychnine receptor), may be more specialized[67]. These receptors are necessary but not sufficient for responses to bitter compounds, suggesting that they function as multimeric complexes[63-65]. A systematic analysis of bitter GRs used *Gr-GAL4* lines to infer that 33 GRs are co-expressed with previously identified, broadly expressed bitter GRs such as *Gr32a*, *Gr33a* and *Gr66a*[68]. Together with *Gr39a.a* and *Gr89a*, these five GRs are expressed in all bitter-responsive taste hairs of the labellum and are therefore thought to constitute the 'core' bitter GRs. Interestingly, labellar taste hairs differ in their physiological responses to bitter chemicals, and these differences correlate with differential expression of non-core bitter GRs. Therefore, it is thought that expression of specific combinations of bitter GRs underlies the functional diversity of *Drosophila* taste hairs. Additionally, a few bitter GRs may also function as pheromone receptors, as they are involved in courtship behavior[63,69-73].

Amino acid taste perception is poorly understood in *Drosophila*, despite some systematic efforts to identify the genes involved[74]. Only one receptor, *Gr8a*, has been implicated in amino acid taste perception[75]. However, *Gr8a* is involved in the avoidance of L-canavanine, a toxic analogue of L-arginine, and is expressed in bitter GRNs. The receptors involved in the detection of more typical amino acids are unknown. A subset of sugar-responsive taste hairs in the labellum showed no responses to 18 common amino acids[19]. Nevertheless, flies can show preference to amino acids and this preference increases with several days of amino acid deprivation[76]. Interestingly, only amino acid deprived flies show PER following labellar (but not tarsal) stimulation[76]. These results suggest that amino acid receptors may reside in the proboscis, most likely in the taste pegs and pharyngeal organs.

1.3.3. Drosophila ionotropic receptors in taste perception

Drosophila IRs are a family distantly related to ionotropic glutamate receptors that participate in chemosensation[77]. A sub-family of 35 genes, the IR20a clade, contains 16 genes that are thought to be expressed in one or multiple *Drosophila* taste organs[39]. Interestingly, some of those appear to be co-expressed with sugar or bitter GRs, but not both, suggesting that they can mediate acceptance or rejection to specific compounds. Some members of the IR20a clade are not co-expressed with GRs; these include the sexually dimorphic *Ir52c* and *Ir52d*. Mutants for these receptors show delayed copulation, demonstrating a role in courtship that is fully consistent with anatomical data[39]. Other IRs that are not members of the IR20a claude may also be expressed in both olfactory and taste organs[78]. Of those, *Ir76b* is required for the detection of low concentrations of salt, which promote food acceptance (Figure 4d)[31]. Deletion of *Ir76b* eliminates attraction to low salt concentrations, but does not affect avoidance to high salt concentrations, suggesting that the 'high salt' receptor is different. Interestingly, comparison of *Ir76b-QF* and *Gr5a-GAL4*, which label the 'low salt' and sweet GRNs respectively, did not reveal co-expression in the labellum, indicating the existence of independent sensory pathways mediating acceptance in *Drosophila*.

1.3.4. Drosophila pickpocket channels in taste perception

Drosophila ppk genes encode degenerin/epithelial Na^+ channels that have been shown to participate in taste perception of water, salt and pheromones. *ppk28* has been shown to be necessary and sufficient for physiological responses to low osmolarity solutions (Figure 4e)[30,41]. Additionally, mutant flies show decreased drinking time and impaired PER with water, but not with sugar solution. *ppk28* is not co-expressed with *Gr5a-GAL4*, indicating that, like low salt

concentrations, it mediates acceptance through a separate pathway. In larvae, *ppk11* and *ppk19* are required for the behavioral preference to low NaCl concentrations, but not for the avoidance of high concentrations[42]. Curiously, in adults the same genes are required for the avoidance of high salt concentrations[42]. A more recent study found that *ppk19* plays a role in choice behavior of larvae for both low and high salt concentrations and identified a non-related gene, *serrano*, as important for the avoidance of high salt concentrations[40]. Finally, *ppk23*[15,43,44], *ppk25*[79,80] and *ppk29*[15] are involved in the courtship behavior of male flies. *ppk23* and *ppk29* are expressed in cells that are mostly different from sweet, bitter or water neurons[15]. While *ppk23* and *ppk29* are expressed in both labellum and leg GRNs, only the latter are involved in courtship. Nevertheless, these genes are probably not pheromone receptor genes, because: (1) ectopic *ppk23*/*ppk29* expression in 'empty' water neurons does not confer sensitivity to pheromones and (2) in pheromone-sensitive leg taste hairs, *ppk23-GAL4* labels two cells, but only one responds to male pheromones, whereas the other responds to female pheromones, suggesting that this specificity is imparted by a different protein.

1.3.5. Drosophila transient receptor potential channels in taste perception

The taste of pungent chemicals, such as isothiocyanates (present in wasabi and mustard) and a few other aversive compounds depends on transient receptor potential (TRP) channels. These channels are necessary and sufficient for aversive responses to specific chemicals: *painless* for isothiocyanates[45], d*TrpA1* for isothiocyanates[81] and aristolochic acid[46] (a toxic anti-feedant) and *TRP*-like (*TRPL*) for camphor[47] (an aversive but non-toxic terpenoid). These genes are mostly expressed in sets of bitter GRNs but not required for aversion of other bitter

compounds. Therefore, distinct receptors and/or pathways exist in the same cells for detection of different aversive tastants.

1.3.6. Taste information processing in sensory neurons

Segregated representation of taste qualities of opposing valence by non-overlapping GRNs is thought to be one of the mechanisms underlying food acceptance and rejection[8,22]. However, the *Drosophila* taste system can also control feeding via other mechanisms. Bitter substances recruit a dual pathway by not only activating bitter GRNs, but also by inhibiting sweet and water GRNs[82]. Bitter GRNs are thought to indirectly inhibit sweet GRNs via GABA (γ-aminobutiric acid) interneurons[83]. Interestingly, flies lacking bitter GRN function can still avoid bitter substances. This latter pathway is thought to involve binding of bitter substances to odorant-binding proteins, which are expressed in taste organs, and direct inhibition of sweet GRNs through them[84-86]. A similar mechanism underlies aversive responses to acids. While *Drosophila* lacks a dedicated 'sour cell', acids can activate bitter GRNs and inhibit sweet GRNs via as yet unidentified receptors and mechanisms[87].

GRN projections in the brain are segregated based on taste quality: sweet taste cells from the labellum have more lateral and anterior projections in the GNG than projections from labellar bitter cells[8,22,88,89] (Figure 5). This spatial segregation suggests that the sweet and bitter taste pathways recruit different downstream neurons to elicit acceptance and rejection, an idea consistent with large-scale functional imaging data[90]. However, GRNs tuned to the same quality also project to spatially segregated regions in the CNS, depending on taste organ (see also section 1.2.3 and Figure 2). Taken together, these observations suggest that flies may be able to differentially process gustatory information depending on stimulus location and produce

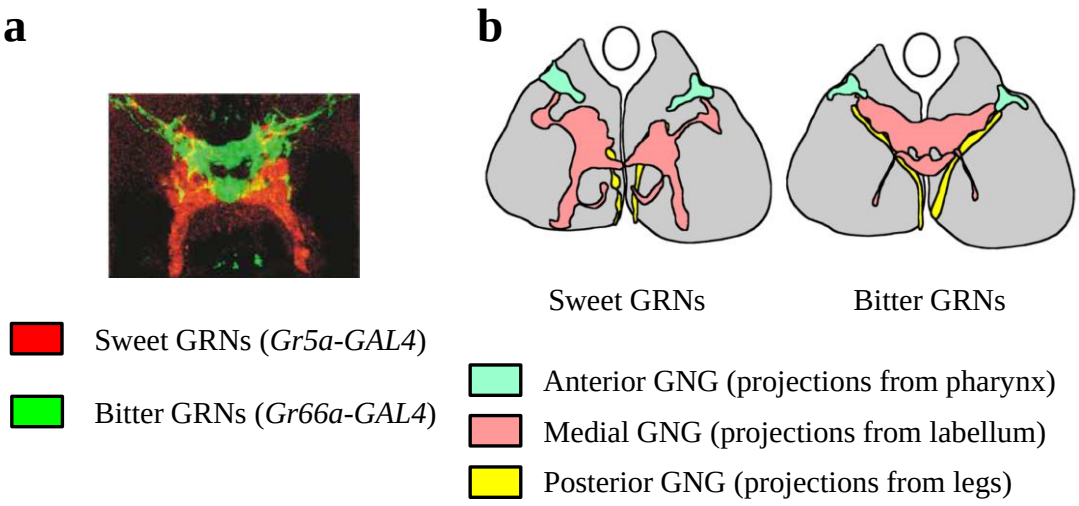

Figure 5: Projections of gustatory receptor neurons are segregated based on taste quality. (a) Overlay of sweet (red) and bitter (green) gustatory receptor neuron projections (labeled by *Gr5a-GAL4* and *Gr66a-GAL4*, respectively) in the gnathal ganglia. From[22]. (b) Schematics of sweet (left) and bitter (right) gustatory receptor neuron projections in the gnathal ganglia. Sweet neurons from the labellum (pink) project more laterally than bitter neurons from the labellum. From[87]. GRNs gustatory receptor neurons; GNG gnathal ganglia.

different behavioral output for the same stimulus[22,88]. In line with this, different subsets of bitter GRNs underlie different functions: bitter cells in the legs are required for aversion to a bitter substance, while pharyngeal bitter cells are needed for female flies' egg laying preference on the same bitter substance[91].

1.3.7. Coordination of feeding behavior

Feeding behavior requires the simultaneous inhibition of competing behavior, such as locomotion. In the larva, activation of a cluster of 20 interneurons expressing the neuropeptide hugin simultaneously suppresses feeding and promotes locomotion. The precise neuronal mechanism by which opposite regulation of these mutually exclusive behaviors occurs is not fully understood. However, hugin cells were proposed to input into two distinct central pattern generators (CPGs), one for feeding-related motor programs and another for locomotion, thereby coordinating their activities[92]. In adult flies, proboscis extension inhibits locomotion. Inhibition

of proboscis extension during movement may involve a pair of VNC interneurons called PER_{in}. These neurons receive mechanosensory input from the legs, presumably transmitted during walking, and are necessary and sufficient for PER inhibition[93].

1.3.8. Functions of 'atypical' taste organs

GRNs in the wings and ovipositor do not typically come into contact with food and have not been implicated in feeding so far. The ovipositor of moths was found to contain taste hairs sensitive to sucrose and fructose, which correlates with these animals' preference to lay eggs in media containing these sugars[94]. It has been speculated that GRNs in the *Drosophila* ovipositor may also be involved in the selection of egg-laying sites[95], but this has not been demonstrated yet. Wing GRNs are important for grooming. These cells are necessary for grooming behavior induced by stimulating the wing margins in decapitated flies. Additionally, optogenetic activation of bitter cells in decapitated flies is sufficient to induce this behavior[96].

1.3.9. Role of taste in courtship behavior

Courtship involves physical contact between the male forelegs or labellum and the female abdomen, behaviors known as 'tapping' and 'licking', respectively[97]. Several bitter GRs are involved in cuticular pheromone perception and are required for suppression of male-male courtship[63,71,72]. One of these GRs, *Gr32a*, is also required for suppression of courtship towards other fruit fly species[69] and is involved in unilateral wing extension during courtship[70]. Two other GRs, *Gr39a*[73] and *Gr68a*[98], are required for male-female courtship. Three pickpocket channels, *ppk23*[15,43,44], *ppk25*[79,80] and *ppk29*[15] are involved in promoting courtship towards females and/or inhibiting courtship towards males. The actual pheromone receptors are probably

heteromeric complexes with additional proteins[15,99]. Receptors *Ir52c* and *Ir52d* are also involved in courtship[39]. Interestingly, these two IRs are expressed in dorsal taste hairs of the forelegs; the same is true of channels *ppk23*[44] and *ppk25*[80]. Dorsal taste hairs are unlikely to contact potential food when walking, but tapping of the female abdomen during courtship occurs with the dorsal male foreleg, making these taste hairs optimally positioned for detecting female pheromones[39].

1.4. Taste processing in the *Drosophila* central nervous system

While taste perception by peripheral sensory neurons is well understood, relatively less is known about processing of taste information in the brain. Anatomical and functional GAL4 screens are a popular strategy for discovering higher-order taste neurons, often with single-cell resolution[93,100-104]. However, this unbiased approach typically results in a very fragmented view of the fly taste circuit, as the neuronal contexts and connectivity of circuit components can be difficult to appreciate. Alternatively, hypothesis-driven approaches[105,106] can uncover the function of specific taste circuit components, but these have so far been restricted to neurons near the input or output sites. Finally, global approaches are useful for demonstrating principles of taste coding in the brain. For example, a recent large-scale functional imaging study revealed that tastant responses are mostly segregated in the brain[90]. However, this approach does not address the behavioral relevance of specific circuit components. This section will focus on three aspects of taste processing in the brain that are relatively well-understood, namely: (1) modulation of taste neurons by starvation; (2) motor neurons involved in feeding behaviors and (3) taste circuits for associative learning.

1.4.1. Modulation of sweet taste neurons by starvation

Internal state can affect feeding behavior. The best understood example is starvation, which regulates the expression of appetitive behaviors such as PER[25]. The mechanism by which this is accomplished involves starvation-dependent modulation of sensory[106,107] and higher-order[100,102] sweet taste neurons. A single ventral unpaired median dopaminergic neuron with a cell body and broad arborizations in the GNG, called TH-VUM, mediates starvation modulation. TH-VUM shows increased activity upon starvation and manipulating its activity changes PER probability[106]. While it is not clear if TH-VUM and sweet GRNs form synapses[106], dopamine (DA) release on GRNs increases during starvation, while a DA receptor in sweet GRNs is necessary and sufficient for the starvation-dependent increase in PER probability[107]. Therefore, it is likely that DA release through TH-VUM decreases the sugar threshold of sweet GRNs. The activity of a paired second-order taste neuron[102] and a paired feeding 'command' neuron[100] were also reported to be positively modulated by starvation. In the case of the former neurons, feeding flies the DA precursor L-3, 4-dihydroxyphenylalanine (L-DOPA) increases the response, indicating that DA is also involved[102]. Taken together, these results suggest that DA modulation in the sweet taste circuit may be the mechanism underlying starvation-dependent control of feeding initiation.

1.4.2. Motor neurons controlling feeding behaviors

The motor neurons underlying some feeding behaviors are also understood. A paired motor neuron in the GNG is necessary for proper execution of the PER motor program, while its activation is sufficient for eliciting PER[101]. This motor neuron pair does not contact sweet GRNs labeled by a *Gr5a* line, suggesting that PER is not a monosynaptic reflex. However, PER is only

the first step of feeding. Ingestion of food requires the function of a pump inside the proboscis, in a compartment called the cibarium. This cibarial pump draws liquid food through the fly's proboscis and propels it toward its esophagus. Proper function of this pump requires the coordinated function of two distinct populations of motor neurons[105]. The action of one population leads to expansion of the cibarium, drawing liquid within it. Consequently, the action of the other population propels the liquid from the cibarium to the esophagus. Coordinated activity in these two populations is likely controlled by an upstream central pattern generator, which may receive feedback from the motor neurons themselves.

1.4.3. Taste circuits for associative learning

Sugar can be associated with odors[108] or visual cues[109] to drive the formation of appetitive memories. The mushroom body (MB) is the brain center where the unconditioned stimulus (US; sugar) and conditioned stimulus (CS; e.g. odor, color) are associated[110,111]. The pathways transmitting sweet taste information to the brain are the subject of intensive study. In sugar-odor conditioning with bees, activation of a ventral unpaired median neuron, VUMmx1, can substitute for the sugar reward[112]. This neuron is octopaminergic[113]. Additionally, injection of octopamine (OA) near the VUMmx1-MB calyx or VUMmx1-antennal lobe convergence sites can substitute for the sugar reward[114]. OA is also important for odor-sugar learning in *Drosophila*[115]. *Drosophila* also has OA neurons anatomically similar to VUMmx1[116], which could transmit sugar information. Interestingly, dopamine (DA) also plays a role in sugar-odor learning. A group of DAergic neurons in the protocerebral anterior medial (PAM) cluster is necessary and sufficient for memory and transmits sugar information through DA receptors expressed in the MB[117]. The current view is that sugar information is transmitted through

OAergic neurons towards subsets of PAM neurons, which in turn convey it to the MB[117,118]. Interestingly, flies can learn the sweet taste and nutritive value of sugars separately, with sweet taste driving the formation of robust short-term memory, but weak long-term memory[119,120]. Sweet taste is conveyed by OAergic neurons[118], while two distinct subsets of PAM neurons convey the sweet taste and nutritional information to the MB[121]. Water can also act as a reward in olfactory conditioning and is conveyed to the MB via a subset of PAM neurons[122].

Bitter taste can drive the formation of aversive memories. For example, hungry flies can learn to suppress PER to sugar, when sugar presentation on the legs (the CS) is paired with application of a bitter chemical on the proboscis (the US)[123]. The MB is required for this aversive taste memory[124,125]. A distinct subset of DA neurons, the paired posterior lateral 1 cluster (PPL1) innervates the MB, responds to bitter tastants (but not sweet) and is necessary and sufficient for conditioned PER suppression[124,125]. In the MB calyx, tastants within the same taste quality activate largely overlapping populations of cells, whereas different taste qualities are mostly separated[124]. Overlapping representations in the MB may explain why flies show a limited ability to distinguish stimuli representing the same taste quality[126].

1.5. *Drosophila* as a model organism

1.5.1. General advantages of Drosophila

The pioneering work of Thomas Hunt Morgan has contributed to establishing *Drosophila melanogaster* as an important model organism in the 20th century, particularly in the field of genetics. In more recent years, *Drosophila* has proved to be a useful model organism for understanding the molecular and neuronal basis of behavior[127]. Fruit flies have basic advantages

such as a short life cycle, an ability to produce many offspring, low cost and ease of maintenance. Moreover, their CNS is numerically simpler than that of mammals, as it only contains an estimated 150000 neurons[128]. However, the most important advantage is its unparalleled genetic tractability[129]. Of particular interest for neuroscience, this includes genetic tools useful for characterizing the anatomy, physiological properties and behavioral function of neurons with excellent resolution[130]. For taste in particular, *Drosophila* is advantageous because: (1) like humans, it can perceive a similar set of taste qualities, suggesting that principles of taste coding discovered in the fly might apply to mammals; (2) unlike mammalian GRNs, *Drosophila* GRNs project directly to the CNS, making it easier to examine taste information coding in the brain[21] and (3) the taste center of the fly brain, the GNG, only contains 6000 neurons, roughly[106].

1.5.2. Genetic tools in Drosophila: GAL4/UAS system

The GAL4/UAS system is a popular method for targeting transgene expression to specific cells of the fruit fly (Figure 6a)[131]. This binary expression system consists of GAL4, a transcription factor from yeast, and an upstream activating sequence (UAS), to which GAL4 can bind. Binding of GAL4 to UAS activates transcription of the transgene placed downstream of this sequence. This transgene, often called the 'effector transgene', can encode any desirable RNA. Of particular use for behavioral analyses are effectors that can be used for activating or silencing neurons, while anatomical analyses rely on expression of green fluorescent protein (GFP) and its variants.

GAL4 expression is controlled by *cis* regulatory elements. For example, a promoter can be cloned and placed upstream of the GAL4-coding sequence to target cells expressing the promoter-associated gene. Using this 'promoter-fusion' strategy, the Carlson lab has generated

lines expressing GAL4 under the control of most GR promoters and confirmed that these direct expression to taste organs[68]. With this approach, GAL4 expression should recapitulate the gene expression pattern, but discrepancies might occur, especially if the cloned enhancer does not include all regulatory sequences[62]. Alternatively, GAL4 can be randomly integrated in the genome to target random subsets of cells. Transgenics generated in this way are called 'enhancer-trap' lines, because endogenous *Drosophila* enhancers are 'trapped' into driving GAL4 expression. Collections of enhancer-trap lines can be used for anatomical and/or

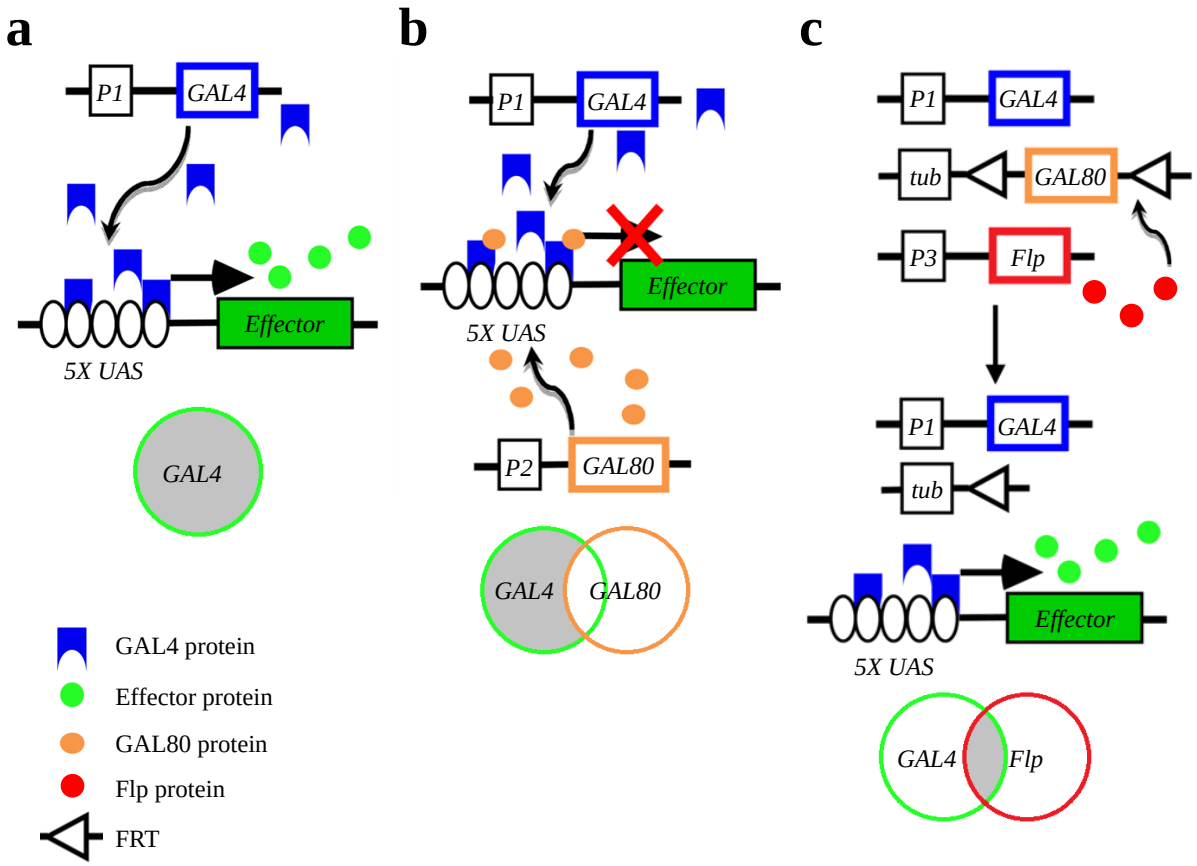

Figure 6: Examples of genetic tools in *Drosophila*. (a) Schematic of the GAL4/UAS system. Effector-expressing population indicated in gray. (b) Expression can be refined by introducing *GAL80*, which limits effector expression to the non-overlapping GAL4-expressing cells (gray in the Venn diagram). (c) Strategy for positive intersection between *GAL4* and *Flp*. Ubiquitously expressed GAL80 is eliminated only in the *Flp*-expressing cells, limiting transgene expression to the overlapping GAL4-expressing cells (gray in Venn diagram). *P1* promoter 1; *5X UAS* upstream activating sequence (5 copies); *P2* promoter 2; *tub* tubulin promoter; *P3* promoter 3; Flp flippase; FRT flippase recognition target. Modified from[129].

functional screens to discover cells of interest in an unbiased manner.

Popular effector transgenes for neuroethology include *UAS-Shibire^{ts1}* and *UAS-Kir2.1* for silencing neurons, as well as *UAS-TrpA1* and various *UAS-Channelrhodopsins* for activating them. *Shibire^{ts1}* (*Shi^{ts1}*) is a temperature-sensitive, dominant-negative allele of Dynamin, a protein required for vesicle recycling at presynapses. Therefore, neurons expressing *Shi^{ts1}* can be silenced by increasing the temperature, since vesicle recycling is blocked at higher temperatures, leading to their depletion[132]. On the other hand, Kir2.1 is a human inwardly rectifying potassium channel (fused to GFP). Expression of *Kir2.1* in neurons leads to membrane hyperpolarization, decreasing the probability of action potential generation and consequently neurotransmitter release[133]. Kir2.1 is complementary to Shi^{ts1}, as it can block neuronal communication through both chemical and electrical synapses. Conversely, the endogenous heat-activated TRP family ion channel TrpA1 can be used to activate neurons by mild elevation of the temperature[134]. Additionally, channelrhodopsins are light-gated ion channels from *Chlamydomonas* that, if expressed in neurons, can lead to depolarization upon exposure to light of appropriate wavelength[135]. Taken together, these tools allow conditional manipulation of neuronal subsets in intact, behaving animals.

1.5.3. Intersectional approaches and other binary expression systems

A problem with GAL4 lines is that they often label additional cells, besides those of interest. To address this caveat, complementary genetic tools can be used with GAL4/UAS. Such intersectional approaches can improve cellular resolution, in some cases allowing the manipulation of individual neurons. For example, GAL80, a protein that binds to GAL4 and blocks its ability to activate transcription, can be used to refine effector transgene expression

(Figure 6b)[136]. Additionally, recombinases like the yeast flippase (Flp) can be used with GAL4/UAS for positive or negative intersections. A strategy for positive intersections additionally relies in the presence of *GAL80* driven by a ubiquitous promoter (e.g. tubulin promoter, *tubP*) and flanked by flippase recognition target (FRT) sequences. Flp can therefore excise *GAL80*, leading to expression of the effector transgene only in cells that express both *GAL4* and *Flp* (Figure 6c). The Flp/FRT and GAL4/UAS systems can be used in combination to label cells in a stochastic[137] or deterministic[138] manner.

Other binary expression systems operate similarly to GAL4/UAS. These include the QF/QS[139] and LexA/LexAop[140] systems. Because QF/QS and LexA/LexAop are independent from GAL4/UAS (i.e. these systems do not interact), they can be used in combination, by having one of the former systems drive expression of a protein that influences GAL4/UAS. For example, LexA/LexAop can be used to drive GAL80 expression to refine a GAL4 line.

2. Materials and Methods

2.1. Fly strains

The following transgenic strains of *Drosophila melanogaster* in a w^{1118} background were used for crosses: *y w hsp70-flp; Sp/CyO; TM2/TM6b*[141], *UAS >CD2 y*$^{+}$ *>mCD8-GFP*[142] (original donor Gary Struhl), *w Gr5a-LexA; Bl/CyO; TM2/TM6b*[101], *w*; *LexAop-GAL80* in attP40 (gift from B. Pfeiffer and G. Rubin, Bloomington #32214), *w; Pin/CyO; UAS-mCD8::GFP*[136], *w;; UAS-Kir2.1::eGFP*[133], *y w LexAop-mCD8::GFP UAS-mCD8::RFP*[143] (gift from B. Pfeiffer and G. Rubin, Bloomington #32229), *w; UAS-mCD8::RFP* (gift from Ilona Kadow), *w;; LexAop-rCD2::GFP*[59], *w; otd-nls-FLPo*[144], *w; Bl/CyO; tub>GAL80>* (Bloomington #38881), *w*; *Gr5a-GAL4/CyO; Dr/TM3*[68], *w*; *Sp/CyO*; *Gr43a-GAL4/TM3*[68], *w; Gr43a-GAL4*[59], *w*; *Gr61a-GAL4/CyO; Dr/TM3*[68], *w*; *Sp/CyO*; *Gr64a-GAL4/TM3*[68], *w*; *Sp/CyO*; *Gr64c-GAL4/TM3*[68], *w*; *Sp/CyO*; *Gr64d-GAL4/TM3*[68], *w*; *Gr64e-GAL4/CyO; Dr/TM3*[68], *w*; *Gr64f-GAL4/CyO; MKRS/TM2*[68], *w;; Gr64f-LexA*[59], *w;; UAS-Shibire*^{ts1} [132] and *white* (w^{1118}). Enhancer-trap GAL4 lines from the Nippon Project collection (*NP-GAL4*s) were ordered from the *Drosophila* Genetic Resource Collection (DGRC) in Kyoto, Japan[145]. Canton S flies were used as the wild-type strain, but the appropriate generic controls (in w^{1118} background) were used for comparisons with experimental groups. Most flies were kept at 25 °C and 60% relative humidity on standard cornmeal medium under a 14 h/10 h light/dark cycle. Only the *NP-GAL4* crosses to *UAS-Shibire*^{ts1} were kept at 18 °C.

2.2. Immunohistochemistry and anatomical analysis

Brains, VNCs, proventriculi, uteri and proboscises of 2-8 d adult female *Drosophila* were dissected as previously described[146], fixed for 45 minutes at room temperature in 4% formaldehyde in phosphate-buffered saline (PBS) with 0.1% Triton X-100 (PBS-Tx), washed with 0.1% PBS-Tx and stained using antiserum to GFP (rabbit, 1:1000, Invitrogen, or rat monoclonal 3H9, 1:100, Chromotek) and RFP (rabbit, 1:100, Clontech). Fixation and immunostaining were avoided for forelegs and some proboscis samples (Figures 16 and 18); these were imaged immediately after dissection. To visualize synaptic neuropil regions, mouse monoclonal antibody for Synapsin[147] (1:100, Developmental Studies Hybridoma Bank; Iowa City, IA) or rat monoclonal antibody for N-Cad (1:100, Developmental Studies Hybridoma Bank; Iowa City, IA) were used. For detection of primary antisera, Alexa 488-tagged goat anti-rabbit (1:1000, Invitrogen), Alexa 488-tagged goat anti-rat (1:200, Invitrogen), Cy3-tagged goat anti-mouse (1:250, Jackson Immunoresearch), Cy3-tagged goat anti-rabbit (1:250, Jackson Immunoresearch), Cy3-tagged goat anti-rat (1:200, Jackson Immunoresearch) and Alexa 633-tagged goat anti-mouse antisera (1:250, Invitrogen) were used. Preparations were mounted in Vectashield (Vector; Burlingame, CA), 70% glycerol in PBS or 70% 2, 2-thiodiethanol in PBS, and imaged with either an Olympus FV-1000 (brains and VNCs) or a Zeiss LSM 780 confocal microscope including a T-PMT device (transmitted light detector for bright field images, for some tarsi and proboscises). All images were processed using Fiji software[148]. For the *NP-GAL4* lines, analysis of expression was followed by image registration, performed as described elsewhere[149].

2.3. Generation of single-cell flp-outs

To generate single-cell flp-outs, freshly eclosed flies carrying *hsp70-flp, UAS >CD2 y^+ >mCD8-GFP and Gr64f-GAL4* were heat-shocked in a 37 ^oC water bath for 30 min and dissected 4-5 days later.

2.4. Behavioral experiments

For the *Gr-GAL4* experiments, genetic crosses were raised at 25 °C. F1 progeny were transferred to fresh food vials and were allowed to feed for at least 24 h prior to starvation. Flies were subsequently starved in moistened vials until a mortality rate of roughly 20% was achieved. As different genotypes vary in starvation resistance, average starvation times ranged between 31-49 h. All flies were 3-7 days old at the time of the experiment. Testing times were distributed throughout the day to minimize effects of circadian rhythm on performance. Behavioral experiments were performed at 25.0 ± 0.3 °C and 60-70% relative humidity.

For the *NP-GAL4* experiments, driver lines that bore P-element insertions on the second or third chromosomes, were homozygous-viable, had readily apparent markers, showed specific expression patterns and bore viable progeny when crossed to *UAS-Shi^{ts1}* were selected. The crosses with *UAS-Shi^{ts1}* were raised at 18 °C to minimize the effects of *Shi^{ts1}* expression during development. Their F1 progeny were transferred to 25 °C 0-3 days after eclosion and kept on fresh food for 5-7 days prior to starvation in order to boost *Shi^{ts1}* expression. Starvation was carried out as above, with starvation times adjusted to allow a minimum of 20% mortality before testing. Flies were incubated at 32-34 °C for 20 min before the experiment, to ensure silencing of

GAL4-expressing neurons. Sugar preference was tested at 32-34 °C and 60-70% relative humidity.

2.4.1. Sugar preference assay

Mixed populations of males and females (about 30-60 flies in total) were tested for sucrose preference (Calbiochem) in a circular arena (Ø 76 mm). Each half of the arena was covered with a semicircular piece of filter paper that had previously been soaked with either 350 µL of water or 350 µL of a 0, 0.1, 0.5, 1 or 2 M sucrose solution; filter papers were subsequently allowed to dry. For the *NP-GAL4* experiments, a 1.7 M sucrose solution was used. The walls of the arena were covered with Fluon (Fluon® GP1, Whitford Plastics Ltd., UK) to prevent flies from climbing. After introduction, flies were allowed to choose between the two sides for 1 min. Fly behavior was video-recorded at 20 frames per second from above (Canon EOS 500D). The videos were processed using Matlab and Fiji software. Automatic fly counting was done as previously described[109] and the preference index (PI) was calculated as:

$$\mathrm{PI} = \frac{(\#\ \text{flies on sugar} - \#\ \text{flies on water})}{(\#\ \text{flies on sugar} + \#\ \text{flies on water})}$$

Pooled PI values (30-60 s) are presented for most experiments. For the *NP-GAL4* experiments, the PIs at 60 s following introduction into the assay were manually calculated. To approximate the dependence of the sugar preference on starvation time and/or sucrose concentration, the following equation was fitted to the corresponding data:

$$y = \frac{ax^b}{c + x^b}$$

In this equation, *x* represents starvation time or sucrose concentration and *y* represents PI.

2.4.2. Proboscis extension reflex

Starved flies were briefly anesthetized under CO_2. Female flies were selected and glued on their back on a cover slide with nail polish. Flies were allowed to recover in a humidified chamber for at least 1 h prior to the experiment. After recovery, flies were presented with water on their tarsi and were allowed to drink *ad libitum*. Unresponsive flies were discarded. After the flies stopped responding to water, sucrose solutions were presented on the tarsi in triplicate, from lowest to highest concentration. Water was given after each presentation to wash the tarsi and ensure that flies remained water-satiated throughout. PER was scored as 0 or 1 (0: no extension; 1: extension). To approximate the dose-response curve, the same equation as above was fitted. Labellar PER was performed as described elsewhere[150].

2.4.3. Olfactory learning

Flies were trained and tested for immediate appetitive olfactory memory as previously described[108,151]. Odors (4-methylcyclohexanol and 3-octanol, diluted 1:80 and 1:100 in paraffin oil; Fluka, Germany) were presented in odor cups with a diameter of 14 mm. A learning index (LI) was calculated as the mean preference of two separate groups of reciprocally trained flies. In half of the experiments the first presented odor was rewarded and in the other half, the second presented odor was rewarded[152]. Aversive memory[152] of starved flies using the same odors served as controls for intact locomotion and odor responses.

2.5. Quantification of fly locomotion

Videos were acquired as described above and analyzed in Matlab. First, the region of interest (circular arena) was selected and RGB images were converted to grayscale. To distinguish flies from the background, images were binarized by applying a user-defined threshold. The binarized background (empty arena) was subtracted from all binarized images. Resulting images were eroded and dilated to remove noise[153]. A cluster of contacting pixels was labeled as one particle. For each particle, its area, its centroid, the diagonal length of its bounding box, and the eccentricity of an ellipse with the same second-moments as the particle were calculated.

The likelihood for each particle representing a fly was calculated based on the diagonal lengths of the bounding box and eccentricity. Particles with low likelihood represented either flies for which the selected threshold was not appropriate, or multiple flies that were merged because of close proximity. The number of flies in low-likelihood particles was estimated by dividing their area with the average area of the high-likelihood particles. Then, the threshold was re-adjusted using an iterative process, until the number of particles in the region matched the estimated number of flies. If this did not occur after forty iterations, those low-likelihood particles were excluded. Ellipses were fitted to all particles as described elsewhere[154].

A closest neighbor approach was then used to identify individual flies in every pair of consecutive frames. First, a pair set was defined as all the possible pairs of ellipses between the two frames and the distances between the centroids of all ellipse pairs were computed. Second, the smallest distance was determined and the corresponding ellipses were identified as a pair. Third, that ellipse pair was eliminated from the pair set. The second and third steps were repeated

until the pair set was emptied. The maximum changes in position and angle of paired ellipses in consecutive frames were set to approximately 7 mm and 90°, respectively. Using this information, the change in position, angle, linear velocity, angular velocity, and absolute angular velocity of each ellipse were computed.

All computations were carried out on a parallel computer LX406Re-2, which consists of 68 nodes. Each node is equipped with a main storage of 128 GB and two groups of 12-core Intel Xeon processors E5-2695v2. The Matlab script outlined above was run on one node. In each node, parallel processing with automatic parallelization, Open Multi-Processing, or Message Passing Interface can be operated up to 24 parallels. The maximum computing performance per node becomes 460.8 GFLOPS (Giga Floating-point Operations Per Second).

2.6. Mathematical model of sugar preference

Flies in the sugar preference assay (Figure 7a) were assigned to four states: free to walk on the sugar side (FS), free to walk on the water side (FW), feeding on the sugar side (S) and feeding on the water side (W) (Fig. 8a). Transitions between states were reversible and controlled by certain rates (constants k). The preference index was obtained using:

$$PI = \frac{[S]+[FS]-[FW]-[W]}{[S]+[FS]+[FW]+[W]}$$

The number of flies in each state were obtained by solving the differential equations describing the transitions:

$$\frac{d[S]}{dt} = -k_{Sout}[S] + k_{\mathrm{Sin}}[FS]$$

$$\frac{d[FS]}{dt} = k_{Sout}[S] - (k_{\mathrm{Sin}} + k_{SW})[FS] + k_{WS}[FW]$$

$$\frac{d[FW]}{dt} = k_{SW}[FS] - (k_{WS} + k_{Win})[FS] + k_{Wout}[W]$$

$$\frac{d[W]}{dt} = k_{Win}[FW] - k_{Wout}[W]$$

An equilibrium was assumed to solve the differential equations and the results were substituted into the PI formula, thereby obtaining:

$$PI = \frac{A + 1 - (1 + D)B}{A + 1 + (1 + D)B}$$

Here, 'sugar affinity' $A = k_{\mathrm{Sin}} / k_{Sout}$, 'speed ratio' $B = k_{SW} / k_{WS}$ and 'water affinity' $D = k_{Win} / k_{Wout}$. Flies were never observed feeding on the water side, so the water affinity was set at an arbitrarily low level (D = 0.001). The relative contributions of sugar affinity and sugar-induced locomotion suppression on PIs was consequently examined by varying parameters A and B (Figure 26b).

To predict PIs for the *Gr5a-GAL4* and Gr(64f–5a) blockades (Figs 8c, d), data from genetic control experiments were first used to determine values of A and B as functions of sucrose concentration. PER upon stimulation of the tarsi with sucrose solutions was reasoned to recapitulate sugar affinity A. Therefore, A was derived as a function of sucrose concentration from the PER data as follows. First, a sigmoidal curve was fitted to the PER data using the equation:

$$PER(\log[Sucrose]) = \frac{1}{1+\exp(-slope(\log[Sucrose]) - thrd_{PER})}$$

where $slope$ and $thrd_{PER}$ are the parameters of the sigmoid function. Second, PER data were transformed to affinity using:

$$A = c\frac{PER(\log[sucrose] - thrd_{shift})}{1 - PER(\log[sucrose] - thrd_{shift})}$$

Here, $thrd_{shift}$ and c are correction factors that account for the different conditions between the PER and sugar preference experiments (values of $c = 0.83$ and $thrd_{shift} = 3.1$ were acquired). The transformation produced a sugar affinity A between zero and infinity that is more appropriate for the model (A = 0 when $k_{\mathrm{Sin}} = 0$ and A = ∞ when $k_{Sout} = 0$). The speed ratio B was calculated from the linear velocity data of genetic controls in the presence or absence of 2 M sucrose. Like sugar affinity, linear velocity was assumed to be a sigmoidal function of sucrose concentration. Additionally, contributions of sugar affinity A and speed ratio B to sugar preference were quantified by simulating PIs of a theoretical sugar affinity mutant (A = D = 0.001) and locomotion suppression mutant (B = 1; Fig. 8e).

2.7. Statistics

Data were evaluated using Prism software (GraphPad, San Diego, CA) as previously described[155], employing Shapiro-Wilk and Bartlett's test. Data are presented as means ± SEM if they are normally distributed and have equal variances and were tested with one-way ANOVA and Bonferroni-corrected pairwise comparisons. Data are presented as medians, with the lower

and upper error bars representing the first and third quartile, respectively, if they are not normally distributed and/or variances are not equal. In that case, the Kruskal-Wallis test and Dunn-corrected pairwise comparisons, the Mann-Whitney U test or the Wilcoxon signed-rank test were used to check for statistically significant differences. An exception was made for PER data, which are presented as means ± SEM for ease of visualization, even though they are not normally distributed. However, nonparametric statistics were applied to check differences in the PER data as described above. Significance levels are indicated as follows: ns $P > 0.05$; * $P < 0.05$; ** $P < 0.01$; *** $P < 0.001$.

3. Results

3.1. Sugar preference assay

The PER assay is a popular choice for quantifying appetitive responses in insects[25], but relies on stimulation of tethered flies. Therefore, the sugar preference assay[156] (Figure 7a) was chosen to quantify early appetitive responses, because it simulates natural foraging better. In these experiments, freely walking flies were introduced into a circular arena and were allowed to choose between two sides, one containing sugar and one without. Flies were video-recorded from above, allowing subsequent quantification of locomotion (see section 3.6).

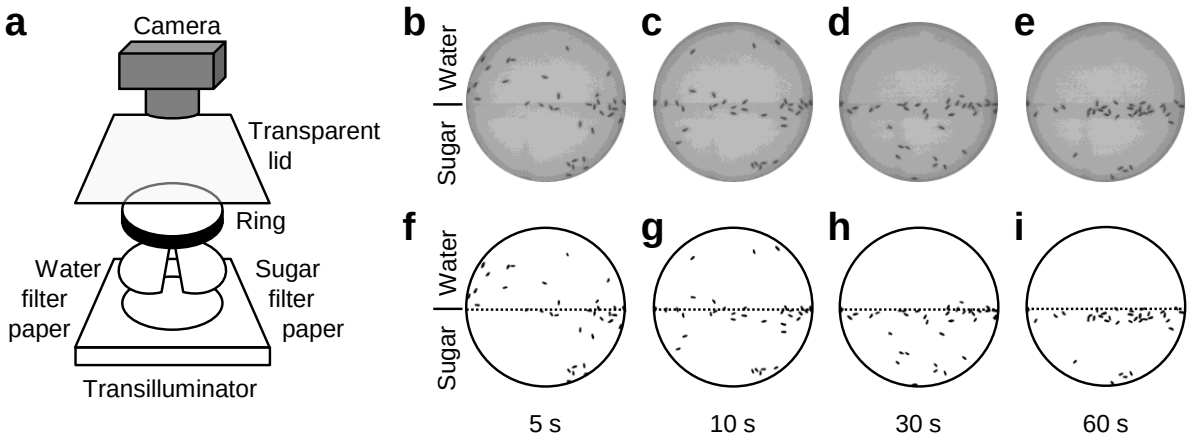

Figure 7: The sugar preference assay. (a) Schematic of the assay. (b-e) Distribution of hungry wild-type flies (36 h starvation) at different time points after introduction (5, 10, 30 and 60 s). The lower semicircle (sugar) was soaked with 350 µL of a 2 M sucrose solution and subsequently dried. 350 µL of water and drying were applied to the upper semicircle (water). (f-i) Same images as above after image binarization. Flies are depicted as black 'particles'. The border between the water/sugar sides is indicated with a dashed line.

The sugar preference assay was characterized using Canton S flies, a wild-type strain of *Drosophila melanogaster*. Starved flies (36 h) showed strong and rapid preference for 2 M sucrose (Figure 7b-e). The great majority of flies (roughly 90%) accumulated on the sugar side approximately 30 s after they were introduced in the assay (Figure 7 d, h). To quantify sugar

preference, a threshold was applied on the grayscale videos, yielding a series of binary images in which flies were depicted as 'particles' (Figure 7f-i). These particles were automatically counted in each image (i.e. frame) and the PIs to sugar were computed. These analyses yielded time series of PIs (Figure 8a, b)

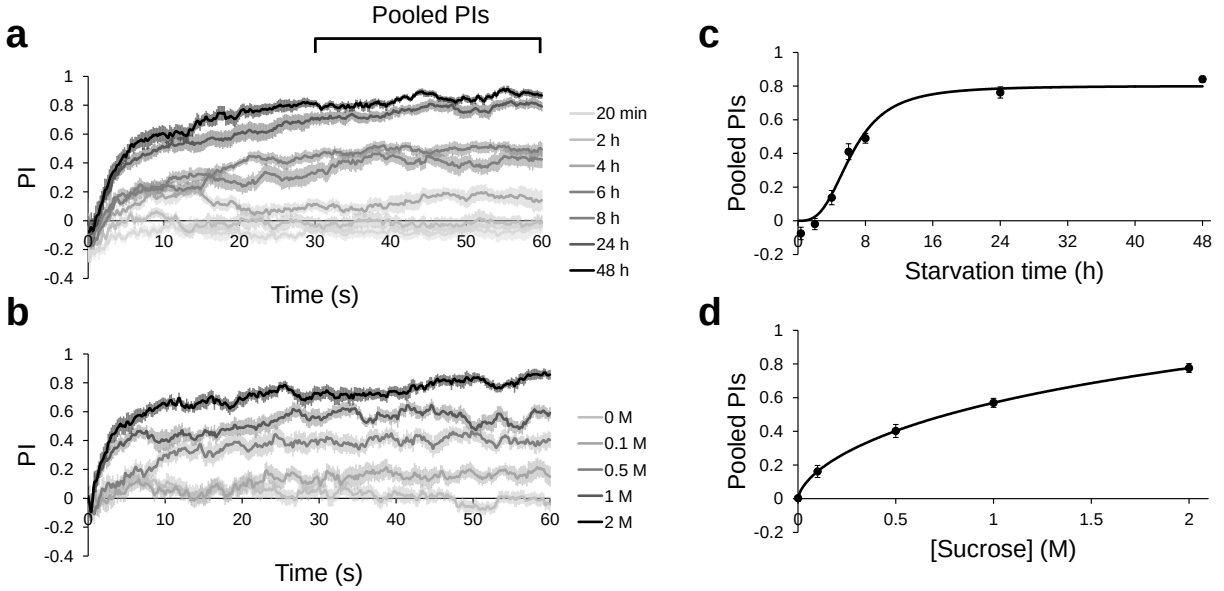

Figure 8: Quantification and characterization of sugar preference in wild-type flies. (a) Time series of PIs of wild-type flies to 2 M sucrose and their dependence on starvation time. Darker shades of gray indicate longer starvation times (labeled on the right). (b) Time series of PIs of wild-type flies to different sucrose concentrations (labeled on the right). Flies were starved to 20% mortality (40 h starvation on average). (c) Starvation-dependency of pooled PIs between 30-60 s. (d) Sucrose concentration-dependency of pooled PIs between 30-60 s. n = 8-15 per starvation interval/sucrose concentration. PI preference index.

The time series of PIs showed that sugar preference generally increased during the first 10-20 s of the experiments and remained mostly constant thereafter (Figure 8a, b). Therefore, PIs between 30-60 s were pooled to quantify sugar choice (Figure 8a and 8c, d). These 'pooled PIs' (referred to as PIs hereafter for the sake of brevity) showed strong dependency on starvation time and sucrose concentration. Increasing starvation time led to a steady increase of PIs during the first 8 hours and reached a plateu between 24-48 hours (Figure 8a, c). Similarly, PIs for strongly starved flies rose with increasing sucrose concentrations (Figure 8b, d). Given the high signal-to-

noise ratio for the maximal starvation/sucrose concentration conditions, strong starvation (i.e. 20% mortality) and a high sucrose concentration (i.e. 2 M) were chosen for subsequent experiments.

3.2. Sweet taste receptor neurons are diferentially required for sugar choice

To examine the role of different taste organs in sugar preference, seven gustatory receptor GAL4 lines (*Gr-GAL4*) were chosen. In these lines, GAL4 expression is controlled by the cloned promoters of different sweet GRs: *Gr5a* (the trehalose receptor) or six closely related GRs (*Gr61a* and 5 members of the *Gr64* cluster; see also Figure 4g). These lines differentially label the labellum[68] and legs[11]. These *Gr-GAL4* lines were crossed to *UAS-Kir2.1* flies (see section 1.5.2) and the progeny tested with the sugar preference assay (Figure 9).

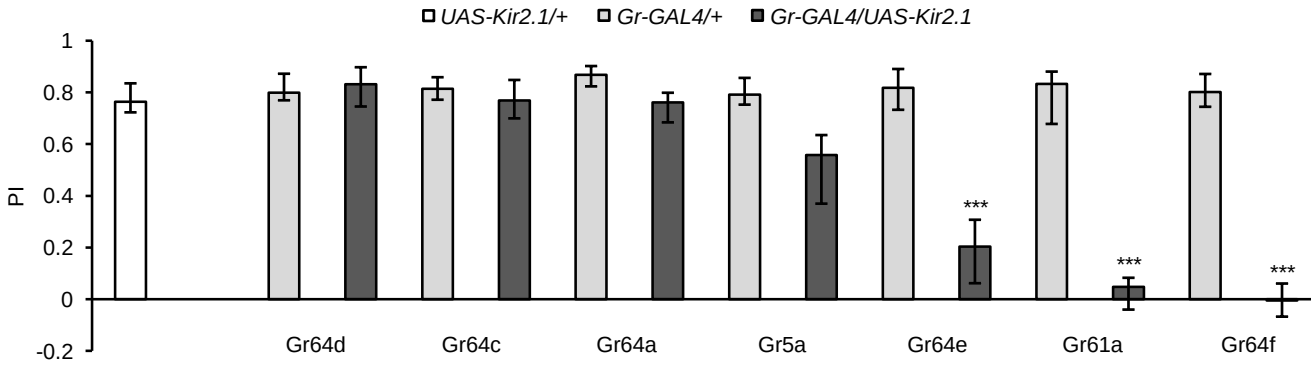

Figure 9: Sweet taste receptor neurons are differentially required for sugar preference. Requirement of different sweet taste receptor neurons for preference to 2 M sucrose. Silencing cells in *Gr64e-GAL4*, *Gr61a-GAL4* and *Gr64f-GAL4* with *UAS-Kir2.1* impaired sucrose preference compared to genetic controls (Kruskal-Wallis test; Dunn's post test; *** $P <$ 0.001). Flies with silenced *Gr61a*- and *Gr64f*-expressing cells were 'sugar-blind' (i.e. preference indices indistinguishable from zero; Wilcoxon signed-rank test, $P > 0.05$). n = 12-23 per group. PI preference index.

Blocking with different *Gr-GAL4* lines differentially affected sugar preference (Figure 9). Only blocking with three of the lines, *Gr64e-GAL4*, *Gr61a-GAL4* and *Gr64f-GAL4* resulted in statistically significant sugar preference reductions. Blocking with *Gr5a-GAL4* yielded a noticeable but statistically insignificant PI reduction, despite this line's broad expression pattern[22,68]. Interestingly, blocking with *Gr61a-GAL4* and *Gr64f-GAL4* completely abolished sugar preference, as these flies' PIs were statistically indistinguishable from zero.

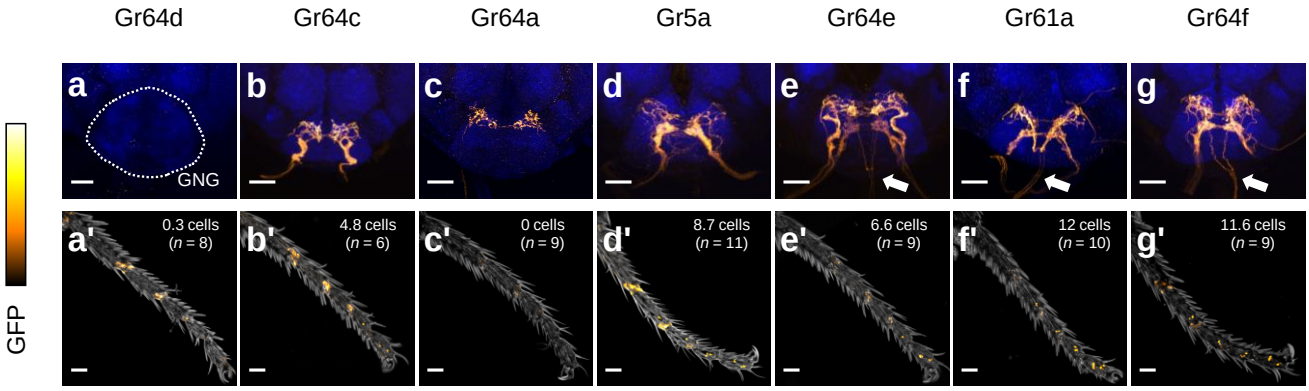

Figure 10: Expression patterns of sweet Gr-GAL4 in the gnathal ganglia and foreleg tarsi. (a-g) Expression patterns of *Gr-GAL4/UAS-mCD8::GFP* flies in the gnathal ganglia (orange). Brains were counter-stained with ubiquitous synaptic marker (Synapsin, in blue). Arrows indicate ascending projections from sweet taste receptor neurons in the legs. Partial projections, scale bars 40 µm. (a'-g') Expression patterns of *Gr-GAL4/UAS-mCD8::GFP* flies in the foreleg tarsi (orange). Mean of cells in tarsi is reported (top right). Strong signals in the tarsal joints are autofluorescence. Scale bars 40 µm; *n* = 6-11. GNG gnathal ganglia; GFP green fluorescent protein.

To better understand these differences, all tested *Gr-GAL4* lines were crossed to *UAS-mCD8::GFP* flies and the GFP expression patterns of the progeny in the gnathal ganglia and forelegs were examined (Figure 10). Analysis of the expression pattern highlighted three key findings:

(1) Labelling of the labial nerves did not predict a sugar preference impairment, because blocking with *Gr64c-GAL4* (Figure 10b) and *Gr5a-GAL4* (Figure 10d) did not affect preference, or reduced it modestly (cf. Figure 9).

(2) Labelling of pharyngeal nerves also failed to predict sugar preference impairment. *Gr64a-GAL4*, which exclusively labelled these nerve terminals in the brain (Figure 10c) but no cells in the foreleg tarsi (Figure 10c'), did not show a PI decrease upon blockade (cf. Figure 9).

(3) Labelling of the maximum number of cells in the foreleg tarsi was the best predictor of a strong sugar preference phenotype. *Gr61a-GAL4* and *Gr64f-GAL4*, both of which labeled the maximum number of cells in the forelegs (approx. 12 cells, Figure 10f, g) were sugar-blind upon blockade.

Taken together, these results suggest that sweet taste receptor neurons in the forelegs are more important than those in the labellum or pharynx for sugar preference.

3.3. *Gr64f* and *Gr5a* lines label overlapping but distinct populations of cells

Gr5a-GAL4 broadly labels sweet GRNs (Figure 10d, d'), including sweet GRNs in all labellar taste hairs[68] and the majority of foreleg taste hairs[11]. Additionally, killing *Gr5a-GAL4* cells results in reduction of PER probability upon stimulating the legs with a 5 mM sucrose solution[22]. Surprisingly, blocking with *Gr5a-GAL4* only yielded a modest (but statistically not significant) decrease in sucrose preference (Figure 9). On the other hand, *Gr64f-GAL4*, which gave a

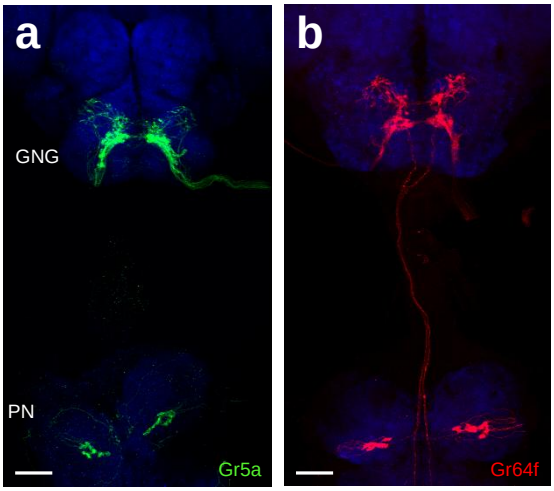

Figure 11: Comparison of *Gr5a-GAL4* (green) and *Gr64f-GAL4* (red) expression in the central nervous system. (a) Expression of *Gr5a-GAL4/UAS-mCD8::GFP*. (b) Expression of *Gr64f-GAL4/UAS-mCD8::GFP*. Partial projections, scale bars 40 µm. GNG gnathal ganglia; PN prothoracic ganglia.

complete phenotype (Figure 9), only labels a few additional cells in the LSO[27] and tarsi[11] (also see Figure 10g, g').

To better understand these subtle differences, the expression patterns of *Gr5a-GAL4* and *Gr64f-GAL4* in the CNS were examined in greater detail (Figure 11). As expected, both lines labeled inputs from the labellum and legs. However, only *Gr64f-GAL4* labeled brain-projecting cells that sent axons through the VNC and CvC and terminated in the posterior GNG (Figure 11b). Interestingly, these brain-projecting cells were included in all *Gr-GAL4* lines that yielded strong sugar preference defects upon blockade (Figure 10e-g, arrows).

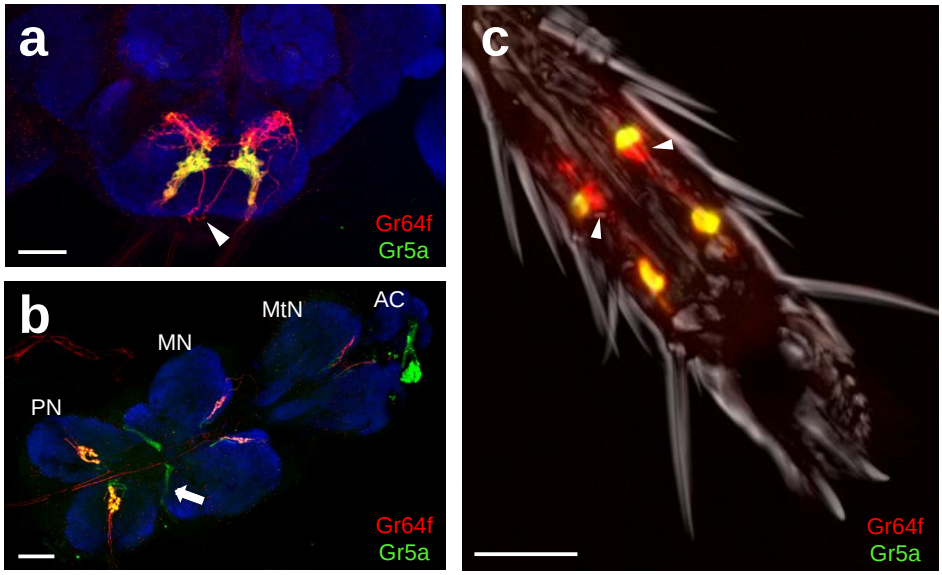

Figure 12: Comparison of *Gr5a-LexA* and *Gr64f-GAL4* in the same fly. Expression patterns of a *Gr5a-LexA/ LexAop-mCD8::GFP UAS-mCD8::RFP; Gr64f-GAL4/+* fly in: (a) the gnathal ganglia (b) the ventral nerve cord and (c) the fifth tarsal segment of the foreleg. Arrowheads indicate projections from ascending tarsal gustatory receptor neurons (in (a)) and their cell bodies (in (c)). Arrow indicates projections from the wings in (b). Partial projections, scale bars 40 μm (a, b) or 20 μm (c). PN prothoracic ganglia; MN mesothoracic ganglia; MtN metathoracic ganglia; AC abdominal center.

To contrast these GRN populations in the same fly, *Gr64f-GAL4* and a LexA line, *Gr5a-LexA*, which has been previously used to label *Gr5a*-expressing cells[101], were used for two-color labeling. Examination of expression in the CNS and the periphery showed that the two lines

greatly overlap (Figure 12). Both lines labeled the labial nerves (Figure 12a, yellow), in line with data showing that the respective GAL4s innervate all labellar taste hairs[68]. In the VNC, only *Gr5a-LexA* labeled projections from wing GRNs (Figure 12b, arrow). Nevertheless, both lines labeled projections from leg GRNs (9-10 cells in the foreleg) that terminated in the pro-, meso- and metathoracic ganglia (Figure 12b, yellow). A few additional cells (2-4 in the foreleg), labeled only by *Gr64f-GAL4*, had cell bodies in the fifth tarsal segment (Figure 12c, arrowheads) and projected towards the brain (Figure 12a, b, red). These two anatomically distinct groups cells will be hereafter referred to as segmental tarsal GRNs (stGRNs) or ascending tarsal GRNs (atGRNs), for the VNC-projecting and brain-projecting neurons, respectively.

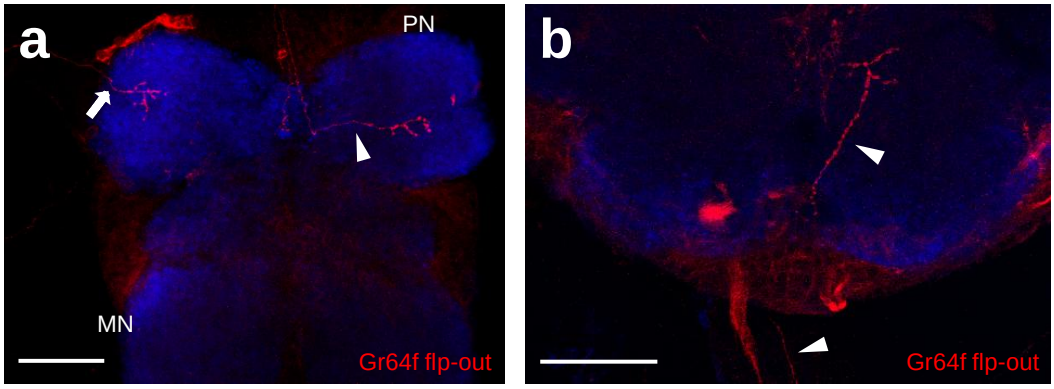

Figure 13: Single-cell labeling of tarsal gustatory receptor neurons in the central nervous system. (a) Distinct projections of an ascending (right; arrowhead) and a segmental (left; arrow) tarsal gustatory receptor neuron in the prothoracic ganglia of the ventral nerve cord. Note axon collaterals in both cells. (b) Projection of an ascending tarsal gustatory receptor neuron in the gnathal ganglia (arrowhead). Partial projections; scale bars 20 μm. PN prothoracic ganglia; MN mesothoracic ganglia.

Finally, to examine stGRN/atGRN projection patterns in detail, the single-cell flp-out technique[142] was used to stochastically label *Gr64f-GAL4* positive neurons. As *Gr64f-GAL4* labels both tarsal populations, this approach allowed examination of the projections of both stGRNs and atGRNs in the CNS (Figure 13). Interestingly, stGRNs and atGRNs showed axon collaterals in the thoracic ganglia, which presumably intermingle between the two groups. Taken

together, these anatomical analyses highlight two distinct populations of sweet GRNs in the legs of *Drosophila*.

3.4. An intersectional approach selectively labels ascending tarsal GRNs

The *Gr-GAL4* screen results (Figures 9 and 10) suggested that atGRNs are critical for sugar preference. Indeed, all 3 *Gr-GAL4*s that yielded statistically significant decreases of PI upon blockade (*Gr64e-GAL4*, *Gr61a-GAL4* and *Gr64f-GAL4*) labeled these cells. However, these lines also labeled additional cells, including stGRNs. Therefore, an intersectional strategy was used to more selectively manipulate atGRNs (Figure 14a).

To refine the *Gr64f-GAL4* expression pattern, *Gr5a-LexA* and *LexAop-GAL80* were introduced to 'subtract' the *Gr5a* pattern (Figure 14a; see also section 1.5.3). For brevity, this approach will be referred to as Gr(64f–5a) hereafter. As both lines label the same labellar GRNs[68] and all stGRNs (Figure

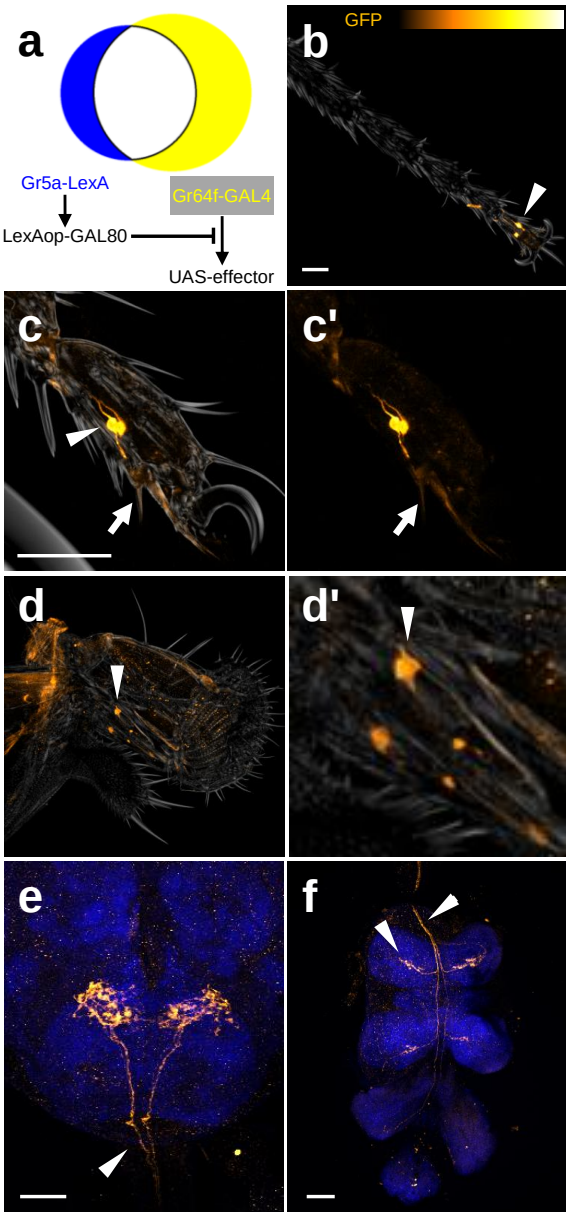

Figure 14: Expression pattern of Gr(64f–5a) flies. (a) Schematic of the intersectional 'subtraction' approach. (b-f) Expression pattern of Gr(64f–5a) in the foreleg (b), the fifth tarsal segment of the foreleg (c, c'), the proboscis (d), the labral sense organ (d'), the gnathal ganglia (e) and the ventral nerve cord (f). *UAS-mCD8::GFP* orange; blue Synapsin. z-stack projections; scale bars 40 μm.

12), this approach should primarily target atGRNs. To test this, the *UAS-mCD8::GFP* expression with Gr(64f–5a) in the CNS and periphery were examined (Figure 14).

As expected, this approach labeled only a small population of 2-4 cells in the distal-most tarsal segment of the foreleg (Figure 14b-c') that had ascending projections in the CNS (Figure 14e, f). Although the labellum and the labellar nerves were not labeled (Figure 14d, e), Gr(64f–5a) additionally labeled four cells in the LSO. Moreover, these experiments revealed that atGRNs innervate a pair of short, distal-most ventral taste hairs in the fifth tarsal segment of the foreleg (Figure 14c, c'). These are likely the taste hairs identified by others as 5V1[55] or f5v[11], which were shown to contain the leg GRNs with the highest sugar sensitivity.

3.5. Ascending sweet taste receptor neurons in the tarsi are required for early appetitive responses

As the genetic subtraction approach labeled atGRNs more selectively than any of the *Gr-GAL4* lines (Figure 10), Gr(64f–5a) was used with *UAS-Kir2.1* to silence these cells. Consequently, several appetitive behaviors were tested (see below). Performance was compared with the results obtained by blocking with *Gr5a-GAL4* in parallel, to better contrast requirements for the two non-overlapping populations of sweet taste receptor neurons.

Blocking with Gr(64f–5a) yielded a strong, but incomplete, sucrose preference reduction across the concentration range (Figure 15a). In contrast, blocking the sum of labellar GRNs and stGRNs with *Gr5a-GAL4* yielded a more modest effect, which failed to reach statistical significance (Figure 15b). Taken together, these results suggest that:

(1) atGRNs are not tuned to specific concentrations of sugar (i.e. high or low);

(2) only blocking all sweet GRNs in the legs results in 'sugar-blind' flies (cf. Figure 9 and 15a);

(3) atGRNs are more important than stGRNs when it comes to sugar preference and

(4) stGRNs may nevertheless still play a smaller role in sugar preference.

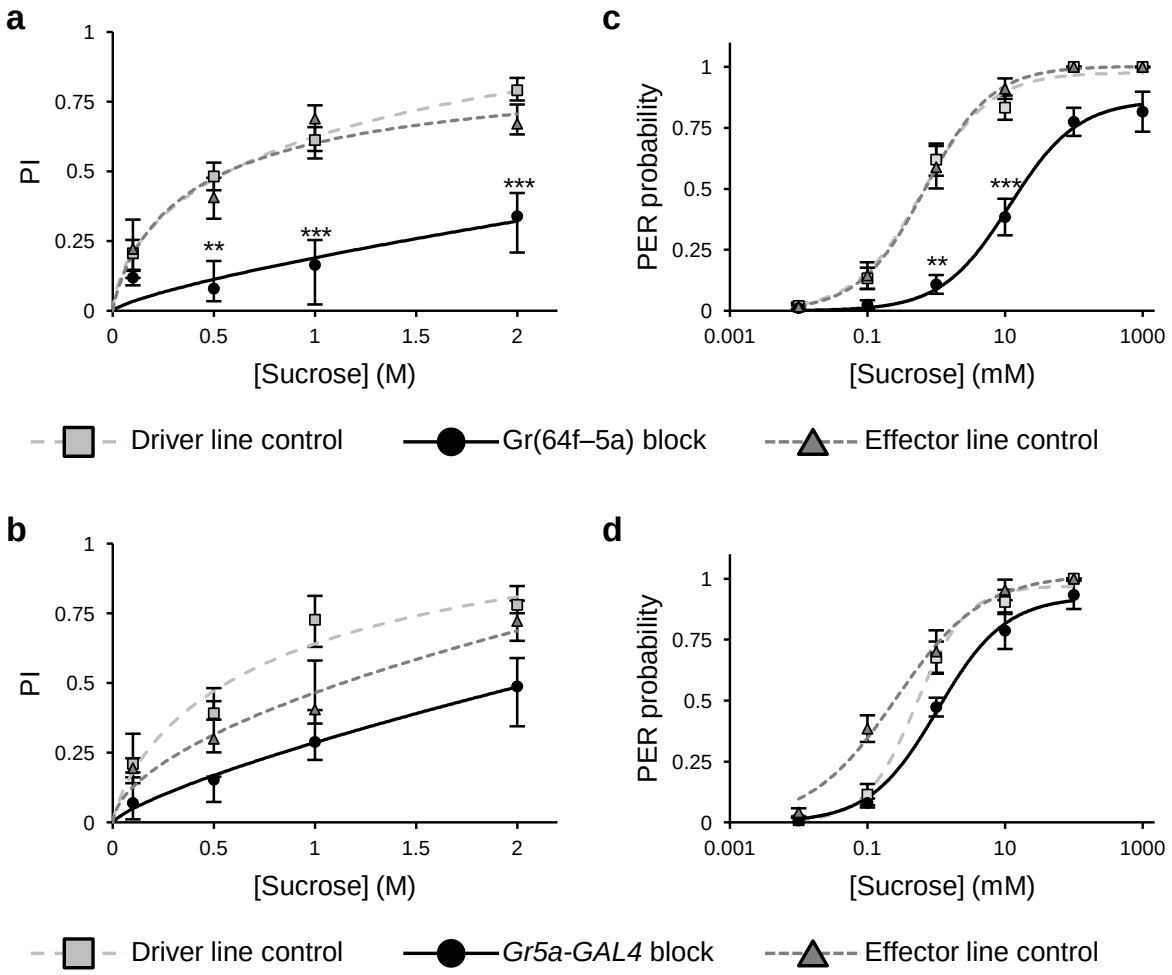

Figure 15: atGRNs are required for sugar preference and feeding initiation. (a) Sucrose preference was significantly reduced upon blocking Gr(64f–5a) cells at 0.5 M, 1 M and 2 M sucrose (Kruskal-Wallis test; Dunn's post test; ** $P < 0.01$; *** $P < 0.001$). n = 9–21 per group. Driver line control *Gr64f-GAL4/+*, Gr(64f–5a) block *Gr5a-LexA/+; Gr64f-GAL4/LexAop-GAL80; UAS-Kir2.1/+*, effector line control *Gr5a-LexA/+; LexAop-GAL80/+; UAS-Kir2.1/+*. (b) Sucrose preference showed a small, statistically not significant decrease when blocking with *Gr5a-GAL4* (Kruskal-Wallis test; Dunn's post test; $P > 0.05$). n = 11–21 per group. Driver line control *Gr5a-GAL4/+*, *Gr5a-GAL4* block *Gr5a-GAL4/UAS-Kir2.1*, effector line control *UAS-Kir2.1/+*. (c) Proboscis extension reflex probability following stimulation of the legs with 1 mM and 10 mM sucrose was significantly reduced when blocking with Gr(64f–5a) (Kruskal-Wallis test; Dunn's post test; ** $P < 0.01$; *** $P < 0.001$). n = 20–50 flies per group. Genotypes as in (a). (d) Proboscis extension reflex probability following stimulation of the legs was not significantly impaired upon blocking *Gr5a-GAL4* cells (Kruskal-Wallis test; Dunn's post test; $P > 0.05$). n = 35–58 flies per group. Genotypes as in (b). PI preference index; PER proboscis extension reflex.

Freely-walking flies in the sugar preference assay can extend their proboscises towards the sugar side and ingest sugar. Therefore, the contributions of additional non-tarsal GRNs, namely LSO GRNs in Gr(64f–5a) (Figure 14d, d') and labellar GRNs in *Gr5a-GAL4* (Figure 11a), cannot be excluded. To focus on the role of tarsal GRNs, flies were tethered and only the legs were stimulated with sucrose solutions. Such stimulation typically produces extension of the proboscis in hungry flies, the first step in feeding[25]. In line with the sugar preference results, PER probability was greatly decreased when atGRNs were blocked (Figure 15c), but was only marginally affected when stGRNs were blocked (Figure 15d). Therefore, atGRNs, but not stGRNs, are required for feeding initiation.

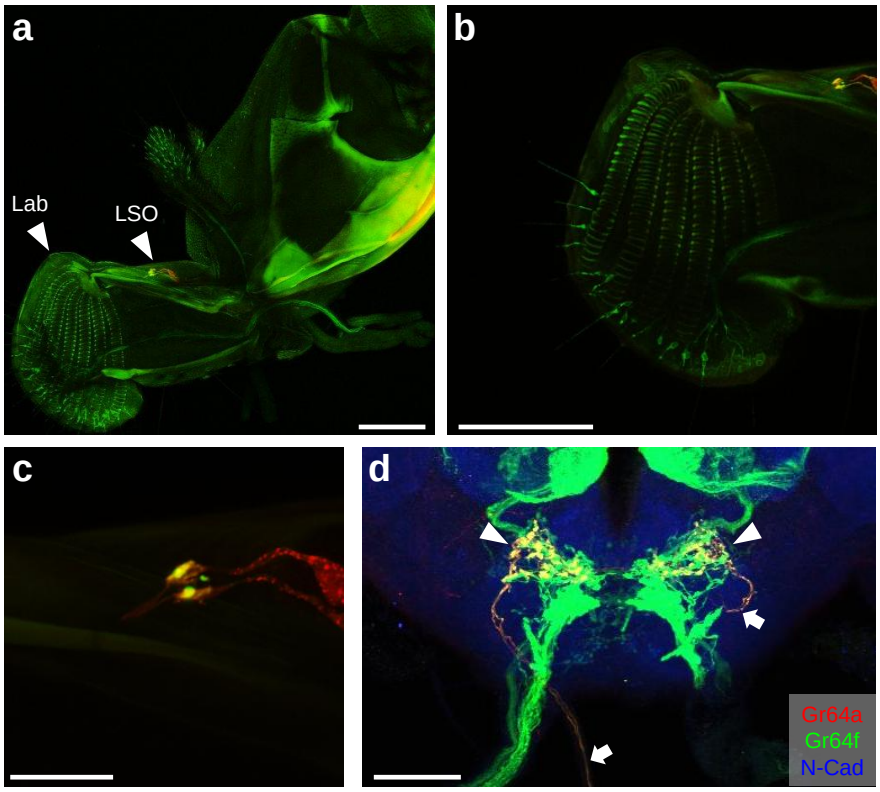

Figure 16: Comparison of *Gr64f-LexA* and *Gr64a-GAL4* expression in the proboscis and brain. Expression pattern of *Gr64a-GAL4/UAS-mCD8::RFP; Gr64f-LexA/LexAop-rCD2::GFP* flies in the proboscis (a), labellum (b), labral sense organ (c) and gnathal ganglia (d). Both lines co-label the labral sense organ and its projections to the gnathal ganglia (yellow; arrows and arrowheads in (d)). Green GFP; red RFP; blue ubiquitous neuropile marker (N-Cad). Partial projections; scale bars 100 µm (a, b), 20 µm (c) or 30 µm (d). Lab labellum; LSO labral sense organ.

To further exclude a role for the GRNs in the LSO in sugar preference, the *Gr64f*-expressing cells were examined in greater detail. As stated earlier, *Gr64a-GAL4* exclusively labeled pharyngeal nerves (Figure 10c, c'), but its blockade did not result in PI reduction (Figure 9), arguing against a role for these cells in sugar preference. To check if the same cells are labeled by a *Gr64f* line, the expression patterns of *Gr64a-GAL4* and *Gr64f-LexA* were compared with double labeling (Figure 16). Both lines labeled the same four cells in the LSO but no cells in the DCSO/VCSO (Figure 16a), similarly to the Gr(64f–5a) strategy (Figure 14d, d') and in agreement with a recent study[27]. Additionally, these lines co-labeled nerves projecting from the pharynx to the brain and their terminals (Figure 16d, arrows and arrowheads respectively). Therefore, the sugar preference defect with the Gr(64f–5a) blockade should be attributed to the atGRNs.

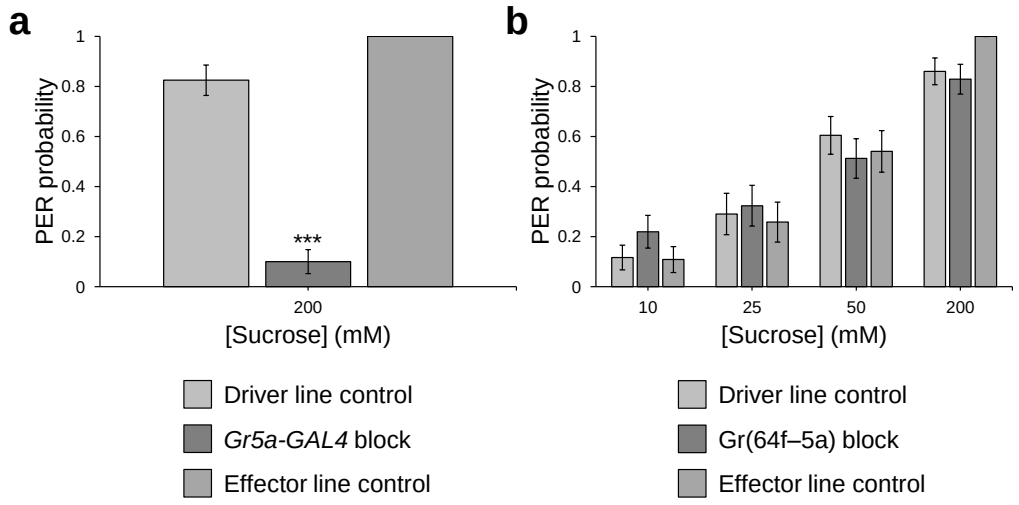

Figure 17: Blocking with Gr(64f–5a) leaves labellar sweet taste receptor neurons functionally intact. (a) Blocking with *Gr5a-GAL4* abolishes proboscis extension reflex in response to labellar stimulation with a 200 mM sucrose solution (Kruskal-Wallis test; Dunn's post test; *** $P < 0.001$). Proboscis extension reflex probability was statistically indistinguishable from zero (Wilcoxon signed-rank test, $P > 0.05$). $n = 40$ flies per group. Driver line control *Gr5a-GAL4/+*; *Gr5a-GAL4* block *Gr5a-GAL4/UAS-Kir2.1*; Effector line control *UAS-Kir2.1/+*. (b) Blocking with Gr(64f–5a) did not affect proboscis extension reflex probability when the labellum was stimulated with sucrose solutions (Kruskal-Wallis test; Dunn's post test; $P > 0.05$). $n = 31–43$ flies per group. Driver line control *Gr64f-GAL4/+*, Gr(64f–5a) block *Gr5a-LexA/+; Gr64f-GAL4/LexAop-GAL80; UAS-Kir2.1/+*, effector line control *Gr5a-LexA/+; LexAop-GAL80/+; UAS-Kir2.1/+*. PER proboscis extension reflex.

To ensure that the Gr(64f–5a) strategy left *Gr5a*-expressing cells intact, stimulation of the labellum was used to test whether labellar GRNs remained functional. Blocking with *Gr5a-GAL4* was expected to abolish PER in response to stimulation of the labellum, because all taste hairs are labeled by this line[68]. In contrast, blocking with Gr(64f–5a) should leave labellar GRNs intact (Figure 14d-e). These predictions were validated by the experiments (Figure 17), showing that only the function of *Gr64f*-positive, *Gr5a*-negative cells was manipulated with the 'subtraction' Gr(64f–5a) approach. Additionally, these results confirmed that sweet GRNs can be effectively silenced with *Gr5a-GAL4*.

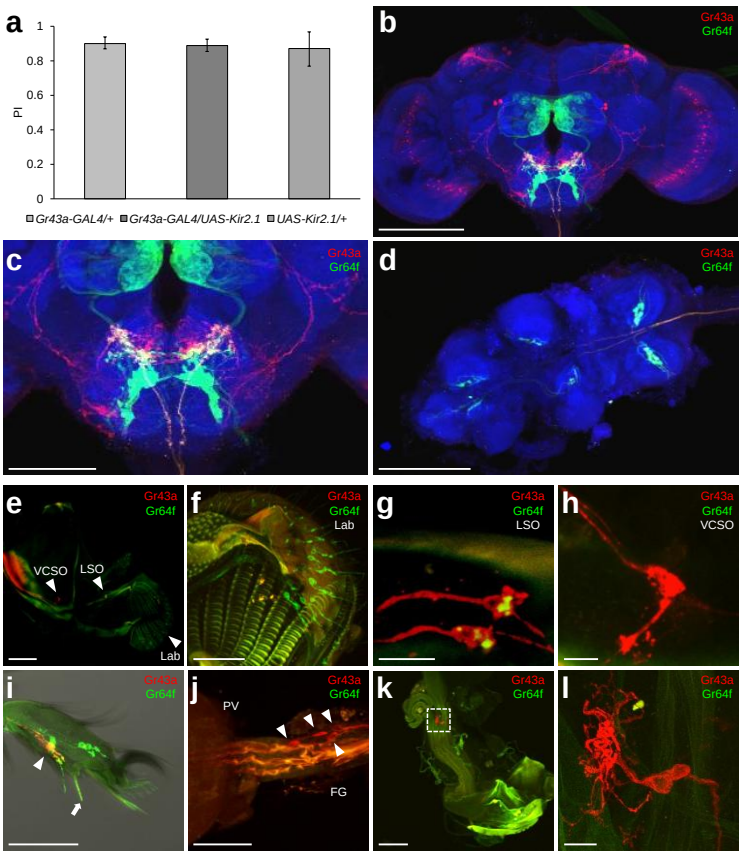

Figure 18: Behavioral and anatomical characterization of *Gr43a-GAL4*. (a) Blocking with *Gr43a-GAL4* did not alter preference index to 2 M sucrose (Kruskal-Wallis test; Dunn's post test; $P > 0.05$). n = 11–12 per group. (b-l) Expression patterns of *Gr43a-GAL4/UAS-mCD8::RFP; Gr64f-LexA/LexAop-rCD2::GFP* flies in the brain (b), gnathal ganglia (c), ventral nerve cord (d), proboscis (e), labellum (f), labral sense organ (g), ventral cibarial sense organ (h), fifth tarsal segment of the foreleg (i), foregut/proventriculus (j) and uterus (k, l). Note additional expression of *Gr43a-GAL4* in internal GRNs (red). Partial projections, scale bars 100 µm (b, d, e, k), 50 µm (c, f, i, j) or 10 µm (g, h, l).GFP green fluorescent protein, green; RFP red fluorescent protein, red; blue ubiquitous neuropile marker (N-Cad); Lab labellum; LSO labral sense organ; VCSO ventral cibarial sense organ; PV proventriculus; FG foregut.

Another line, *Gr43a-GAL4*, has been reported to label atGRNs, in addition to multiple sweet taste receptor neurons in the brain and other internal organs[11,59,157]. However, blocking with this line did not alter sugar preference (Figure 18a). Off-target cells labeled by *Gr43a-GAL4*

are not labeled by *Gr64f-LexA* (Figure 18b-l), suggesting that this discrepancy can be attributed to silencing of internal GRNs in the brain or elsewhere. In line with this interpretation, the Amrein lab showed that blocking brain cells in *Gr43a-GAL4* specifically leads to overconsumption of a nutritive sugar[59]. Taken together, these results suggest that the genetic 'subtraction' strategy is more specific and therefore more appropriate for addressing the role of atGRNs. Indeed, the Gr(64f–5a) phenotype was duplicated by Gr(61a–5a) (Figure 19), which labels the same cells[11] (Figure 10f, f').

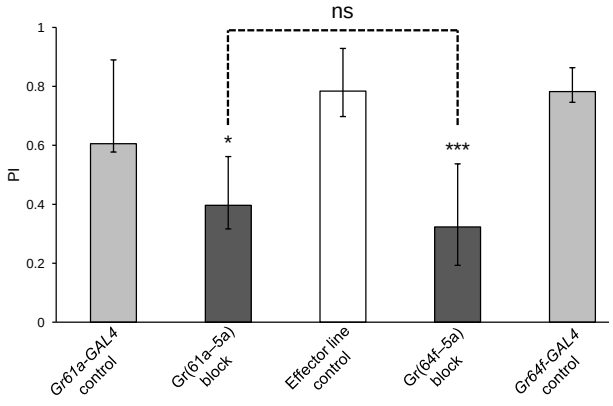

Figure 19: Blocking atGRNs with Gr(61a–5a) decreases 2 M sucrose preference. The decrease was as severe as the blockade with Gr(64f–5a) (Kruskal-Wallis test; Dunn's post test; * $P < 0.05$; *** $P < 0.001$; ns $P > 0.05$). n = 15-21 per group. *Gr61a-GAL4* control *Gr61a-GAL4/+*, Gr(61a–5a) block *Gr5a-LexA/+; Gr61a-GAL4/LexAop-GAL80; UAS-Kir2.1/+*, effector line control *Gr5a-LexA/+; LexAop-GAL80/+; UAS-Kir2.1/+*, Gr(64f–5a) block *Gr5a-LexA/+; Gr64f-GAL4/LexAop-GAL80; UAS-Kir2.1/+*, *Gr64f-GAL4* control *Gr64f-GAL4/+*.

In addition to driving early appetitive responses, sugar can also lead to the formation of appetitive olfactory memory[108]. To test if subsets of sweet GRNs were differentially required for sugar-odor learning, flies with blocked *Gr5a-GAL4* or Gr(64f–5a) cells were trained with a 2 M sucrose reward (identical to the preference assay experiments in Figure 9) and consequently tested for short-term memory (Figure 20a, b). Blocking atGRNs with Gr(64f–5a) significantly reduced appetitive memory. In contrast, blocking the sum of labellar and stGRNs with *Gr5a-GAL4* had no effect. Importantly, the observed effects were not the results of general defects in odor perception or learning, as both experimental groups performed well in aversive odor-electric shock conditioning (Figure 20c, d). The simplest interpretation of these results is that

early appetitive responses controlled by atGRNs, such as feeding initiation, are essential for sugar reward.

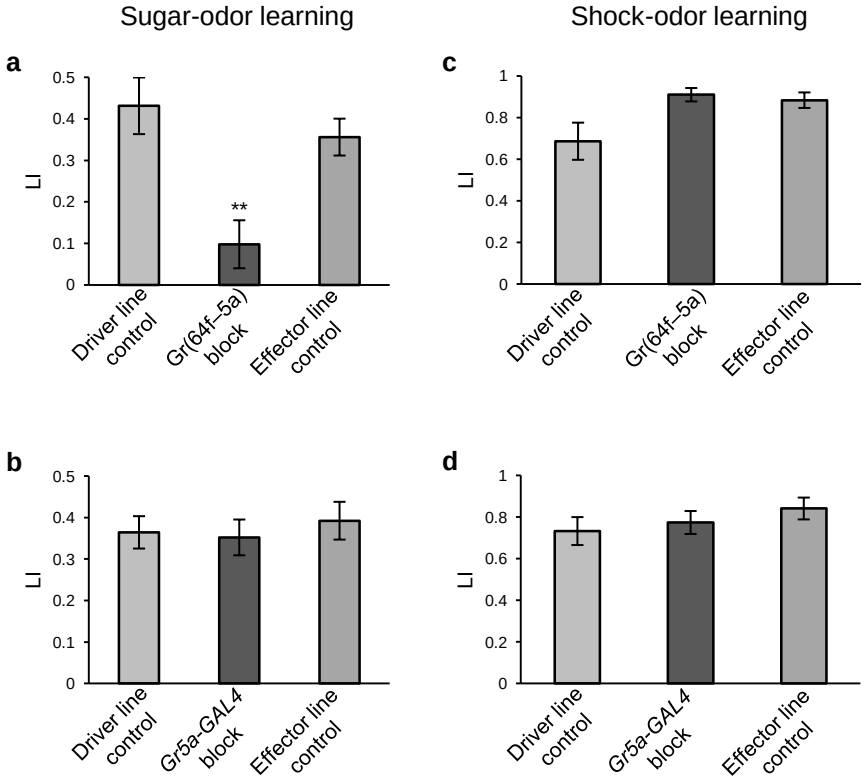

Figure 20: Blocking atGRNs impairs short-term appetitive olfactory learning. (a) Short-term appetitive olfactory memory was abolished when atGRNs were blocked with Gr(64f–5a) (one-way ANOVA; Bonferroni's multiple comparison test; ** $P < 0.01$). n = 11–12 per group. Driver line control *Gr64f-GAL4/+*, Gr(64f–5a) block *Gr5a-LexA/+; Gr64f-GAL4/LexAop-GAL80; UAS-Kir2.1/+*, effector line control *Gr5a-LexA/+; LexAop-GAL80/+; UAS-Kir2.1/+*. (b) Short-term appetitive olfactory memory was not affected when labellar GRNs and stGRNs were blocked with *Gr5a-GAL4* (one-way ANOVA; Bonferroni's multiple comparison test; $P > 0.05$). n = 9–10 per group. Driver line control *Gr5a-GAL4/+*; *Gr5a-GAL4* block *Gr5a-GAL4/UAS-Kir2.1*; Effector line control *UAS-Kir2.1/+*. (c) Short-term aversive memory was not changed when Gr(64f–5a) cells were blocked (one-way ANOVA; Bonferroni's multiple comparison test; $P > 0.05$). n = 8 per group. Genotypes as in (a). (d) Short-term aversive memory was not changed when *Gr5a-GAL4* was blocked (one-way ANOVA; Bonferroni's multiple comparison test; $P > 0.05$). n = 8 per group. Genotypes as in (b). LI learning index.

3.6. Sugar detection triggers rapid suppression of locomotion

The lack of a strong requirement for the stGRNs in all the appetitive behaviors tested suggested that these cells control other aspects of feeding behavior. Because stGRNs project

locally in the VNC, it is possible that they interact with neuronal networks controlling locomotion. In line with this hypothesis, flies from the *Gr5a-GAL4* blockade were observed to be restless on the sugar side of the preference assay, despite the fact that they did not show a strong defect in sugar choice (Figures 9 and 15b).

Wild-type flies and genetic control groups were observed to move more slowly, or even cease moving entirely, after crossing over to the sugar side of the sugar preference assay. To simplify the paradigm, the choice was eliminated by testing flies either in the absence (Figure 21a) or in the presence (Figure 21b) of 2 M sucrose. The same stimulus was used in the sugar preference assay (Figure 9), making results from these experiments comparable. Even without quantification, it was evident that wild-type flies greatly suppressed their locomotion in the presence of 2 M sucrose (Figure 21).

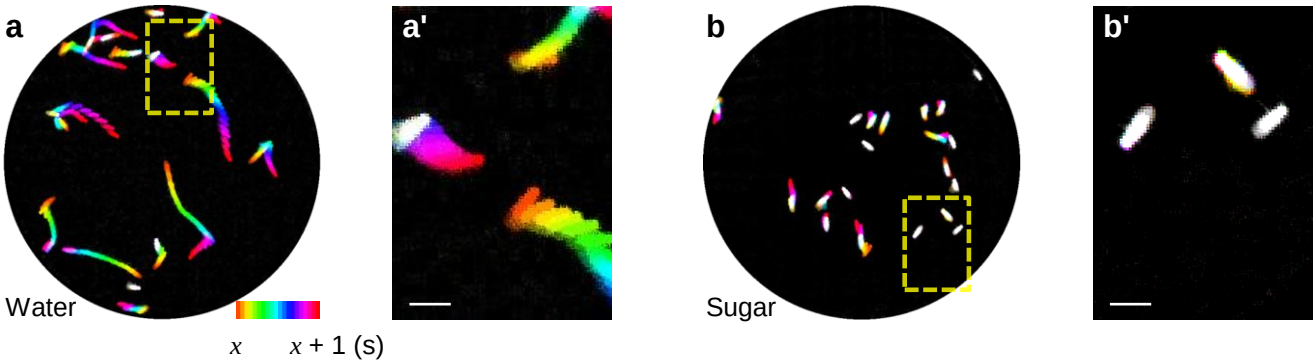

Figure 21: Hungry wild-type flies suppress their locomotion in the presence of sugar. (a) Locomotion of starved Canton S flies in the absence of sugar. (a') Blow-up of (a). (b) Locomotion of starved Canton S flies in the presence of 2 M sucrose. (b') Blow-up of (b). Images represent one second of fly movement behavior, sampled at 20 frames per second. Frames are color-coded according to the inset of panel (a) and overlaid. Immobile flies are thus shown in white. x = 55 s in (a); x = 57 s in (b). Scale bars 3 mm.

To quantify locomotion, an algorithm was developed to analyze videos of fly behavior. Briefly, flies were detected by applying a threshold, similarly to the sugar preference videos (Figure 7b-i). Consequently, ellipses were fitted to the flies and flies were paired between

consecutive frames using a closest neighbor approach. Finally, the changes in centroid position and body axis angle were computed for each fly and the linear and angular velocities were calculated from these parameters (Figure 22a, b). The accuracy of pairing flies was assessed by examining over a thousand fly pairs from random video frames. Pairing was done correctly for the majority of the flies, but there were errors in rare cases (error rate 0.7%). Additionally, the body axis angle and center of flies were validated by examining a hundred random flies. The error rates in these parameters were 2.2 ± 0.2^{o} and 0.108 ± 0.006 mm (approx. 5% of body length), respectively. These errors are comparable to those of a fly tracking algorithm[158] and were deemed acceptable to allow further analyses.

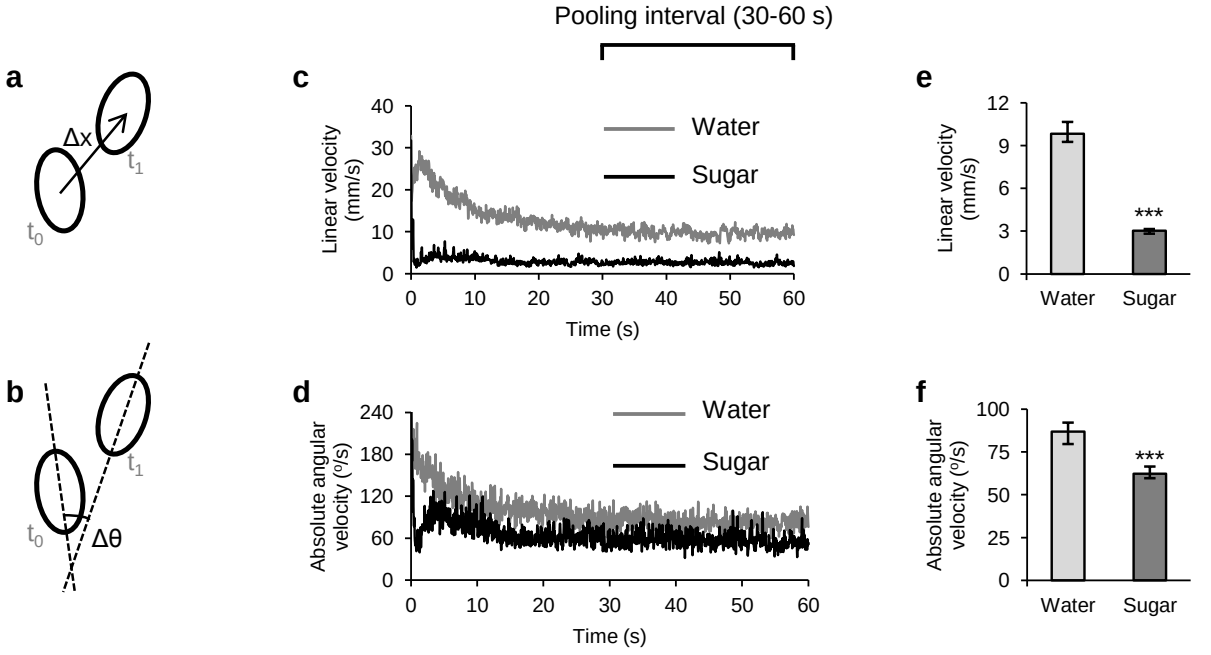

Figure 22: Quantification of sugar-induced suppression of locomotion in wild-type flies. (a) Calculation of linear velocity by computing the change in the centroid position in ellipse-fitted flies (Δx). (b) Calculation of angular velocity by computing the change in the major axis' angle in ellipse-fitted flies (Δθ). (c) Time series of average linear velocity of starved wild-type flies in the presence (black) or absence (gray) of 2 M sucrose. (d) Time series of average absolute angular velocity of starved wild-type flies in the presence (black) or absence (gray) of 2 M sucrose. (e) Average linear velocity between 30-60 s of starved wild-type flies in the presence (dark gray) or absence (light gray) of 2 M sucrose. Sucrose significantly reduced average linear velocity (Mann-Whitney U tests; *** $P < 0.001$). (f) Average absolute angular velocity between 30-60 s of starved wild-type flies in the presence (dark gray) or absence (light gray) of 2 M sucrose. Sucrose significantly reduced angular velocity (Mann-Whitney U tests; *** $P < 0.001$). n = 11-12. t_0 starting time; t_1 time in subsequent frame (typically 0.05 s later); Δx change in centroid position; Δθ change in major axis' angle.

Quantification of locomotion of hungry, wild-type flies revealed that sugar-induced locomotion suppression is strong and robust and reflected in both the linear and absolute angular velocities of the flies (Figure 22c-f). In the absence of sugar, locomotion was initially high, perhaps reflecting a startle response accompanying aspiration of the flies into the arena. Both linear and absolute angular velocity gradually dropped, mostly stabilizing after 30 s (Figure 22c, d). In comparison, locomotion was consistently lower in the presence of sugar and the initial high-locomotion startle response was not observed (on the contrary, locomotion dropped immediately after introduction into the arena, Figure 22c, d). Because both parameters were stabilized after 30 s, they were pooled between 30-60 s (pooling interval in Figure 22c) and an average linear velocity and absolute angular velocity were calculated (Figure 22e, f). Both parameters were significantly reduced in the presence of sugar.

3.7. Segmental tarsal sweet taste receptor neurons are required for sugar-induced locomotion suppression.

Blocking the sum of labellar sweet GRNs and stGRNs with *Gr5a-GAL4* revealed that these cells were necessary for sugar-induced suppression of turning (Figure 23a-d) and walking (Figure 24). Strikingly, sugar-induced suppression of turning was entirely abolished (Figure 23d). On the other hand, linear velocity was noticeably, albeit not significantly, decreased in the presence of sugar, suggesting that atGRNs are also involved in locomotion suppression, at least to a more limited extent (Figure 24). In contrast, when atGRNs were blocked using Gr(64f–5a), flies were still able to suppress turning on sugar (Figure 23e-h) and showed a significantly reduced linear velocity in the presence of sugar (Figure 24). These results suggest that stGRNs

are more crucial than atGRNs for sugar-induced locomotion suppression, in surprising contrast to their more limited role in sugar preference and feeding initiation (Figure 15b, d).

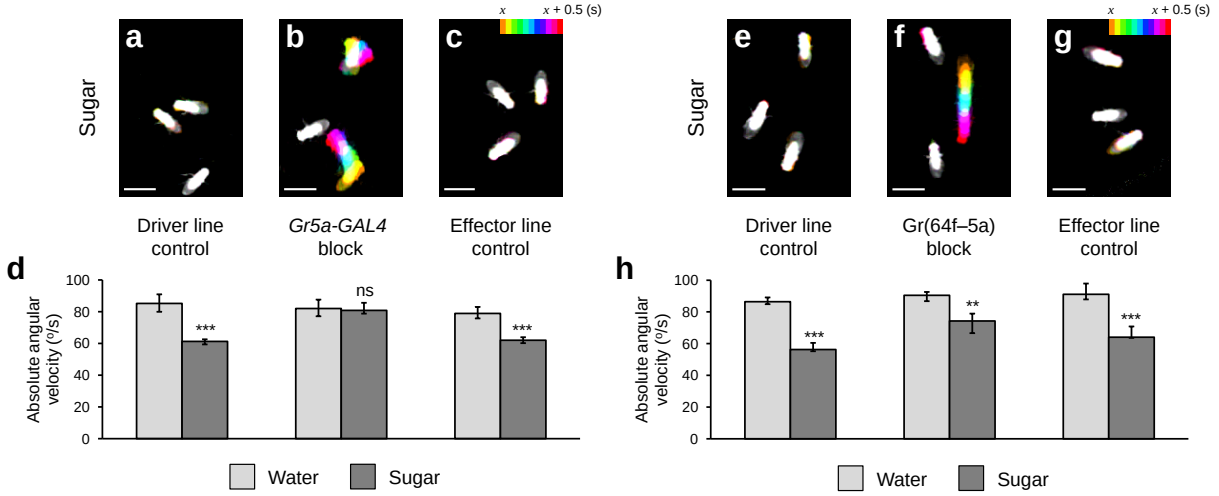

Figure 23: *Gr5a* cells are necessary for sugar-induced turning suppression. (a-c) Examples of locomotion of *Gr5a-GAL4/+* (a), *Gr5a-GAL4/UAS-Kir2.1* (b) and *UAS-Kir2.1/+* (c) flies during half-second intervals (x = 46.4 s in (a); x = 55.5 s in (b); x = 50 s in (c)). Flies from different frames are color-coded according to time (inset of panel (c)). (d) Average absolute angular velocity of all flies between 30-60 s of the experiments in the absence (light gray) or presence (dark gray) of 2 M sucrose. Sucrose significantly reduced angular velocity for genetic controls, but not for the experimental group (Mann-Whitney U tests; *** $P < 0.001$; ns $P > 0.05$). n = 15-17. (e-g) Examples of locomotion of *Gr64f-GAL4/+* (e), *Gr5a-LexA/+; Gr64f-GAL4/LexAop-GAL80; UAS-Kir2.1* (f) and *Gr5a-LexA/+; LexAop-GAL80/+; UAS-Kir2.1* (g) flies during half-second intervals (x = 49.5 s in (e); x = 47.6 s in (f); x = 51.7 s in (g)). Flies are color-coded as in (a-c). (h) Average absolute angular velocity of all flies between 30-60 s of the experiments in the absence (light gray) or presence (dark gray) of 2 M sucrose. Sucrose significantly reduced angular velocity for all groups (Mann-Whitney U tests; *** $P < 0.001$; ** $P < 0.01$). n = 8-11. Scale bars 3 mm.

Because *Gr5a-GAL4* includes sweet taste receptor neurons in the labellum in addition to labeling stGRNs, it is possible that labellar GRNs are involved in the sugar-induced suppression of locomotion. To test this possibility, another intersectional approach was used to limit silencing to the labellum. A line driving flippase expression in the head, *otd-nls-FLPo*[144,159], along with an ubiquitously-expressing, FRT-flanked GAL80 line (*tub>GAL80>*) were used in conjunction with *Gr5a-GAL4* and *UAS-Kir2.1* to limit silencing to the labellum (see also section 1.5.3). These flies showed normal sugar-induced locomotion suppression (Figure 25), indicating that

stGRNs, and not the labellar GRNs, are responsible for controlling locomotion suppression upon sugar detection.

Taken together, these findings support the idea that both sets of tarsal GRNs, atGRNs and stGRNs, are required for different aspects of the early appetitive response to sugar. atGRNs are more crucial in feeding initiation (Figure 15c), whereas stGRNs are tuned to controlling locomotion suppression upon sugar encounter (Figures 23-25). Both of these behaviors are important for sugar choice, as blocking either GRN population yielded a decrease in preference (Figures 9 and 15a, b). However, feeding initiation appears to be more important than sugar-induced locomotion suppression, as the effect of atGRN blockade was more severe. Finally, only blocking both populations of tarsal GRNs in the legs abolishes sugar responses (Figure 9), suggesting a non-linear interaction between these two classes of sweet taste receptor neurons.

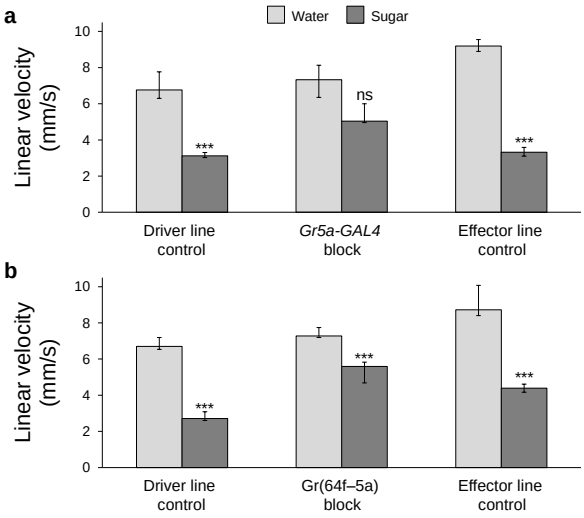

Figure 24: *Gr5a* cells are necessary for sugar-induced linear velocity suppression. Average linear velocity of all flies between 30-60 s of the experiment in the absence (light gray) or presence (dark gray) of 2 M sucrose. (a) Blocking with *Gr5a-GAL4* did not result in a statistically significant sugar-induced locomotion suppression, in contrast to genetic controls (Mann-Whitney U tests; *** $P < 0.001$; ns $P > 0.05$). Driver line control *Gr5a-GAL4/+*, *Gr5a-GAL4* block *Gr5a-GAL4/UAS-Kir2.1*, effector line control *UAS-Kir2.1/+*. n = 15-17. (b) Blocking with Gr(64f–5a) yielded statistically significant sugar-induced locomotion suppression (Mann-Whitney U tests; *** $P < 0.001$). Driver line control *Gr64f-GAL4/+*, Gr(64f–5a) block *Gr5a-LexA/+; Gr64f-GAL4/LexAop-GAL80; UAS-Kir2.1/+*, effector line control *Gr5a-LexA/+; LexAop-GAL80/+; UAS-Kir2.1/+*. n = 8-11.

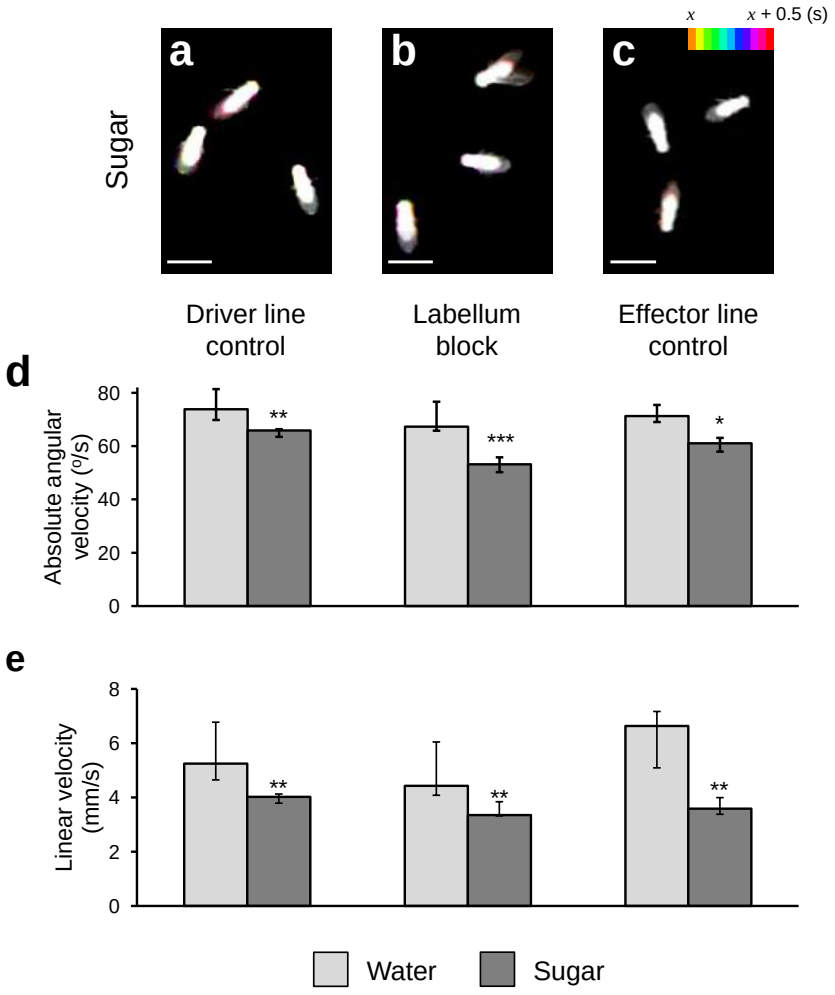

Figure 25: Sweet taste receptor neurons in the labellum are not required for sugar-induced locomotion suppression. (a-c) Examples of locomotion of *Gr5a-GAL4/+; tub>GAL80>/+* (a), *Gr5a-GAL4/otd-nls-FLPo; tub>GAL80>/ UAS-Kir2.1* (b) and *otd-nls-FLPo/+; UAS-Kir2.1/+* (c) flies during half-second intervals (x = 56 s in (a); x = 51.8 s in (b); x = 31.6 s in (c)). Flies from different frames are color-coded according to time (inset of panel (c)). (d) Average absolute angular velocity of all flies between 30-60 s of the experiments in the absence (light gray) or presence (dark gray) of 2 M sucrose. Sucrose significantly reduced angular velocity for all groups (Mann-Whitney U tests; *** $P < 0.001$; ** $P < 0.01$; * $P < 0.05$). (e) Average linear velocity of all flies between 30-60 s of the experiments in the absence (light gray) or presence (dark gray) of 2 M sucrose. Sucrose significantly reduced angular velocity for all groups (Mann-Whitney U tests; ** $P < 0.01$). n = 13-14; scale bars 3 mm.

3.8. A mathematical model accurately predicts sugar preference

To understand the mechanism by which sugar preference is controlled, a dynamic state transition model was devised to mathematically predict PIs. In this model, inspired by chemical

equilibriums, flies were assigned to the mutually exclusive ‘free to walk’ and ‘feeding’ states on the sugar and water sides, for a total of four states (Figure 26a). By definition, only the flies in the ‘free to walk’ states (FS and FW in Figure 26a) can cross the border and therefore move from one side to the other. ‘Free to walk’ flies can also transition to a ‘feeding’ state on either side (S and W in Figure 26a). Transitions between the four states are controlled by certain rates (constants k on the transition arrows in Figure 26a).

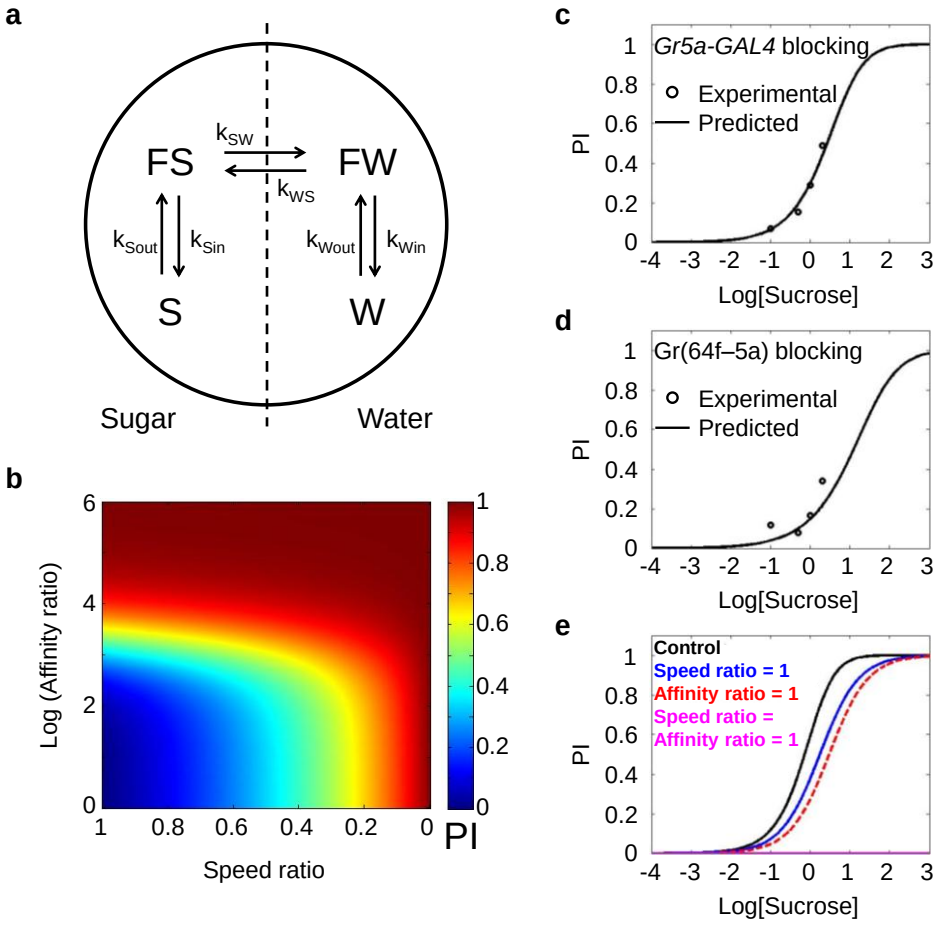

Figure 26: A mathematical model can predict sugar preference. (a) Graphical depiction of the model. Flies can reversibly transition between ‘free to walk’ (FS and FW) and ‘feeding’ states (S and W) on the sugar and water sides of the preference assay. The transitions (arrows) are controlled by constant transition rates k. (b) Effect of the sugar/water speed and affinity ratios on the sugar preference index. (c) Quantitative prediction of the model for the *Gr5a-GAL4* blockade. Actual data are also shown (open circles) for comparison. (d) Quantitative prediction of the model for the Gr(64f–5a) blockade. Actual data are also shown (open circles) for comparison. (e) Effect of loss of sugar-induced locomotion suppression (blue), loss of sugar affinity (red) and both (magenta) on the preference indices of wild-type flies (black). FS freely moving on sugar; FW freely moving on water; S feeding on sugar; W feeding on water;PI preference index.

Transition rates between the 'free to walk' states (FS and FW) were equated to the linear velocities on sugar and on water (Figure 24). Their sugar/water ratio will be referred to as 'speed ratio' hereafter. Additionally, the ratio of the transitions between each 'free to walk' and the corresponding 'feeding' state (k_{in}/k_{out} in Figure 26a) was assumed to represent stimulus affinity. Stimulus affinity was therefore derived from the PER data (Figure 15c, d). The sugar/water affinity ratio will be referred to as 'affinity ratio' hereafter.

The effect of the speed ratio and affinity ratio on the sugar preference was examined by calculating the PIs for different values of the two ratios (Figure 26b). Sugar preference was dependent on both parameters, but showed greater dependence on the affinity ratio. This is in line with neuronal silencing experiments, which showed that blocking atGRNs (controlling PER, i.e. affinity) had a greater effect on preference than blocking stGRNs (controlling speed). Next, experimental data (shown in Figures 15c, d and 24) were inputted to the model to predict the PI dose-response curves for the *Gr5a-GAL4* and Gr(64f–5a) blockades (Figure 26c, d). The model was successful in making accurate quantitative predictions, as experimental data were in good agreement with theoretical values. Finally, three theoretical cases were examined:

(1) Sugar affinity is abolished (i.e. affinity ratio = 1).

(2) Sugar-induced locomotion suppression is abolished (i.e. speed ratio = 1).

(3) Both behaviors are abolished (i.e. affinity ratio = speed ratio = 1).

Once again, the results showed that loss of affinity had a greater effect on sugar preference than loss of sugar-induced locomotion suppression (Figure 26e). Importantly, sugar preference was entirely abolished only when both behaviors were abolished. These results highlight the non-linear interaction between distinct populations of tarsal GRNs and correctly predict that only by

blocking all tarsal GRNs (e.g. with *Gr61a-GAL4* and *Gr64f-GAL4*, Figure 9) will sugar preference be completely abolished.

3.9. A neuronal silencing screen reveals candidate neurons for sugar preference

To identify additional components of the circuit that drives early appetitive responses, a large-scale neuronal silencing screen was conducted using the sugar preference assay (Figure 7a). This functional screen utilized GAL4 lines from the NP collection (*NP-GAL4s*)[145]. Initially, lines with homozygous-viable GAL4 insertions on the second or third chromosomes and relatively narrow expression patterns in the brain were chosen (1081 lines; Figure 27a). These lines were crossed to *UAS-Shi^{ts1}* and their progeny were starved and tested for sugar preference

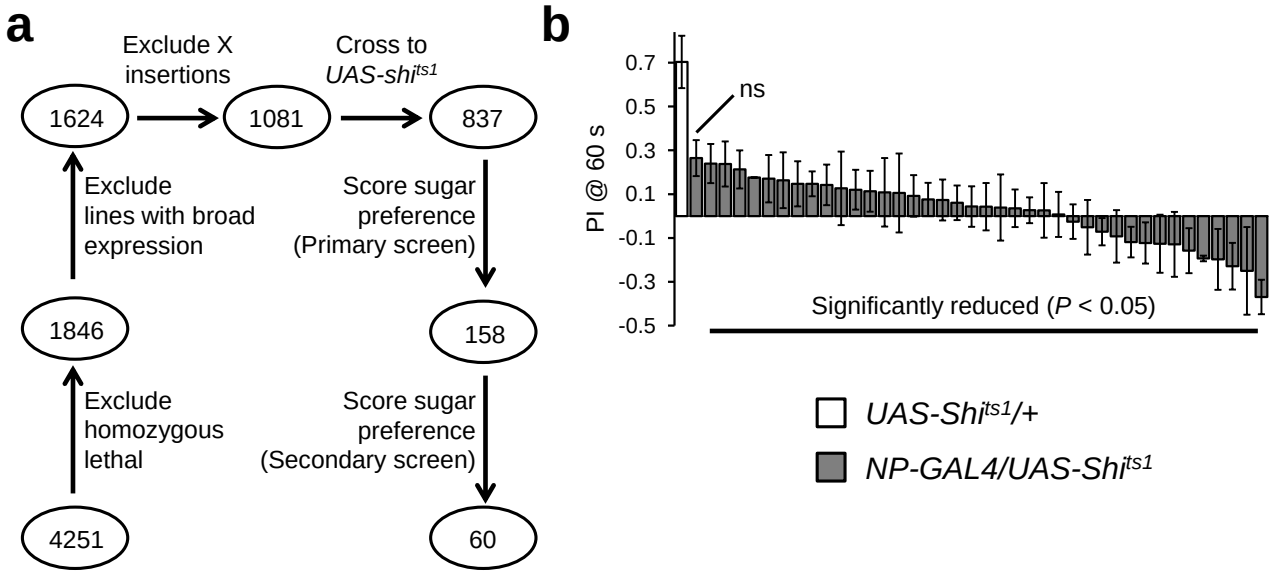

Figure 27: A neuronal silencing screen for identification of neurons involved in sugar preference. (a) Schematic outlining the strategy for identification of enhancer-trap GAL4 lines labeling neurons required for sugar preference. Numbers in the ellipses indicate the number of *NP-GAL4* lines examined at each stage of selection. (b) Preference indices of silenced *NP-GAL4* lines to 1.7 M sucrose (gray) compared to the *UAS-Shi^{ts1}* genetic control (white). Only the 40 lines with the lowest preference indices are shown. Except for one case (ns; not significant), blocking with *UAS-Shi^{ts1}* significantly reduced sugar preference (two-sample t-test assuming unequal variances; $P < 0.05$). On average, 6 experiments per group were performed. PI @ 60 s Preference Index 60 s after fly introduction into the sugar preference assay.

by Dr. Christine Damrau[156]. This preliminary screen isolated 158 lines defective in sugar preference (Figure 27a).

To confirm these results and exclude false positives, a more thorough secondary screen was carried out using *UAS-Shi^{ts1}* to silence neurons in candidate GAL4s. In contrast to the primary screen, which focused on high throughput[156], the secondary screen focused on assessing reproducibility through multiple experiments per line and improved quantification over the primary screen. Overall, this multi-step selection process (summarized in Figure 27a) yielded 60 *NP-GAL4* lines: 40 lines which showed strong PI reduction (Figure 27b) and 20 lines with milder impairments but more specific expression patterns. These lines showed no visible locomotion defect even after prolonged inactivation and should therefore label neurons required for sugar preference.

To identify candidate neurons required for sugar preference in these *NP-GAL4s*, GAL4 expression in the periphery, brain and VNCs was analyzed in detail. Additionally, image registration was used to compare expression patterns in these lines[160]. Manual examination and computational analysis of expression patterns revealed that some *NP-GAL4*s showed patterns reminiscent of GRN projections in the CNS (Figure 28a). However, some lines showed no detectable labeling of some projections and labeled neurons with cell bodies in the CNS. An interesting pair of candidate neurons was labeled by three *NP-GAL4s* (Figure 28b). These cells had cell bodies in the GNG and projected medially towards the esophagus. Taken together, these resources provide an entry point to characterizing the neuronal circuits that control early appetitive responses in *Drosophila*.

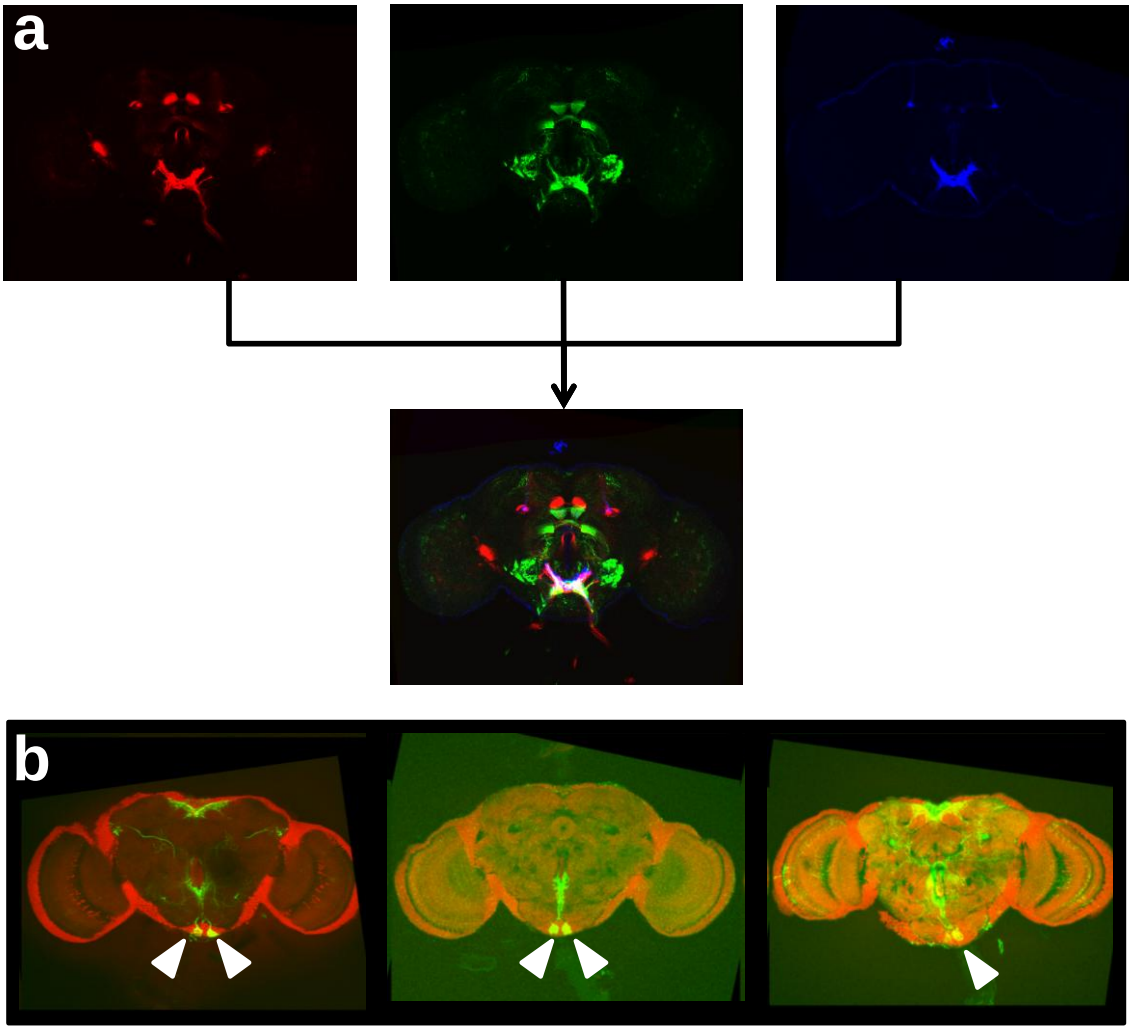

Figure 28: Candidate neurons for sugar preference. (a) Image registration of expression patterns of three different *NP-GAL4*s. These lines show impaired sugar preference upon blockade with *UAS-Shi*^{ts1}. Note overlapping expression in projections in the gnathal ganglia, reminiscent of GRN terminals in the same region (white). (b) A pair of candidate sugar neurons in the brain (arrowheads) is labeled by three different *NP-GAL4*s that show impaired sugar preference upon blockade with *UAS-Shi*^{ts1}.

4. Discussion

4.1. Summary of results

It has long been known that insects have hundreds of taste sensilla, located in taste organs[25], but their specific contributions to feeding have been unclear. Here, the sweet taste receptor neurons of *Drosophila* were used as a model to understand the importance of different GRNs in feeding. The results presented here show that sweet GRNs in the legs, but not the labellum or LSO, are essential for sugar preference (Figure 9). Strikingly, additional functional specialization exists within the legs themselves, with different sets of GRNs (Figures 11-13) controlling different components of the early appetitive response. The smaller population of brain-projecting cells, atGRNs (Figure 14), controls feeding initiation (Figure 15). In contrast, the larger population of VNC-projecting cells, stGRNs, is more important for suppression of locomotion following encounter with food (Figures 23-25). Both of these behaviors are important for sugar preference and can be used to accurately predict it (Figure 26). Sugar preference also requires identified higher-order neurons in the brain (Figures 27b and 28b) which presumably receive information from sweet GRNs in the periphery.

4.2. Sensillar position relates to gustatory receptor neuron function

The importance of tarsal GRNs in sugar choice fits well with the fact that legs are the first appendages to contact food. In line with this, bitter GRNs in the foreleg tarsi, but not in the labellum or pharynx, are specifically required for aversion to lobeline, a bitter chemical[91]. Taken

together, these findings show that control of choice behavior by leg GRNs can be generalized to both appetitive and aversive stimuli.

It has been suggested that taste hairs in the legs and wings may be particularly advantageous to insects, as they are much smaller than their favored foods (e.g. fruits) and spend considerable time on them[2]. Therefore, tarsal GRNs may play an active role in short-range foraging, an idea supported by the experiments with freely-walking flies (Figures 9, 15a, b and 23-25). In contrast, in larger animals like mammals, the taste system is more likely a devoted 'gatekeeper' that controls the decision between ingestion and rejection. For such a function, taste receptor cells exclusively located in the mouth are apparently sufficient.

The presence of multiple taste organs may also be advantageous to insects because of additional GRNs with functions besides feeding. For example, taste receptor neurons in the wings may not be involved in feeding, as wings are less likely to contact food during walking. Nevertheless, bitter GRNs in the wings were recently shown to control grooming in response to noxious stimuli[96]. Additionally, specific tarsal GRNs are known to be involved in controlling courtship behavior[97]. Interestingly, these studies highlight the important relationship between GRN location and function. For example, some of the GRNs involved in courtship innervate dorsal taste hairs in the forelegs, but not the midlegs or hindlegs[39]. These dorsal taste hairs are unlikely to contact food during walking. However, during courtship the male 'taps' the female abdomen with the dorsal surface of its foreleg[39]. Therefore, these IR-expressing GRNs are optimally positioned with regards to their function.

Results presented here suggest that the same principle applies to atGRNs. atGRNs innervate a pair of distal-most ventral taste hairs just beneath the leg claws (Figure 14c, c').

Therefore, they are likely to be in frequent contact with potential food during walking. Two recent studies show that GRNs innervating taste hairs beneath the claws have the highest sugar sensitivity of all leg GRNs tested[11,55]. These cells are most likely the atGRNs. Arrangement of GRNs that are sensitive and important for feeding initiation (Figure 15c) to the most food-accessible location in the legs is an optimal cellular configuration. Moreover, the direct projection of these atGRNs to the taste center of the brain may ensure rapid and efficient feeding initiation. Interestingly, bees also have GRNs with high sugar sensitivity in their tarsi[161] and antennae[162], which are presumably the first organs to contact nectar. Therefore, optimization of sensillar position with regards to its function may be a general principle in the insect taste system.

4.3. Functional dissociation in tarsal sweet taste receptor neurons

While the atGRNs are involved in feeding initiation, the stGRNs are preferentially tuned to suppression of locomotion upon sugar encounter (Figures 23-25). Therefore, distinct facets of the early appetitive response are controlled by distinct tarsal sweet taste receptor neurons (Figure 29). Because stGRNs project exclusively to the VNC, they may have

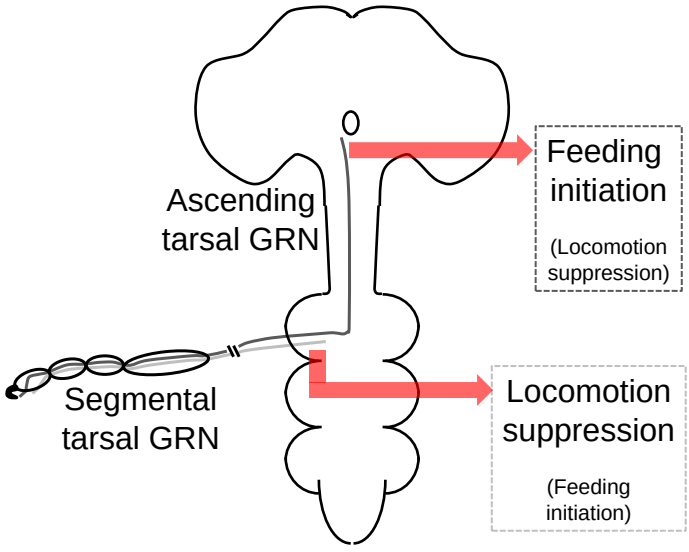

Figure 29: Distinct subsets of tarsal sweet taste receptor neurons are tuned to different facets of the early appetitive response. Ascending tarsal gustatory receptor neurons (dark gray) primarily control feeding initiation (i.e. proboscis extension), with a minor contribution in sugar-induced locomotion suppression. Segmental tarsal gustatory receptor neurons (light gray) control sugar-induced locomotion suppression, with a minor contribution to feeding initiation. GRN gustatory receptor neuron.

better access to the local circuits that control movement of the legs, making them well-suited for this function. Mechanistically, having two neuronal populations that respond to sugar and control distinct but related behaviors facilitates coordination of these responses.

Despite the apparent specialization, the roles of these sensors are unlikely to be mutually exclusive. For example, blocking atGRNs yielded proportionately lower sugar-induced locomotion suppression compared to genetic controls (Figures 23h and 25b), while blocking *Gr5a-GAL4* still showed a tendency for sugar-induced linear velocity suppression (Figure 25a), although none of these effects were statistically significant. These results suggest that atGRNs can contribute to sugar-induced locomotion suppression, albeit to a more limited extent. atGRNs may be able to influence locomotion directly through their VNC collaterals (Figure 13a), or indirectly, by controlling proboscis extension (Figure 15c). Fixing the proboscis in the extended position negatively regulates movement[93], demonstrating that additional mechanisms are in play, to ensure that flies stay immobile while feeding.

On the other hand, blocking stGRNs with *Gr5a-GAL4* showed a small reduction in PER probability when the legs were stimulated with sugar (Figure 15d). Although it was not significant, this reduction is consistent with a previous study, in which ablating *Gr5a-GAL4* cells significantly reduced PER probability following stimulation of the legs[22]. Differences in the magnitude of this effect may be related to the differences in starvation. The stronger starvation used for the experiments presented here may attenuate the effect of stGRN blockage on PER. Conversely, blocking atGRNs did not eliminate PER, indicating that stGRNs alone can induce this behavior, albeit with considerably lower efficiency (Figure 15c). In line with this, thermogenetic activation of stGRNs is sufficient for PER induction[123]. Collectively, these findings suggest that a parallel pathway indirectly relays sweet taste information from stGRNs to

the brain. The stGRNs may exert a small influence on feeding initiation through this pathway. The existence of parallel pathways to the brain may be advantageous for retaining appetitive responses, should one of the two pathways become compromised.

4.4. Roles of different taste organs in *Drosophila*

While sweet taste receptor neurons in the legs are important for early appetitive responses, GRNs in the labellum and pharynx may come into play in later stages of feeding. This is reasonable, considering that stimulation of labellar GRNs requires extension of the proboscis towards a potential food, while stimulation of pharyngeal GRNs requires ingestion (or at least its initiation). Functional specialization of different taste organs is additionally supported by anatomical and physiological data:

(1) Projections from GRNs tuned to the same quality, but located in different taste organs, are segregated in the CNS (Figure 2).

(2) Sugar stimulation of different taste organs yields unique Ca^{2+} activation patterns in higher brain structures (MB calyx), suggesting differential representation of taste organs in the brain[124].

The roles of GRNs in the labellum and pharynx are discussed below, with particular emphasis on feeding. More generally, the roles of different taste organs in controlling fly behavior are summarized in Figure 30.

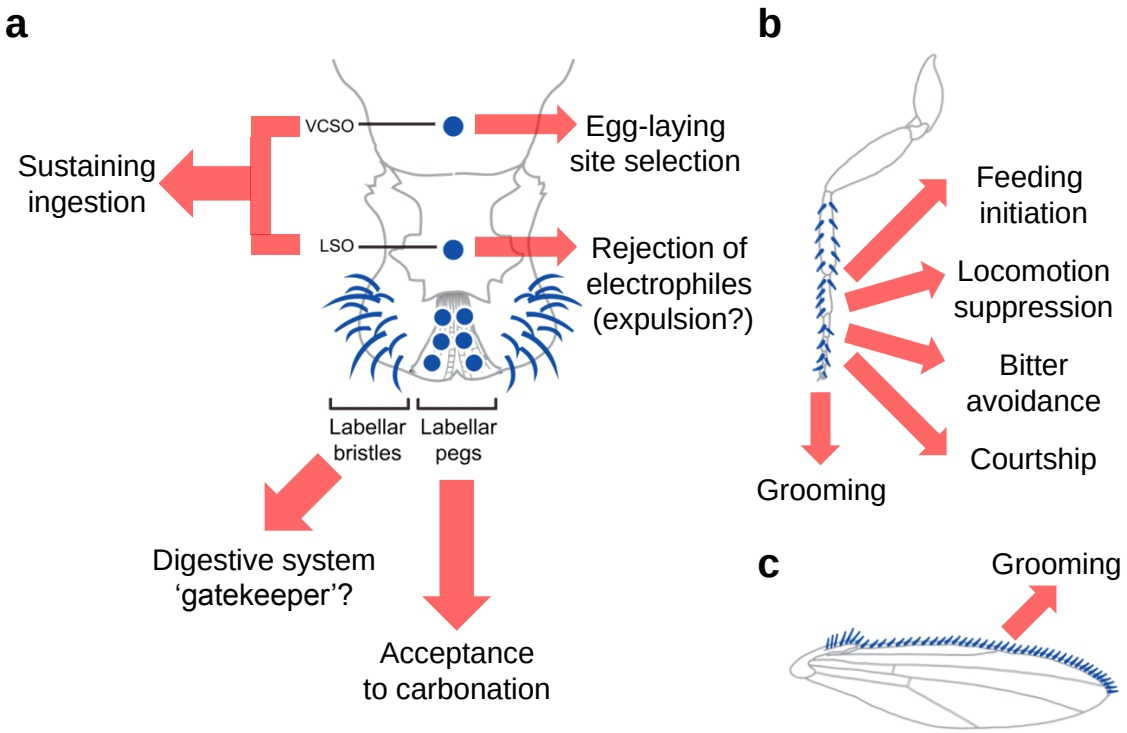

Figure 30: Roles of taste receptor neurons in different taste organs of *Drosophila*. (a) Roles of different taste organs in the proboscis. The dorsal cibarial taste organ (DCSO) is not shown, but has not been attributed to a specific function yet. (b) Roles of taste hairs in the tarsi. (c) Bitter taste hairs in the wings promote grooming. Speculative roles are marked with a question mark. The ovipositor is not shown, but it may be involved in the selection of egg-laying sites. Schematic from[38]. LSO labral sense organ; VCSO ventral cibarial sense organ.

4.4.1. Role of labellar GRNs

As with legs, stimulation of the labellum can also cause proboscis extension[25,150]. However, flies typically keep their proboscises retracted[2], limiting direct contact of the labellum with potential food. Therefore, the labellum is less likely to play an important role in early appetitive responses. In line with this, blocking all sweet GRNs of the labellum with *Gr5a-GAL4* did not cause a large impairment in sugar preference (Figures 9 and 15b).

Although there have been no focused attempts to characterize the role of the labellum in feeding behavior, it is notable that this organ is also not crucial for sugar-induced locomotion suppression (Figure 25), odor-sugar learning (Figure 20b), long-term preference to sugars[27],

regulation of sugar consumption[27] and lobeline aversion[91]. This is striking, considering that it is sometimes thought of as the main taste organ of *Drosophila*[8]. Nevertheless, its position at the entrance to the digestive system indicates that it may function as a 'gatekeeper' before ingestion. In accordance with this, stimulation of the legs with sugar, followed by application of a bitter compound on the labellum of the (extended) proboscis, leads to immediate proboscis retraction[123-125]. Therefore, when faced with stimuli of opposing valence, primacy of the labellum over the legs dictates the fly's response.

The Carlson lab has systematically analyzed *Gr-GAL4* expression and physiological responses of taste hairs in the labellum[68] and legs[11]. Two key findings from these studies point to a unique role for the labellum:

(1) Most bitter GRNs in the labellum express far more bitter GRs than bitter GRNs in the forelegs. In the labellum, they express 15 ± 2 bitter GRs (Mean ± SEM; range 6-28) whereas in the forelegs, they express 8 ± 3 bitter GRs (Mean ± SEM; range 5-18).

(2) Maximal physiological responses to bitter compounds are consistently higher in the labellum than the forelegs for the great majority of tested compounds.

These results suggest that the labellum is better suited to carrying out rigorous quality control of potential food, in line with its ability to 'veto' appetitive responses induced by leg stimulation. To conclude, the labellum may be functionally more analogous to the mammalian tongue than any of the other fly taste organs.

4.4.2. Role of pharyngeal GRNs

Sweet taste receptor neurons in the LSO and VCSO were recently shown to be required for sugar preference in a long-term (2 hour) assay[27]. In this assay, flies are allowed to ingest

agarose with or without food, differentially labeled with dyes. Preference is scored by counting flies whose abdomens are differentially colored by the dyes. Interestingly, eliminating all GRNs in the legs and labellum with a *poxn* mutant had a minor effect on this ingestion-based preference. This result shows that, if flies are allowed to remain on food for a long period, feeding can be initiated spontaneously, without any input from peripheral GRNs. However, for immediate appetitive responses (i.e. 1 min or less), sweet GRNs in the LSO appear to be dispensable (Figures 9, 10c, c' and 16). The authors of the study also show that blocking the sweet GRNs in the LSO/VCSO reduces sugar consumption. Therefore, they conclude that these pharyngeal cells regulate ingestion, an interpretation consistent with the location of the pharyngeal organs.

The role of bitter GRNs in the pharynx is less intuitive. Logically, it would be safer and more economical to reject potentially harmful stimuli before initiation of ingestion. However, rejection of electrophiles (aversive chemicals that include allyl isothiocyanate, a pungent chemical in wasabi) depends on bitter GRNs in the LSO and is mediated by dTrpA1, an ion channel that also plays a role in heat perception[81]. The same study also revealed that ingestion of these chemicals is necessary for the aversive response: mixtures of sugar and aversive electrophiles elicit PER when the tarsi are stimulated, but if the flies are allowed to ingest the mixture, they suppress PER in subsequent trials. It is unclear why the presence of such specialized GRNs exclusively in the LSO is advantageous. Nevertheless, it seems tempting to speculate that these specialized cells drive fluid expulsion in response to certain aversive stimuli, thus terminating feeding without allowing complete ingestion.

Bitter GRNs in the VCSO and DCSO are further along the pharynx. Both are located near the cibarial pump, which draws food from the environment and propels it through the esophagus.

Therefore, they may interact with nearby motor neurons that coordinate the muscles controlling this pump[105]. In line with this, these motor neurons respond to tastants, including caffeine, a bitter compound. It is therefore plausible that detection of bitters in the VCSO/DCSO could reverse the motor program of the cibarial pump, switching ingestion to expulsion as soon as an aversive tastant is detected.

While bitter substances are undesirable in food, they may be advantageous under other circumstances. The Heberlein lab and others have shown that female flies prefer to lay their eggs on lobeline, a bitter chemical, despite the fact that it is aversive to them[91]. This egg-laying preference is controlled by bitter GRNs in the VCSO. Strikingly, the ovipositor has not yet been implicated in selection of the site for egg laying, despite long-standing speculation that this is its role[6]. Control of egg-laying preference by pharyngeal GRNs may seem counter-intuitive, but females appear to actively search for egg-laying sites[95]. This search behavior includes proboscis extension. It seems reasonable to assume that limited ingestion also occurs during this search behavior, which could explain the involvement of pharyngeal GRNs.

4.5. Higher order neurons for sugar preference

Some of the *NP-GAL4*s isolated in the silencing screen have off-target expression in GRNs (Figure 28a). *Gr64f-LexA* and *LexAop-GAL80* should therefore be used to refine expression. *NP-GAL4*s that continue to show impaired sugar preference upon blockade will most likely contain interneurons crucial for sugar choice. Because sugar preference integrates multiple appetitive responses (Figure 26), interneurons should be further characterized using strategies that were successfully applied for GRNs.

To explore interactions of GRNs and higher-order taste neurons, two-color labeling or GFP reconstitution across synaptic partners (GRASP) are often used to highlight contacts. However, most such experiments use *Gr5a* lines to label the sweet GRNs[93,100-103,106]. Therefore, contacts with atGRNs are typically overlooked. Given the role of atGRNs in feeding initiation, it will be important to examine their interactions with higher-order brain neurons. Future studies using the GAL4 resources, intersectional strategies and computer algorithms established here should provide deeper mechanistic understanding about how processing in the CNS controls preference in *Drosophila*.

References

1 Breslin, P. A. & Spector, A. C. Mammalian taste perception. *Current biology : CB* **18**, R148-155, doi:10.1016/j.cub.2007.12.017 (2008).

2 Yarmolinsky, D. A., Zuker, C. S. & Ryba, N. J. Common sense about taste: from mammals to insects. *Cell* **139**, 234-244, doi:10.1016/j.cell.2009.10.001 (2009).

3 Li, X., Li, W., Wang, H., Cao, J., Maehashi, K., Huang, L., Bachmanov, A. A., Reed, D. R., Legrand-Defretin, V., Beauchamp, G. K. & Brand, J. G. Pseudogenization of a sweet-receptor gene accounts for cats' indifference toward sugar. *PLoS genetics* **1**, 27-35, doi:10.1371/journal.pgen.0010003 (2005).

4 Zhao, H., Yang, J. R., Xu, H. & Zhang, J. Pseudogenization of the umami taste receptor gene Tas1r1 in the giant panda coincided with its dietary switch to bamboo. *Molecular biology and evolution* **27**, 2669-2673, doi:10.1093/molbev/msq153 (2010).

5 Liman, E. R., Zhang, Y. V. & Montell, C. Peripheral coding of taste. *Neuron* **81**, 984-1000, doi:10.1016/j.neuron.2014.02.022 (2014).

6 Stocker, R. F. The organization of the chemosensory system in *Drosophila melanogaster*: a review. *Cell and tissue research* **275**, 3-26 (1994).

7 Shanbhag, S. R., Park, S. K., Pikielny, C. W. & Steinbrecht, R. A. Gustatory organs of *Drosophila melanogaster*: fine structure and expression of the putative odorant-binding protein PBPRP2. *Cell and tissue research* **304**, 423-437 (2001).

8 Thorne, N., Chromey, C., Bray, S. & Amrein, H. Taste perception and coding in *Drosophila*. *Current biology : CB* **14**, 1065-1079, doi:10.1016/j.cub.2004.05.019 (2004).

9 Gendre, N., Luer, K., Friche, S., Grillenzoni, N., Ramaekers, A., Technau, G. M. & Stocker, R. F. Integration of complex larval chemosensory organs into the adult nervous system of *Drosophila*. *Development* **131**, 83-92, doi:10.1242/dev.00879 (2004).

10 Stocker, R. F. & Schorderet, M. Cobalt filling of sensory projections from internal and external mouthparts in *Drosophila*. *Cell and tissue research* **216**, 513-523 (1981).

11 Ling, F., Dahanukar, A., Weiss, L. A., Kwon, J. Y. & Carlson, J. R. The molecular and cellular basis of taste coding in the legs of *Drosophila*. *The Journal of neuroscience : the official journal of the Society for Neuroscience* **34**, 7148-7164, doi:10.1523/JNEUROSCI.0649-14.2014 (2014).

12 Nayak, S. V. & Singh, R. N. Sensilla on the tarsal segments and mouthparts of adult *Drosophila melanogaster* meigen (Diptera : Drosophilidae). *International Journal of Insect Morphology and Embryology* **12**, 273-291, doi:http://dx.doi.org/10.1016/0020-7322(83)90023-5 (1983).

13 Meunier, N., Ferveur, J. F. & Marion-Poll, F. Sex-specific non-pheromonal taste receptors in *Drosophila*. *Current biology : CB* **10**, 1583-1586 (2000).

14 Possidente, D. R. & Murphey, R. K. Genetic control of sexually dimorphic axon morphology in *Drosophila* sensory neurons. *Developmental biology* **132**, 448-457 (1989).

15 Thistle, R., Cameron, P., Ghorayshi, A., Dennison, L. & Scott, K. Contact chemoreceptors mediate male-male repulsion and male-female attraction during *Drosophila* courtship. *Cell* **149**, 1140-1151, doi:10.1016/j.cell.2012.03.045 (2012).

16 Nelson, G., Hoon, M. A., Chandrashekar, J., Zhang, Y., Ryba, N. J. & Zuker, C. S. Mammalian sweet taste receptors. *Cell* **106**, 381-390 (2001).

17 Falk, R., Bleiser-Avivi, N. & Atidia, J. Labellar taste organs of *Drosophila melanogaster*. *Journal of Morphology* **150**, 327-341, doi:10.1002/jmor.1051500206 (1976).

18 Ito, K., Shinomiya, K., Ito, M., Armstrong, J. D., Boyan, G., Hartenstein, V., Harzsch, S., Heisenberg, M., Homberg, U., Jenett, A., Keshishian, H., Restifo, L. L., Rossler, W., Simpson, J. H., Strausfeld, N. J., Strauss, R., Vosshall, L. B. & Insect Brain Name Working, G. A systematic nomenclature for the insect brain. *Neuron* **81**, 755-765, doi:10.1016/j.neuron.2013.12.017 (2014).

19 Dahanukar, A., Lei, Y. T., Kwon, J. Y. & Carlson, J. R. Two Gr genes underlie sugar reception in *Drosophila*. *Neuron* **56**, 503-516, doi:10.1016/j.neuron.2007.10.024 (2007).

20 Kwon, J. Y., Dahanukar, A., Weiss, L. A. & Carlson, J. R. A map of taste neuron projections in the *Drosophila* CNS. *Journal of biosciences* **39**, 565-574 (2014).

21 Miyazaki, T. & Ito, K. Neural architecture of the primary gustatory center of *Drosophila melanogaster* visualized with GAL4 and LexA enhancer-trap systems. *The Journal of comparative neurology* **518**, 4147-4181, doi:10.1002/cne.22433 (2010).

22 Wang, Z., Singhvi, A., Kong, P. & Scott, K. Taste representations in the *Drosophila* brain. *Cell* **117**, 981-991, doi:10.1016/j.cell.2004.06.011 (2004).

23 Masek, P. & Keene, A. C. *Drosophila* fatty acid taste signals through the PLC pathway in sugar-sensing neurons. *PLoS genetics* **9**, e1003710, doi:10.1371/journal.pgen.1003710 (2013).

24 Hiroi, M., Meunier, N., Marion-Poll, F. & Tanimura, T. Two antagonistic gustatory receptor neurons responding to sweet-salty and bitter taste in *Drosophila*. *Journal of neurobiology* **61**, 333-342, doi:10.1002/neu.20063 (2004).

25 Dethier, V. G. *The hungry fly : a physiological study of the behavior associated with feeding / V. G. Dethier*. (Harvard University Press, 1976).

26 Galizia, G. & Lledo, P. M. *Neurosciences - From Molecule to Behavior: a university textbook*. (SpringerSpektrum, 2013).

27 LeDue, E. E., Chen, Y. C., Jung, A. Y., Dahanukar, A. & Gordon, M. D. Pharyngeal sense organs drive robust sugar consumption in *Drosophila*. *Nature communications* **6**, 6667, doi:10.1038/ncomms7667 (2015).

28 Pool, A. H. & Scott, K. Feeding regulation in *Drosophila*. *Current opinion in neurobiology* **29**, 57-63, doi:10.1016/j.conb.2014.05.008 (2014).

29 Ishimoto, H. & Tanimura, T. Molecular neurophysiology of taste in *Drosophila*. *Cellular and molecular life sciences : CMLS* **61**, 10-18, doi:10.1007/s00018-003-3182-9 (2004).

30 Cameron, P., Hiroi, M., Ngai, J. & Scott, K. The molecular basis for water taste in *Drosophila*. *Nature* **465**, 91-95, doi:10.1038/nature09011 (2010).

31 Zhang, Y. V., Ni, J. & Montell, C. The molecular basis for attractive salt-taste coding in *Drosophila*. *Science* **340**, 1334-1338, doi:10.1126/science.1234133 (2013).

32 Chandrashekar, J., Mueller, K. L., Hoon, M. A., Adler, E., Feng, L., Guo, W., Zuker, C. S. & Ryba, N. J. T2Rs function as bitter taste receptors. *Cell* **100**, 703-711 (2000).

33 Nelson, G., Chandrashekar, J., Hoon, M. A., Feng, L., Zhao, G., Ryba, N. J. & Zuker, C. S. An amino-acid taste receptor. *Nature* **416**, 199-202, doi:10.1038/nature726 (2002).

34 Chaudhari, N., Landin, A. M. & Roper, S. D. A metabotropic glutamate receptor variant functions as a taste receptor. *Nature neuroscience* **3**, 113-119, doi:10.1038/72053 (2000).

35 San Gabriel, A., Uneyama, H., Yoshie, S. & Torii, K. Cloning and characterization of a novel mGluR1 variant from vallate papillae that functions as a receptor for L-glutamate stimuli. *Chemical senses* **30 Suppl 1**, i25-26, doi:10.1093/chemse/bjh095 (2005).

36 Clyne, P. J., Warr, C. G. & Carlson, J. R. Candidate taste receptors in *Drosophila*. *Science* **287**, 1830-1834 (2000).

37 Robertson, H. M., Warr, C. G. & Carlson, J. R. Molecular evolution of the insect chemoreceptor gene superfamily in *Drosophila melanogaster*. *Proceedings of the National Academy of Sciences of the United States of America* **100 Suppl 2**, 14537-14542, doi:10.1073/pnas.2335847100 (2003).

38 Zhang, H. J., Anderson, A. R., Trowell, S. C., Luo, A. R., Xiang, Z. H. & Xia, Q. Y. Topological and functional characterization of an insect gustatory receptor. *PloS one* **6**, e24111, doi:10.1371/journal.pone.0024111 (2011).

39 Koh, T. W., He, Z., Gorur-Shandilya, S., Menuz, K., Larter, N. K., Stewart, S. & Carlson, J. R. The *Drosophila* IR20a clade of ionotropic receptors are candidate taste and pheromone receptors. *Neuron* **83**, 850-865, doi:10.1016/j.neuron.2014.07.012 (2014).

40 Alves, G., Salle, J., Chaudy, S., Dupas, S. & Maniere, G. High-NaCl perception in *Drosophila melanogaster*. *The Journal of neuroscience : the official journal of the Society for Neuroscience* **34**, 10884-10891, doi:10.1523/JNEUROSCI.4795-13.2014 (2014).

41 Chen, Z., Wang, Q. & Wang, Z. The amiloride-sensitive epithelial Na+ channel PPK28 is essential for *drosophila* gustatory water reception. *The Journal of neuroscience : the official journal of the Society for Neuroscience* **30**, 6247-6252, doi:10.1523/JNEUROSCI.0627-10.2010 (2010).

42 Liu, L., Leonard, A. S., Motto, D. G., Feller, M. A., Price, M. P., Johnson, W. A. & Welsh, M. J. Contribution of *Drosophila* DEG/ENaC genes to salt taste. *Neuron* **39**, 133-146 (2003).

43 Lu, B., LaMora, A., Sun, Y., Welsh, M. J. & Ben-Shahar, Y. ppk23-Dependent chemosensory functions contribute to courtship behavior in *Drosophila melanogaster*. *PLoS genetics* **8**, e1002587, doi:10.1371/journal.pgen.1002587 (2012).

44 Toda, H., Zhao, X. & Dickson, B. J. The *Drosophila* female aphrodisiac pheromone activates ppk23(+) sensory neurons to elicit male courtship behavior. *Cell reports* **1**, 599-607, doi:10.1016/j.celrep.2012.05.007 (2012).

45 Al-Anzi, B., Tracey, W. D., Jr. & Benzer, S. Response of *Drosophila* to wasabi is mediated by painless, the fly homolog of mammalian TRPA1/ANKTM1. *Current biology : CB* **16**, 1034-1040, doi:10.1016/j.cub.2006.04.002 (2006).

46 Kim, S. H., Lee, Y., Akitake, B., Woodward, O. M., Guggino, W. B. & Montell, C. *Drosophila* TRPA1 channel mediates chemical avoidance in gustatory receptor neurons. *Proceedings of the National Academy of Sciences of the United States of America* **107**, 8440-8445, doi:10.1073/pnas.1001425107 (2010).

47 Zhang, Y. V., Raghuwanshi, R. P., Shen, W. L. & Montell, C. Food experience-induced taste desensitization modulated by the *Drosophila* TRPL channel. *Nature neuroscience* **16**, 1468-1476, doi:10.1038/nn.3513 (2013).

48 Jones, W. D., Cayirlioglu, P., Kadow, I. G. & Vosshall, L. B. Two chemosensory receptors together mediate carbon dioxide detection in *Drosophila*. *Nature* **445**, 86-90, doi:10.1038/nature05466 (2007).

49 Kwon, J. Y., Dahanukar, A., Weiss, L. A. & Carlson, J. R. The molecular basis of CO2 reception in *Drosophila*. *Proceedings of the National Academy of Sciences of the United States of America* **104**, 3574-3578, doi:10.1073/pnas.0700079104 (2007).

50 Ni, L., Bronk, P., Chang, E. C., Lowell, A. M., Flam, J. O., Panzano, V. C., Theobald, D. L., Griffith, L. C. & Garrity, P. A. A gustatory receptor paralogue controls rapid warmth avoidance in *Drosophila*. *Nature* **500**, 580-584, doi:10.1038/nature12390 (2013).

51 Xiang, Y., Yuan, Q., Vogt, N., Looger, L. L., Jan, L. Y. & Jan, Y. N. Light-avoidance-mediating photoreceptors tile the *Drosophila* larval body wall. *Nature* **468**, 921-926, doi:10.1038/nature09576 (2010).

52 Chyb, S., Dahanukar, A., Wickens, A. & Carlson, J. R. *Drosophila* Gr5a encodes a taste receptor tuned to trehalose. *Proceedings of the National Academy of Sciences of the United States of America* **100 Suppl 2**, 14526-14530, doi:10.1073/pnas.2135339100 (2003).

53 Dahanukar, A., Foster, K., van der Goes van Naters, W. M. & Carlson, J. R. A Gr receptor is required for response to the sugar trehalose in taste neurons of *Drosophila*. *Nature neuroscience* **4**, 1182-1186, doi:10.1038/nn765 (2001).

54 Ueno, K., Ohta, M., Morita, H., Mikuni, Y., Nakajima, S., Yamamoto, K. & Isono, K. Trehalose sensitivity in *Drosophila* correlates with mutations in and expression of the gustatory receptor gene Gr5a. *Current biology : CB* **11**, 1451-1455 (2001).

55 Miyamoto, T., Chen, Y., Slone, J. & Amrein, H. Identification of a *Drosophila* glucose receptor using Ca2+ imaging of single chemosensory neurons. *PloS one* **8**, e56304, doi:10.1371/journal.pone.0056304 (2013).

56 Jiao, Y., Moon, S. J. & Montell, C. A *Drosophila* gustatory receptor required for the responses to sucrose, glucose, and maltose identified by mRNA tagging. *Proceedings of the National Academy of Sciences of the United States of America* **104**, 14110-14115, doi:10.1073/pnas.0702421104 (2007).

57 Wisotsky, Z., Medina, A., Freeman, E. & Dahanukar, A. Evolutionary differences in food preference rely on Gr64e, a receptor for glycerol. *Nature neuroscience* **14**, 1534-1541, doi:10.1038/nn.2944 (2011).

58 Jiao, Y., Moon, S. J., Wang, X., Ren, Q. & Montell, C. Gr64f is required in combination with other gustatory receptors for sugar detection in *Drosophila*. *Current biology : CB* **18**, 1797-1801, doi:10.1016/j.cub.2008.10.009 (2008).

59 Miyamoto, T., Slone, J., Song, X. & Amrein, H. A fructose receptor functions as a nutrient sensor in the *Drosophila* brain. *Cell* **151**, 1113-1125, doi:10.1016/j.cell.2012.10.024 (2012).

60 Slone, J., Daniels, J. & Amrein, H. Sugar receptors in *Drosophila*. *Current biology : CB* **17**, 1809-1816, doi:10.1016/j.cub.2007.09.027 (2007).

61 Freeman, E. G., Wisotsky, Z. & Dahanukar, A. Detection of sweet tastants by a conserved group of insect gustatory receptors. *Proceedings of the National Academy of Sciences of the United States of America* **111**, 1598-1603, doi:10.1073/pnas.1311724111 (2014).

62 Fujii, S., Yavuz, A., Slone, J., Jagge, C., Song, X. & Amrein, H. *Drosophila* sugar receptors in sweet taste perception, olfaction, and internal nutrient sensing. *Current biology : CB* **25**, 621-627, doi:10.1016/j.cub.2014.12.058 (2015).

63 Moon, S. J., Lee, Y., Jiao, Y. & Montell, C. A *Drosophila* gustatory receptor essential for aversive taste and inhibiting male-to-male courtship. *Current biology : CB* **19**, 1623-1627, doi:10.1016/j.cub.2009.07.061 (2009).

64 Moon, S. J., Kottgen, M., Jiao, Y., Xu, H. & Montell, C. A taste receptor required for the caffeine response in vivo. *Current biology : CB* **16**, 1812-1817, doi:10.1016/j.cub.2006.07.024 (2006).

65 Lee, Y., Moon, S. J. & Montell, C. Multiple gustatory receptors required for the caffeine response in *Drosophila*. *Proceedings of the National Academy of Sciences of the United States of America* **106**, 4495-4500, doi:10.1073/pnas.0811744106 (2009).

66 Lee, Y., Kim, S. H. & Montell, C. Avoiding DEET through insect gustatory receptors. *Neuron* **67**, 555-561, doi:10.1016/j.neuron.2010.07.006 (2010).

67 Lee, Y., Moon, S. J., Wang, Y. & Montell, C. A *Drosophila* Gustatory Receptor Required for Strychnine Sensation. *Chemical senses*, doi:10.1093/chemse/bjv038 (2015).

68 Weiss, L. A., Dahanukar, A., Kwon, J. Y., Banerjee, D. & Carlson, J. R. The molecular and cellular basis of bitter taste in *Drosophila*. *Neuron* **69**, 258-272, doi:10.1016/j.neuron.2011.01.001 (2011).

69 Fan, P., Manoli, D. S., Ahmed, O. M., Chen, Y., Agarwal, N., Kwong, S., Cai, A. G., Neitz, J., Renslo, A., Baker, B. S. & Shah, N. M. Genetic and neural mechanisms that inhibit *Drosophila* from mating with other species. *Cell* **154**, 89-102, doi:10.1016/j.cell.2013.06.008 (2013).

70 Koganezawa, M., Haba, D., Matsuo, T. & Yamamoto, D. The shaping of male courtship posture by lateralized gustatory inputs to male-specific interneurons. *Current biology : CB* **20**, 1-8, doi:10.1016/j.cub.2009.11.038 (2010).

71 Lacaille, F., Hiroi, M., Twele, R., Inoshita, T., Umemoto, D., Maniere, G., Marion-Poll, F., Ozaki, M., Francke, W., Cobb, M., Everaerts, C., Tanimura, T. & Ferveur, J. F. An inhibitory sex pheromone tastes bitter for *Drosophila* males. *PloS one* **2**, e661, doi:10.1371/journal.pone.0000661 (2007).

72 Miyamoto, T. & Amrein, H. Suppression of male courtship by a *Drosophila* pheromone receptor. *Nature neuroscience* **11**, 874-876, doi:10.1038/nn.2161 (2008).

73 Watanabe, K., Toba, G., Koganezawa, M. & Yamamoto, D. Gr39a, a highly diversified gustatory receptor in *Drosophila*, has a role in sexual behavior. *Behavior genetics* **41**, 746-753, doi:10.1007/s10519-011-9461-6 (2011).

74 Toshima, N., Hara, C., Scholz, C. J. & Tanimura, T. Genetic variation in food choice behaviour of amino acid-deprived *Drosophila*. *J Insect Physiol* **69**, 89-94, doi:10.1016/j.jinsphys.2014.06.019 (2014).

75 Lee, Y., Kang, M. J., Shim, J., Cheong, C. U., Moon, S. J. & Montell, C. Gustatory receptors required for avoiding the insecticide L-canavanine. *The Journal of neuroscience : the official journal of the Society for Neuroscience* **32**, 1429-1435, doi:10.1523/JNEUROSCI.4630-11.2012 (2012).

76 Toshima, N. & Tanimura, T. Taste preference for amino acids is dependent on internal nutritional state in *Drosophila melanogaster*. *The Journal of experimental biology* **215**, 2827-2832, doi:10.1242/jeb.069146 (2012).

77 Benton, R., Vannice, K. S., Gomez-Diaz, C. & Vosshall, L. B. Variant ionotropic glutamate receptors as chemosensory receptors in *Drosophila*. *Cell* **136**, 149-162, doi:10.1016/j.cell.2008.12.001 (2009).

78 Croset, V., Rytz, R., Cummins, S. F., Budd, A., Brawand, D., Kaessmann, H., Gibson, T. J. & Benton, R. Ancient protostome origin of chemosensory ionotropic glutamate receptors and the evolution of insect taste and olfaction. *PLoS genetics* **6**, e1001064, doi:10.1371/journal.pgen.1001064 (2010).

79 Lin, H., Mann, K. J., Starostina, E., Kinser, R. D. & Pikielny, C. W. A *Drosophila* DEG/ENaC channel subunit is required for male response to female pheromones. *Proceedings of the National Academy of Sciences of the United States of America* **102**, 12831-12836, doi:10.1073/pnas.0506420102 (2005).

80 Starostina, E., Liu, T., Vijayan, V., Zheng, Z., Siwicki, K. K. & Pikielny, C. W. A *Drosophila* DEG/ENaC subunit functions specifically in gustatory neurons required for male courtship behavior. *The Journal of neuroscience : the official journal of the Society for Neuroscience* **32**, 4665-4674, doi:10.1523/JNEUROSCI.6178-11.2012 (2012).

81 Kang, K., Pulver, S. R., Panzano, V. C., Chang, E. C., Griffith, L. C., Theobald, D. L. & Garrity, P. A. Analysis of *Drosophila* TRPA1 reveals an ancient origin for human chemical nociception. *Nature* **464**, 597-600, doi:10.1038/nature08848 (2010).

82 Meunier, N., Marion-Poll, F., Rospars, J. P. & Tanimura, T. Peripheral coding of bitter taste in *Drosophila*. *Journal of neurobiology* **56**, 139-152, doi:10.1002/neu.10235 (2003).

83 Chu, B., Chui, V., Mann, K. & Gordon, M. D. Presynaptic gain control drives sweet and bitter taste integration in *Drosophila*. *Current biology : CB* **24**, 1978-1984, doi:10.1016/j.cub.2014.07.020 (2014).

84 French, A. S., Sellier, M. J., Moutaz, A. A., Guigue, A., Chabaud, M. A., Reeb, P. D., Mitra, A., Grau, Y., Soustelle, L. & Marion-Poll, F. Dual mechanism for bitter avoidance

in *Drosophila*. *The Journal of neuroscience : the official journal of the Society for Neuroscience* **35**, 3990-4004, doi:10.1523/JNEUROSCI.1312-14.2015 (2015).

85 Jeong, Y. T., Shim, J., Oh, S. R., Yoon, H. I., Kim, C. H., Moon, S. J. & Montell, C. An odorant-binding protein required for suppression of sweet taste by bitter chemicals. *Neuron* **79**, 725-737, doi:10.1016/j.neuron.2013.06.025 (2013).

86 Swarup, S., Morozova, T. V., Sridhar, S., Nokes, M. & Anholt, R. R. Modulation of feeding behavior by odorant-binding proteins in *Drosophila melanogaster*. *Chemical senses* **39**, 125-132, doi:10.1093/chemse/bjt061 (2014).

87 Charlu, S., Wisotsky, Z., Medina, A. & Dahanukar, A. Acid sensing by sweet and bitter taste neurons in *Drosophila melanogaster*. *Nature communications* **4**, 2042, doi:10.1038/ncomms3042 (2013).

88 Isono, K. & Morita, H. Molecular and cellular designs of insect taste receptor system. *Frontiers in cellular neuroscience* **4**, 20, doi:10.3389/fncel.2010.00020 (2010).

89 Marella, S., Fischler, W., Kong, P., Asgarian, S., Rueckert, E. & Scott, K. Imaging taste responses in the fly brain reveals a functional map of taste category and behavior. *Neuron* **49**, 285-295, doi:10.1016/j.neuron.2005.11.037 (2006).

90 Harris, D. T., Kallman, B. R., Mullaney, B. C. & Scott, K. Representations of Taste Modality in the *Drosophila* Brain. *Neuron* **86**, 1449-1460, doi:10.1016/j.neuron.2015.05.026 (2015).

91 Joseph, R. M. & Heberlein, U. Tissue-specific activation of a single gustatory receptor produces opposing behavioral responses in *Drosophila*. *Genetics* **192**, 521-532, doi:10.1534/genetics.112.142455 (2012).

92 Schoofs, A., Huckesfeld, S., Schlegel, P., Miroschnikow, A., Peters, M., Zeymer, M., Spiess, R., Chiang, A. S. & Pankratz, M. J. Selection of motor programs for suppressing food intake and inducing locomotion in the *Drosophila* brain. *PLoS biology* **12**, e1001893, doi:10.1371/journal.pbio.1001893 (2014).

93 Mann, K., Gordon, M. D. & Scott, K. A pair of interneurons influences the choice between feeding and locomotion in *Drosophila*. *Neuron* **79**, 754-765, doi:10.1016/j.neuron.2013.06.018 (2013).

94 Maher, N., Thiery, D. & Städler, E. Oviposition by *Lobesia botrana* is stimulated by sugars detected by contact chemoreceptors. *Physiological Entomology* **31**, 14-22, doi:10.1111/j.1365-3032.2005.00476.x (2006).

95 Yang, C. H., Belawat, P., Hafen, E., Jan, L. Y. & Jan, Y. N. *Drosophila* egg-laying site selection as a system to study simple decision-making processes. *Science* **319**, 1679-1683, doi:10.1126/science.1151842 (2008).

96 Yanagawa, A., Guigue, A. M. & Marion-Poll, F. Hygienic grooming is induced by contact chemicals in *Drosophila melanogaster*. *Frontiers in behavioral neuroscience* **8**, 254, doi:10.3389/fnbeh.2014.00254 (2014).

97 Yamamoto, D. & Koganezawa, M. Genes and circuits of courtship behaviour in *Drosophila* males. *Nature reviews. Neuroscience* **14**, 681-692, doi:10.1038/nrn3567 (2013).

98 Bray, S. & Amrein, H. A putative *Drosophila* pheromone receptor expressed in male-specific taste neurons is required for efficient courtship. *Neuron* **39**, 1019-1029 (2003).

99 Liu, T., Starostina, E., Vijayan, V. & Pikielny, C. W. Two *Drosophila* DEG/ENaC channel subunits have distinct functions in gustatory neurons that activate male courtship.

The Journal of neuroscience : the official journal of the Society for Neuroscience **32**, 11879-11889, doi:10.1523/JNEUROSCI.1376-12.2012 (2012).

100 Flood, T. F., Iguchi, S., Gorczyca, M., White, B., Ito, K. & Yoshihara, M. A single pair of interneurons commands the *Drosophila* feeding motor program. *Nature* **499**, 83-87, doi:10.1038/nature12208 (2013).

101 Gordon, M. D. & Scott, K. Motor control in a *Drosophila* taste circuit. *Neuron* **61**, 373-384, doi:10.1016/j.neuron.2008.12.033 (2009).

102 Kain, P. & Dahanukar, A. Secondary taste neurons that convey sweet taste and starvation in the *Drosophila* brain. *Neuron* **85**, 819-832, doi:10.1016/j.neuron.2015.01.005 (2015).

103 Miyazaki, T., Lin, T. Y., Ito, K., Lee, C. H. & Stopfer, M. A gustatory second-order neuron that connects sucrose-sensitive primary neurons and a distinct region of the gnathal ganglion in the *Drosophila* brain. *Journal of neurogenetics*, 1-26, doi:10.3109/01677063.2015.1054993 (2015).

104 Pool, A. H., Kvello, P., Mann, K., Cheung, S. K., Gordon, M. D., Wang, L. & Scott, K. Four GABAergic interneurons impose feeding restraint in *Drosophila*. *Neuron* **83**, 164-177, doi:10.1016/j.neuron.2014.05.006 (2014).

105 Manzo, A., Silies, M., Gohl, D. M. & Scott, K. Motor neurons controlling fluid ingestion in *Drosophila*. *Proceedings of the National Academy of Sciences of the United States of America* **109**, 6307-6312, doi:10.1073/pnas.1120305109 (2012).

106 Marella, S., Mann, K. & Scott, K. Dopaminergic modulation of sucrose acceptance behavior in *Drosophila*. *Neuron* **73**, 941-950, doi:10.1016/j.neuron.2011.12.032 (2012).

107 Inagaki, H. K., Ben-Tabou de-Leon, S., Wong, A. M., Jagadish, S., Ishimoto, H., Barnea, G., Kitamoto, T., Axel, R. & Anderson, D. J. Visualizing neuromodulation in vivo:

TANGO-mapping of dopamine signaling reveals appetite control of sugar sensing. *Cell* **148**, 583-595, doi:10.1016/j.cell.2011.12.022 (2012).

108 Tempel, B. L., Bonini, N., Dawson, D. R. & Quinn, W. G. Reward learning in normal and mutant *Drosophila*. *Proceedings of the National Academy of Sciences of the United States of America* **80**, 1482-1486 (1983).

109 Schnaitmann, C., Vogt, K., Triphan, T. & Tanimoto, H. Appetitive and aversive visual learning in freely moving *Drosophila*. *Frontiers in behavioral neuroscience* **4**, 10, doi:10.3389/fnbeh.2010.00010 (2010).

110 Keene, A. C. & Waddell, S. *Drosophila* olfactory memory: single genes to complex neural circuits. *Nature reviews. Neuroscience* **8**, 341-354, doi:10.1038/nrn2098 (2007).

111 Vogt, K., Schnaitmann, C., Dylla, K. V., Knapek, S., Aso, Y., Rubin, G. M. & Tanimoto, H. Shared mushroom body circuits underlie visual and olfactory memories in *Drosophila*. *eLife* **3**, e02395, doi:10.7554/eLife.02395 (2014).

112 Hammer, M. An identified neuron mediates the unconditioned stimulus in associative olfactory learning in honeybees. *Nature* **366**, 59-63 (1993).

113 Kreissl, S., Eichmuller, S., Bicker, G., Rapus, J. & Eckert, M. Octopamine-like immunoreactivity in the brain and subesophageal ganglion of the honeybee. *The Journal of comparative neurology* **348**, 583-595, doi:10.1002/cne.903480408 (1994).

114 Hammer, M. & Menzel, R. Multiple sites of associative odor learning as revealed by local brain microinjections of octopamine in honeybees. *Learning & memory* **5**, 146-156 (1998).

115 Schwaerzel, M., Monastirioti, M., Scholz, H., Friggi-Grelin, F., Birman, S. & Heisenberg, M. Dopamine and octopamine differentiate between aversive and appetitive

olfactory memories in *Drosophila*. *The Journal of neuroscience : the official journal of the Society for Neuroscience* **23**, 10495-10502 (2003).

116 Busch, S., Selcho, M., Ito, K. & Tanimoto, H. A map of octopaminergic neurons in the *Drosophila* brain. *The Journal of comparative neurology* **513**, 643-667, doi:10.1002/cne.21966 (2009).

117 Liu, C., Placais, P. Y., Yamagata, N., Pfeiffer, B. D., Aso, Y., Friedrich, A. B., Siwanowicz, I., Rubin, G. M., Preat, T. & Tanimoto, H. A subset of dopamine neurons signals reward for odour memory in *Drosophila*. *Nature* **488**, 512-516, doi:10.1038/nature11304 (2012).

118 Burke, C. J., Huetteroth, W., Owald, D., Perisse, E., Krashes, M. J., Das, G., Gohl, D., Silies, M., Certel, S. & Waddell, S. Layered reward signalling through octopamine and dopamine in *Drosophila*. *Nature* **492**, 433-437, doi:10.1038/nature11614 (2012).

119 Burke, C. J. & Waddell, S. Remembering nutrient quality of sugar in *Drosophila*. *Current biology : CB* **21**, 746-750, doi:10.1016/j.cub.2011.03.032 (2011).

120 Fujita, M. & Tanimura, T. *Drosophila* evaluates and learns the nutritional value of sugars. *Current biology : CB* **21**, 751-755, doi:10.1016/j.cub.2011.03.058 (2011).

121 Yamagata, N., Ichinose, T., Aso, Y., Placais, P. Y., Friedrich, A. B., Sima, R. J., Preat, T., Rubin, G. M. & Tanimoto, H. Distinct dopamine neurons mediate reward signals for short- and long-term memories. *Proceedings of the National Academy of Sciences of the United States of America* **112**, 578-583, doi:10.1073/pnas.1421930112 (2015).

122 Lin, S., Owald, D., Chandra, V., Talbot, C., Huetteroth, W. & Waddell, S. Neural correlates of water reward in thirsty *Drosophila*. *Nature neuroscience* **17**, 1536-1542, doi:10.1038/nn.3827 (2014).

123 Keene, A. C. & Masek, P. Optogenetic induction of aversive taste memory. *Neuroscience* **222**, 173-180, doi:10.1016/j.neuroscience.2012.07.028 (2012).

124 Kirkhart, C. & Scott, K. Gustatory learning and processing in the *Drosophila* mushroom bodies. *The Journal of neuroscience : the official journal of the Society for Neuroscience* **35**, 5950-5958, doi:10.1523/JNEUROSCI.3930-14.2015 (2015).

125 Masek, P., Worden, K., Aso, Y., Rubin, G. M. & Keene, A. C. A dopamine-modulated neural circuit regulating aversive taste memory in *Drosophila*. *Current biology : CB* **25**, 1535-1541, doi:10.1016/j.cub.2015.04.027 (2015).

126 Masek, P. & Scott, K. Limited taste discrimination in *Drosophila*. *Proceedings of the National Academy of Sciences of the United States of America* **107**, 14833-14838, doi:10.1073/pnas.1009318107 (2010).

127 Weiner, J. *Time, Love, Memory: A Great Biologist and His Quest for the Origins of Behavior*. (Vintage, 2000).

128 Jenett, A., Rubin, G. M., Ngo, T. T., Shepherd, D., Murphy, C., Dionne, H., Pfeiffer, B. D., Cavallaro, A., Hall, D., Jeter, J., Iyer, N., Fetter, D., Hausenfluck, J. H., Peng, H., Trautman, E. T., Svirskas, R. R., Myers, E. W., Iwinski, Z. R., Aso, Y., DePasquale, G. M., Enos, A., Hulamm, P., Lam, S. C., Li, H. H., Laverty, T. R., Long, F., Qu, L., Murphy, S. D., Rokicki, K., Safford, T., Shaw, K., Simpson, J. H., Sowell, A., Tae, S., Yu, Y. & Zugates, C. T. A GAL4-driver line resource for *Drosophila* neurobiology. *Cell reports* **2**, 991-1001, doi:10.1016/j.celrep.2012.09.011 (2012).

129 Bellen, H. J., Tong, C. & Tsuda, H. 100 years of *Drosophila* research and its impact on vertebrate neuroscience: a history lesson for the future. *Nature reviews. Neuroscience* **11**, 514-522, doi:10.1038/nrn2839 (2010).

130 White, B. H. & Peabody, N. C. Neurotrapping: cellular screens to identify the neural substrates of behavior in *Drosophila*. *Frontiers in molecular neuroscience* **2**, 20, doi:10.3389/neuro.02.020.2009 (2009).

131 Brand, A. H. & Perrimon, N. Targeted gene expression as a means of altering cell fates and generating dominant phenotypes. *Development* **118**, 401-415 (1993).

132 Kitamoto, T. Conditional modification of behavior in *Drosophila* by targeted expression of a temperature-sensitive shibire allele in defined neurons. *Journal of neurobiology* **47**, 81-92 (2001).

133 Baines, R. A., Uhler, J. P., Thompson, A., Sweeney, S. T. & Bate, M. Altered electrical properties in *Drosophila* neurons developing without synaptic transmission. *The Journal of neuroscience : the official journal of the Society for Neuroscience* **21**, 1523-1531 (2001).

134 Hamada, F. N., Rosenzweig, M., Kang, K., Pulver, S. R., Ghezzi, A., Jegla, T. J. & Garrity, P. A. An internal thermal sensor controlling temperature preference in *Drosophila*. *Nature* **454**, 217-220, doi:10.1038/nature07001 (2008).

135 Klapoetke, N. C., Murata, Y., Kim, S. S., Pulver, S. R., Birdsey-Benson, A., Cho, Y. K., Morimoto, T. K., Chuong, A. S., Carpenter, E. J., Tian, Z., Wang, J., Xie, Y., Yan, Z., Zhang, Y., Chow, B. Y., Surek, B., Melkonian, M., Jayaraman, V., Constantine-Paton, M., Wong, G. K. & Boyden, E. S. Independent optical excitation of distinct neural populations. *Nature methods* **11**, 338-346, doi:10.1038/nmeth.2836 (2014).

136 Lee, T. & Luo, L. Mosaic analysis with a repressible cell marker for studies of gene function in neuronal morphogenesis. *Neuron* **22**, 451-461 (1999).

137 Struhl, G. & Basler, K. Organizing activity of wingless protein in *Drosophila*. *Cell* **72**, 527-540 (1993).

138 Bohm, R. A., Welch, W. P., Goodnight, L. K., Cox, L. W., Henry, L. G., Gunter, T. C., Bao, H. & Zhang, B. A genetic mosaic approach for neural circuit mapping in *Drosophila*. *Proceedings of the National Academy of Sciences of the United States of America* **107**, 16378-16383, doi:10.1073/pnas.1004669107 (2010).

139 Potter, C. J., Tasic, B., Russler, E. V., Liang, L. & Luo, L. The Q system: a repressible binary system for transgene expression, lineage tracing, and mosaic analysis. *Cell* **141**, 536-548, doi:10.1016/j.cell.2010.02.025 (2010).

140 Lai, S. L. & Lee, T. Genetic mosaic with dual binary transcriptional systems in *Drosophila*. *Nature neuroscience* **9**, 703-709, doi:10.1038/nn1681 (2006).

141 Xu, T. & Rubin, G. M. Analysis of genetic mosaics in developing and adult *Drosophila* tissues. *Development* **117**, 1223-1237 (1993).

142 Wong, A. M., Wang, J. W. & Axel, R. Spatial representation of the glomerular map in the *Drosophila* protocerebrum. *Cell* **109**, 229-241 (2002).

143 Pfeiffer, B. D., Ngo, T. T., Hibbard, K. L., Murphy, C., Jenett, A., Truman, J. W. & Rubin, G. M. Refinement of tools for targeted gene expression in *Drosophila*. *Genetics* **186**, 735-755, doi:10.1534/genetics.110.119917 (2010).

144 Asahina, K., Watanabe, K., Duistermars, B. J., Hoopfer, E., Gonzalez, C. R., Eyjolfsdottir, E. A., Perona, P. & Anderson, D. J. Tachykinin-expressing neurons control male-specific aggressive arousal in *Drosophila*. *Cell* **156**, 221-235, doi:10.1016/j.cell.2013.11.045 (2014).

145 Hayashi, S., Ito, K., Sado, Y., Taniguchi, M., Akimoto, A., Takeuchi, H., Aigaki, T., Matsuzaki, F., Nakagoshi, H., Tanimura, T., Ueda, R., Uemura, T., Yoshihara, M. & Goto, S. GETDB, a database compiling expression patterns and molecular locations of a collection of Gal4 enhancer traps. *Genesis* **34**, 58-61, doi:10.1002/gene.10137 (2002).

146 Wu, J. S. & Luo, L. A protocol for dissecting *Drosophila melanogaster* brains for live imaging or immunostaining. *Nature protocols* **1**, 2110-2115, doi:10.1038/nprot.2006.336 (2006).

147 Klagges, B. R., Heimbeck, G., Godenschwege, T. A., Hofbauer, A., Pflugfelder, G. O., Reifegerste, R., Reisch, D., Schaupp, M., Buchner, S. & Buchner, E. Invertebrate synapsins: a single gene codes for several isoforms in *Drosophila*. *The Journal of neuroscience : the official journal of the Society for Neuroscience* **16**, 3154-3165 (1996).

148 Schindelin, J., Arganda-Carreras, I., Frise, E., Kaynig, V., Longair, M., Pietzsch, T., Preibisch, S., Rueden, C., Saalfeld, S., Schmid, B., Tinevez, J. Y., White, D. J., Hartenstein, V., Eliceiri, K., Tomancak, P. & Cardona, A. Fiji: an open-source platform for biological-image analysis. *Nature methods* **9**, 676-682, doi:10.1038/nmeth.2019 (2012).

149 Templier, T. *Biological and computational framework for the identification of neuronal circuits in Drosophila brains* Diploma thesis, Technische Universitat Munchen, (2011).

150 Shiraiwa, T. & Carlson, J. R. Proboscis extension response (PER) assay in *Drosophila*. *Journal of visualized experiments : JoVE*, 193, doi:10.3791/193 (2007).

151 Thum, A. S., Jenett, A., Ito, K., Heisenberg, M. & Tanimoto, H. Multiple memory traces for olfactory reward learning in *Drosophila*. *The Journal of neuroscience : the official*

journal of the Society for Neuroscience **27**, 11132-11138, doi:10.1523/JNEUROSCI.2712-07.2007 (2007).

152 Knapek, S., Gerber, B. & Tanimoto, H. Synapsin is selectively required for anesthesia-sensitive memory. *Learning & memory* **17**, 76-79, doi:10.1101/lm.1661810 (2010).

153 Burger, W. & Burge, M. J. *Digital Image Processing*. 177-178 (Springer London, 2008).

154 Mulchrone, K. F. & Choudhury, K. R. Fitting an ellipse to an arbitrary shape: implications for strain analysis. *Journal of Structural Geology* **26**, 143-153, doi:http://dx.doi.org/10.1016/S0191-8141(03)00093-2 (2004).

155 Knapek, S., Sigrist, S. & Tanimoto, H. Bruchpilot, a synaptic active zone protein for anesthesia-resistant memory. *The Journal of neuroscience : the official journal of the Society for Neuroscience* **31**, 3453-3458, doi:10.1523/JNEUROSCI.2585-10.2011 (2011).

156 Damrau, C. *Aversive and Appetitive stimuli response in Drosophila*. Diploma thesis, Julius-Maximilians-Univeristät, (2010).

157 Miyamoto, T. & Amrein, H. Diverse roles for the *Drosophila* fructose sensor Gr43a. *Fly* **8**, 19-25, doi:10.4161/fly.27241 (2014).

158 Branson, K., Robie, A. A., Bender, J., Perona, P. & Dickinson, M. H. High-throughput ethomics in large groups of *Drosophila*. *Nature methods* **6**, 451-457, doi:10.1038/nmeth.1328 (2009).

159 Gao, Q. & Finkelstein, R. Targeting gene expression to the head: the *Drosophila* orthodenticle gene is a direct target of the Bicoid morphogen. *Development* **125**, 4185-4193 (1998).

160 Peng, H., Chung, P., Long, F., Qu, L., Jenett, A., Seeds, A. M., Myers, E. W. & Simpson, J. H. BrainAligner: 3D registration atlases of *Drosophila* brains. *Nature methods* **8**, 493-500, doi:10.1038/nmeth.1602 (2011).

161 de Brito Sanchez, M. G., Lorenzo, E., Su, S., Liu, F., Zhan, Y. & Giurfa, M. The tarsal taste of honey bees: behavioral and electrophysiological analyses. *Frontiers in behavioral neuroscience* **8**, 25, doi:10.3389/fnbeh.2014.00025 (2014).

162 de Brito Sanchez, M. G. Taste perception in honey bees. *Chemical senses* **36**, 675-692, doi:10.1093/chemse/bjr040 (2011).

Acknowledgements

First and foremost, I thank Prof. Hiromu Tanimoto for his support, for fostering a collaborative and friendly atmosphere in his laboratory, for initiating productive collaborations and for the many intellectually fruitful discussions throughout my PhD. I would like to think that I have learnt a lot during these last five years, both as a young scientist and as a human being.

Second, I would like to thank my thesis committees, both in Japan and Europe, for their consistent support and helpful advice: Profs. Daisuke Yamamoto, Masayuki Koganezawa, Kosei Sato and Nobuhiro Yamagata (in Japan) and Prof. Alexander Borst, Dr. Ilona Kadow and Dr. Matthieu Louis (in Europe).

I am deeply indebted to Profs. Shogo Arai and Koichi Hashimoto, as well as to Mr. Pudith Sirigrivatanawong, for our collaboration on the locomotion quantification algorithm. Similarly, the mathematical model for fly preference would not have been possible without Dr. Hiroshi Kohsaka, to whom I extend my appreciation. Dr. Shoh Asano provided a useful Matlab script for this project, while Jessika Binder and Christian Garbers developed preliminary software to estimate fly locomotion, which is not presented here but was nevertheless a useful first step. Finally, Dr. Pavel Mašek was happy to share his expertise in *Drosophila* feeding behaviour, and Maijana Lenk contributed to experiments not presented here. I am grateful to all five of them for their help and contributions.

In addition, I would like to express my appreciation to all members of the Tanimoto lab, past and present, with who I had the pleasure to work or interact with. Special thanks go to Drs. Stephan Knapek and Marion Hartl for their anatomical expertise and substantial contributions to the work presented here. The help of Anja Friedrich was crucial both with *Drosophila* anatomy

and life in Germany. The same goes for Toshiharu Ichinose and Abe Ayako, for life in Japan. Dr. Christine Damrau's help and guidance was valuable during the start of my PhD. Last but not least, I would like to thank Dr. Katrin Vogt, Tuba Oguz and Toshi Ichinose (again) for their support and for critical readings of my thesis.

I am grateful to the International Max Planck Research School for Life Sciences, for providing a fascinating opportunity to do research in one of the best institutes in Europe, and in particular to Dr. Hans Joerg Schaeffer, Dr. Ingrid Wolf and Mrs. Maximiliane Reif for organizing an excellent doctoral program. In addition, I am grateful to the Max Planck society as well as to Tohoku university for financial support.

Finally, I thank Hubert Amrein, John Carlson, Barret Pfeiffer, Gerald M. Rubin, Kristin Scott, Ilona Kadow, David Anderson and the Kyoto DGRC and Bloomington Stock Centres for fly stocks.

Non-self contributions

The majority of the confocal image data were acquired by Dr. Stephan Knapek, with contributions from Dr. Marion Hartl, Anja Friedrich, Ayako Abe, Igor Siwanowicz and Thomas Templier. Mr. Templier also implemented the image registration algorithm. Learning experiments were performed by Dr. Stephan Knapek. The locomotion quantification algorithm was developed in collaboration with Prof. Shogo Arai, Prof. Koichi Hashimoto and Pudith Sirigrivatanawong. The mathematical model for sugar preference was developed with Dr. Hiroshi Kohsaka, who also implemented it. The secondary *NP-GAL4* screen was carried out in collaboration with Dr. Christine Damrau, who also developed the sugar preference assay.